Simulation Study on the Active Motion Compensation of an offshore gangway

Master of Science Thesis

M.Y. Boumzaouad

October 24th, 2017

For the degree of Master of Science in Offshore and Dredging Engineering at Delft University of Technology

-Confidential-

TU Delft
Delft University of Technology

KENZFIGEE GROUP

Master of Science Thesis:

Simulation Study on the Active Motion Compensation of an Offshore Gangway

Author:

Mohamed Yassine Boumzaouad

Thesis Committee:

Delft of University of Technology	Prof. dr. A.V. Metrikine (Chairman)
	Dr. ir. A. Jarquin Laguna
	Dr. ir. K.N. van Dalen
Kenz Figee bv	Ir. S. Herman
	Ir. F. Van den Hoogen

ABSTRACT

During offshore installations in harsh sea conditions, the involved gangway system must satisfy rigorous requirements in terms of safety and accuracy. The forces resulting from the vessel motion have an extensive effect on the overall gangway structure and its lifetime. Moreover, vessel motion handicaps the operator during fine positioning of the gangway during connection to a platform. Hence, an active motion compensation system for the gangway is used. An impression of the gangway structure can be seen in Figure 1 below. In this thesis, a 2D-model for the gangway system is developed in order to simulate the Active Motion Compensation (AMC) required to compensate wave induced vessel motions. The model can be used to estimate the power required by the system, needed to compensate the motions in order to minimize the movements of the connection point. The model is developed using software Matlab Simscape.

The gangway is capable of performing single stage telescoping motion, activated by a winch that pulls the telescoping section back and forth, luffing motion by activating of the hydraulic cylinders and slewing motions by means of a slewing bearing. In order to develop an as accurate as possible model, the whole gangway system is divided in three sub-systems: the mechanical, the hydraulic and the control sub-system. The main outputs of the mechanical sub-system are the movements, velocities and accelerations of the gangway system relative to its mass and center of gravity and based on the RAO's of the vessel. For the hydraulic luffing system, all relevant hydraulic components are modeled. A directional proportional (control) valve in the hydraulic sub-system is used to regulate the amount of flow through the system. In order to compensate the gangway tip, a feedback on the position and a feedforward on the velocity of the compensation point is applied. The inputs from the MRU, which are the imposed ship motions (heave, sway and roll), are converted to the motion of the tip of the gangway by a PLC controller. These converted signals are used to determine the control set points for the luffing and telescoping actuators. A basic proportional controller is used for the Active Motion Compensation system of the gangway.

Figure 1: Impression of the active motion compensated gangway with the 3 degrees of freedom indicated

In order to validate the numerical model, the simulation results are compared with experimental results from quayside tests. During these tests, different sinusoidal signals are applied for the 3 possible motions: translation in vertical direction which mimics the heave motion, translation in the horizontal direction which mimics the sway motion and a rotation around the main hinge which mimics the roll motion of the vessel. When applying only the roll motion or the sway motion, the luffing function and the telescoping function respectively could be assessed separately. Besides these three signals, combinations of these motions are also provided to assess the total performance of the system. Several variables are logged during the tests of which the compensation error, the measured set points, and pressures in the hydraulic cylinder are analyzed thoroughly and compared with the simulation results. It is observed that the simulation results show important similarities in the dynamic response of the gangway on the imposed ship motions.

The current model provides a good insight in the behavior of the gangway system and can be used to simulate offshore tests in different virtual weather windows before testing the real gangway offshore. This is the main advantage compared to the case before this thesis is conducted. It is recommended to extend the 2D simulation into a 3D simulation by adding the slewing function. It's also recommended to further study the controller design in order to improve the AMC performance.

ACKNOWLEDGMENT

This thesis is the final course of my Master of Science study in Offshore and Dredging Engineering at the Delft University of Technology. It has been performed in cooperation with the Engineering department of Kenz Figee bv in Zaandam. I would like to express my gratitude towards all the people that provided any kind of support during the full duration of this thesis.

At the Delft University of Technology, I would like to thank prof. dr. A.V. Metrikine for accepting me as one of his graduation students and for lecturing the inspiring course 'Structural Dynamics' which was in my opinion the most interesting course of the curriculum. Also I would like to thank dr. ir. A. Jarquin Laguna for his helpful support and participation in the graduation committee.

At Kenz Figee, I would like to thank ir. S. Herman for offering me the opportunity to graduate on this challenging assignment as well as giving me appreciated feedback during my thesis. Furthermore I want to express my big gratitude to my daily supervisor ir. F. van den Hoogen for his enormous amount of support, guidance and constructive feedback during my graduation thesis. In particular the enthusiastic weekly meetings where very motivational. Thanks to the daily conversations with ir. F. van den Hoogen, a huge development in the application of academic knowledge in practice during the thesis is performed and a strong fundament for the first step in my engineering career is created.

Nomenclature (Abbreviations)

Abbreviations	Definition
AMC	Active Motion Compensation
AOPS	Automatic Overload Protection System
APS	Automatic Protection System
BP	Back Pressure
CCTV	Closed Circuit Television
CCW	Counter-ClockWise
CW	ClockWise
DPS	Dynamic Positioning System
EH	Electric-Hydraulic
EMC	ElectroMagnetic Compatibility
FAT	Factory Acceptance Test
GW	GangWay
GWTX	GangWay Tip X lever arm
GWTZ	GangWay Tip Z lever arm
HAT	Harbour Acceptance Test
HMI	Human Machine Interface
HPU	Hydraulic Power Unit
MBL	Minimum Breaking Load
MCC	Main Control Centre
MOPS	Manual Overload Protection System
MPS	Manual Protection System
MRU	Motion Reference Unit
N/A	Not applicable
NDT	Non-Destructive Testing
OS	OffShore
PMC	Passive Motion Compensation
PLC	Programmable Logic Controller
PTT	Press-To-Talk
PWM	Pulse Width Modulation
QRC	Quick Release Coupling
RAO	Response Amplitude Operator
SAT	Site Acceptance Test
SLI	Safe Load Indicator
SPI	Safe Position Indicator
SWH	Significant Wave Height
SWL	Safe Working Load
TGS	Telescoping Gangway System
UPS	Uninterrupted Power Supply

Contents

1 Introduction

1.1 Kenz Figee Group B.V.

This thesis has been conducted at the engineering department of Kenz Figee Group B.V. This company combines almost 200 years of experience in the design, production and maintenance of offshore- and harbor cranes. The roots in designing and building harbor-and land-based cranes date as far back as 1836 in Haarlem, The Netherlands. However, with the increase in offshore drilling and production activities in the North Sea, Kenz Figee expanded the product portfolio towards offshore hoisting and lifting equipment in the 1980's and moved the headquarter to the Amsterdam area.

Nowadays, the company is specialized in fulfilling all sorts of customer demands ranging from custom offshore cranes to gangways and other specialized offshore equipment from the head office in the Netherlands and the local office in Singapore. Ram luffing, knuckle boom and boom hoist cranes are the common projects at the company of which the latter is built the most frequent. Servicing, refurbishing and adjusting used cranes is also part of its business. Kenz Figee has developed and built in total three gangways of which the latter one is active motion compensated. In 2016 a lot of effort was put on the design and production of the Active Motion Compensated P340 SIEM Offshore gangway and this will be continued in the coming years.

1.2 Active Motion Compensated Gangway

Before addressing the problem in chapter 2, the reader requires knowledge on the motion compensated gangway system in question, the AMC system. This section therefore explains the design, functioning and purpose of the AMC gangway system. Since many certification authorities make demands on offshore crane/gangway safety, the regulations regarding the gangway in personal transfer mode are investigated to take notice of the design requirements in section 1.3. Thereafter, in the next chapter the problem of this research and the scope of the work conducted during this master thesis is formulated.

1.2.1 General description of the Active Motion Compensated gangway

An offshore gangway can be considered as a bridge between a service operation vessel and a platform or wind turbine. It's one of the many access tools for crew and cargo transfer from ship to the turbines or platforms for maintenance, installation and other services. Therefore, often the term 'walk-to-work gangway' is used. Motion compensated gangways are the new offshore gangway solution from the Netherlands in order to minimize the motions of the gangway tip. This section will provide a functional description of the first active motion compensated gangway, designed and built by Kenz Figee: **Kenz EH 16-26/1800 O.S. GW.** This is an electric-hydraulic pedestal mounted active motion compensated offshore telescopic gangway system built for Siem Offshore Contractors GmbH for installation on service operations vessel Siddis Mariner. In figure 1.1 a 3D model of the gangway is shown.

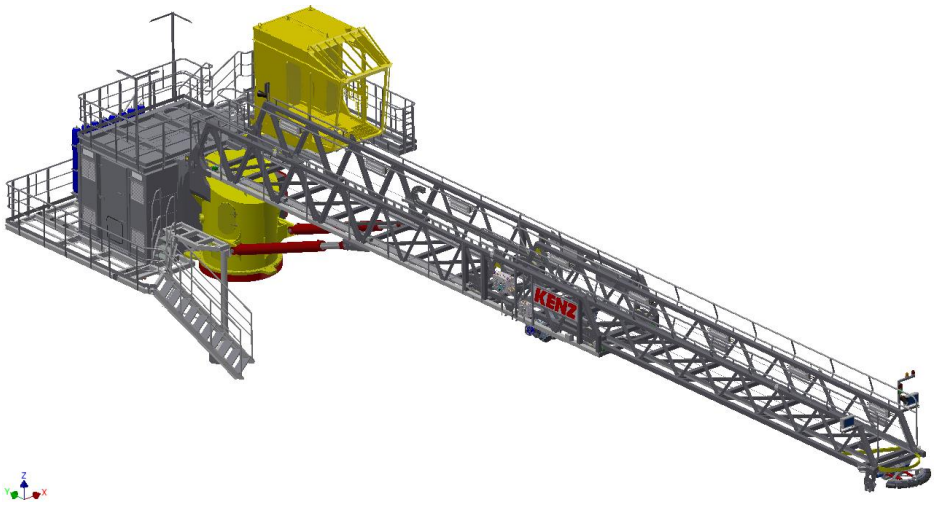

Figure 1.1 - Kenz EH 16-26/1800 O.S. GW electric-hydraulic pedestal mounted active motion compensated offshore gangway

The gangway system enables personnel transfer between the vessel and a fixed offshore platform. The nomenclature of the gangway system is shown in figure 1.2. This design incorporates a pedestal mounted mainframe featuring the slewing bearing and gear units. The pedestal is of a so called X-wing design, which provides the support and is welded to the vessel's structure. A MCC room containing the motor starter panels is mounted on the X-Wing pedestal. The operator's cabin is mounted to the left-hand side of the mainframe. The hydraulic tank and the power packs are located in the machinery house at the back of the mainframe. Stairs and walkways provide access to the cabin, gangway, machinery house, MCC room and the mainframe.

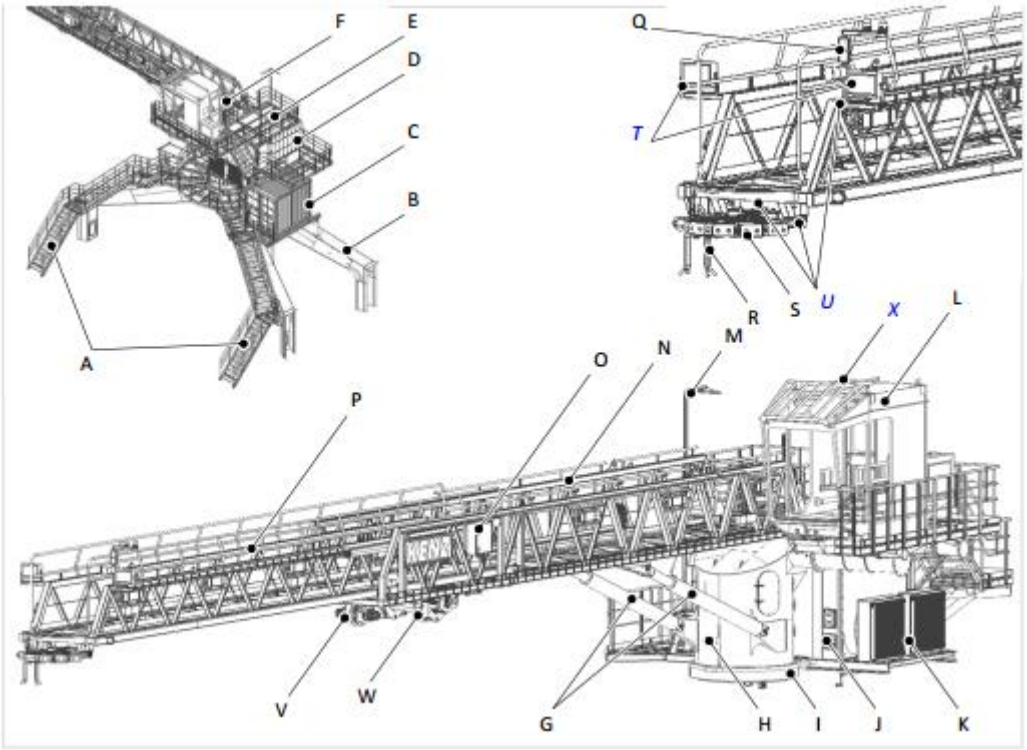

Legend

A. Access stairs	J. Machinery house	R. Hook storage frame
B. X-wing pedestal	K. Hydraulic oil/air coolers	S. Bumper
C. MCC room	L. Operator's cabin	*T. Floodlights*
D. Hydraulic accumulators	M. Lighting fixtures *& cameras*	*U. Cameras*
E. Gangway access waiting platform	N. Fixed gangway section	V. Main hoist winch
F. Signal lights & warning horn	O. Remote I/O panel 53X182	W. Telescoping winch
G. Luffing cylinders	P. Telescoping gangway section	*X. Wind speed sensor*
H. Mainframe	Q. Flash beacons, signal lights & warning horn	
I. Slewing ring		

Figure 1.2 - Gangway System Nomenclature

The gangway consists of a fixed and a telescoping section. The fixed section is attached to the pivot points at the top of the mainframe and supported by twin luffing cylinders. The telescoping winch is mounted on the underside of the fixed section. Connection to the offshore platform is made by means of a bumper system attached to the tip of the telescoping section. A hoist winch is mounted on the underside of the fixed section in front of the telescoping winch. The layout of the sheaves ensures that the main hoist hook stays at the same level during telescoping. A hook storage frame is provided at the tip of the telescoping section to store the hook when the gangway is parked in the boom rest and during personnel transfer. Standard fail-safe features have been included in the design of the control system, including a secondary (back-up) PLC, automatic zero return operating levers, full-size pressure relief valves and hydraulic lock valves.

The gangway has two operation modes: the personnel transfer mode and the crane hook mode. In the personnel transfer mode the gangway is able to transfer a live load of 500 kg up to a significant wave height of 3.0 meters. In the crane mode, the gangway can realize hoisting operations of cargo loads up to 1000 kg. The gangway has in total 4 degrees of freedom to perform the motions in the two described modes: luffing, slewing, telescoping and hoisting. This research will focus only on the personnel transfer mode which means that the fourth degree of freedom of hoisting will not be considered and will be left out in the simulation model. In figure 1.3 the relevant degrees of freedom of the gangway system are indicated.

Figure 1.3 - Gangway System with the 3 degrees of freedom indicated

The gangway is capable of performing slewing motions by means of a slewing bearing activated by two slewing gears, single stage telescopic motion by means of a winch that pulls the telescopic gangwag back and forth and luffing motions by means of two hydraulic cylinders. In section 2.6 the different used coordinate systems during this thesis will be discussed.

1.2.2 Active Motion Compensation System

The gangway system is PLC controlled, which means that all (safety) functions – such as end limits, SLI functions etc. – are guarded by the PLC. The Active Motion Compensation implies a system powered by an external power supply that reduces or cancels (compensates) the effect of the vessel motions (from one degree of freedom to all 6 degrees of freedom) on the gangway structure. The Dynamic Positioning System (DPS) maintains the vessel's position and heading with an accuracy of approx. 1m, but will not compensate the motion due to heave, pitch and roll. During operation, the resulting motion of the tip of the gangway would make accurate positioning difficult. The Active Motion Compensation system compensates this motion. This leaves only minor adjustments to be made by the operator for controlled, accurate and safe positioning. AMC can be activated in both personnel transfer mode and hoisting mode, when the tip of the gangway is positioned overboard the side of the vessel.

A MRU installed in the mainframe measures all motions of the ship. The MRU can be placed at every location, since it measures the ship motion at the COG of the ship. This will be further explained in chapter 8. The inputs from the MRU are converted to the displacement of the tip of the gangway by the PLC. The calculated displacement is used to control the pumps. The motion of the vessel will never be compensated completely, but the system has been calibrated to achieve a minimal displacement of the gangway tip in relation to the stationary platform.

1.2.3 Detailed description of the (main) components

In this thesis a simulation study on the active motion compensation system of the described gangway will be conducted. Due to the time restriction, a strong simplification of the gangway will be made. In chapter 4 a system decomposition will be made of the total gangway system. The total system and the sub-systems will be defined. In order to obtain an accurate model which generates relevant results a good analyses of the sub-systems of the gangway is necessary. Before the decomposition in the sub-systems it's important to have a good understanding of the design configuration and working principle of the main components of the gangway.

The KENZ gangway system is an Electric Hydraulic (EH) walk-to-work solution which is placed on the X-Wing Pedestal. The gangway is designed as a type 2 gangway according to DNV-GL-ST-0358 gangway rules (December 2015). Figure 1.4 provides an overview of the main components of the structure and in figure 1.6 the dimmensions and weights of the gangway structure are displayed.

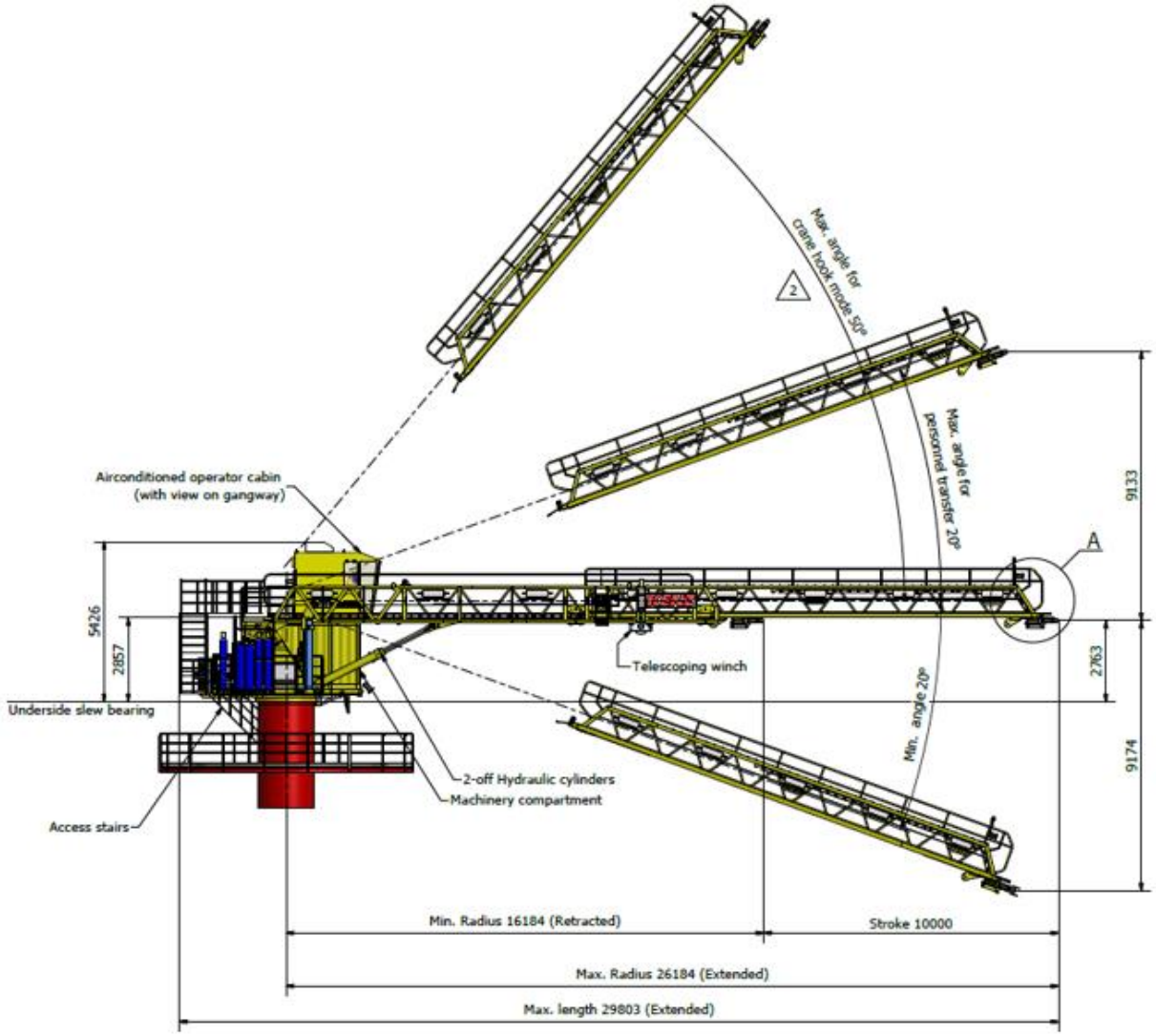

Figure 1.4 - Overview of the gangway geometry

Weights and dimension of the gangway structure

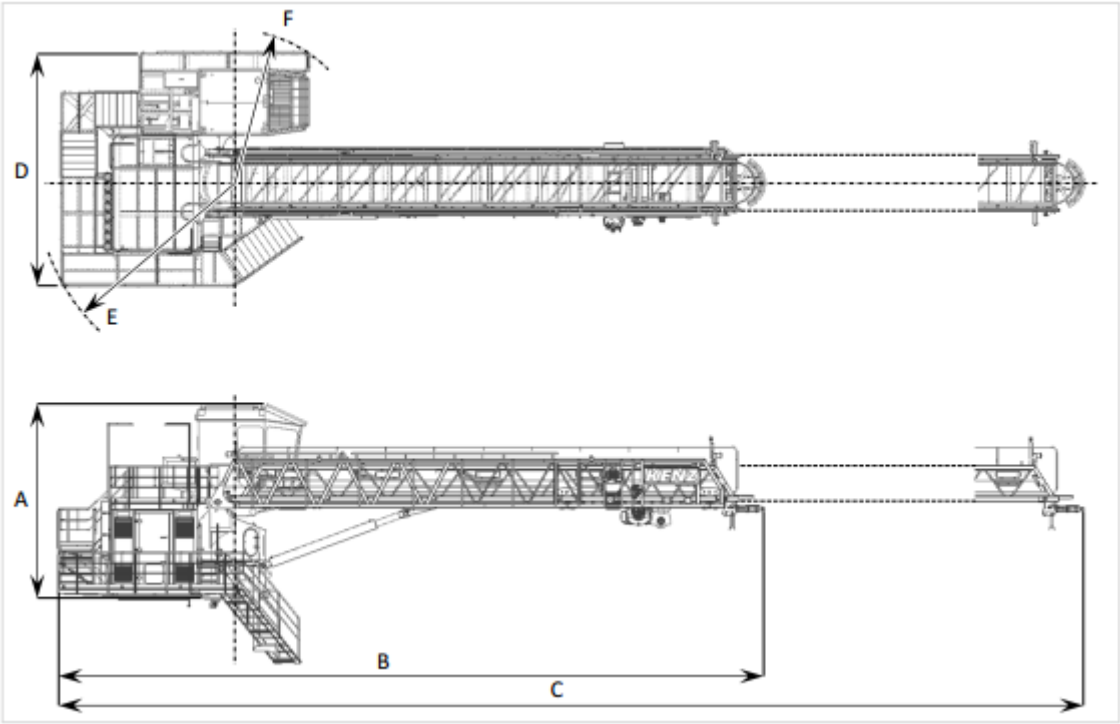

Total weight (excl. X-wing)		:	*49,190*	kg (± 5%)
Height, gangway horizontal	[A]	:	6.0	m from underside slewing bearing
Overall length (retracted)	[B]	:	21.8	m
Overall length (extended)	[C]	:	31.8	m
Overall width	[D]	:	7.1	m
Tail radius	[E]	:	6.3	m
Front radius	[F]	:	4.5	m

Figure 1.5 - Dimensions and weight (excl. X-Wing) of the gangway structure

Mainframe
The mainframe is of a tubular construction, with a bedplate incorporating the mounting flange for the slewing bearing foundation for the slewing gearboxes and jacking supports to facilitate slewing bearing maintenance or replacement. A door at the right-hand side of the mainframe provides maintenance access to the slewing gears. In figure 1.6 the details of the mainframe are shown.

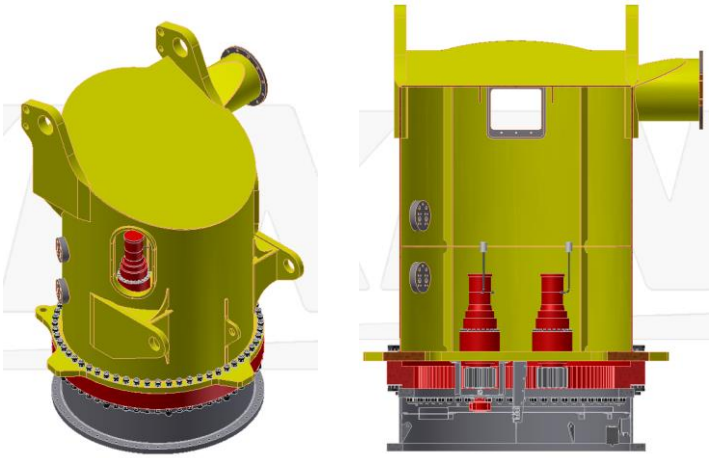

Figure 1.6 - Drawing of the mainframe (left) and cross-section (right) of the mainframe

Telescoping Gangway
The gangway consists of a fixed section and a telescoping section. It has a total length of 16.2 m when fully retracted or 26.2 m when fully extended. In figure 1.7 the fixed section is shown.
The fixed section is attached to the pivot points at the top of the mainframe and supported by twin luffing cylinders. The shafts of the gangway pivot and luffing cylinder attachment points are made of high grade steel, turning in advanced self-lubricating composite marine bearings and spherical plain bearings respectively.

A winch mounted on the underside of the fixed section drives the telescoping section (figure 1.7). The telescoping motion is guided by sets of horizontal and vertical guide rollers, while the vertical forces are transferred to the fixed structure by means of four sets of bogies. The telescoping distance is measured by a redundant encoder on the winch drum. A hardwired final limit switch is installed at the fully extended position.

Figure 1.7 - Fixed Section of the gangway

The main hoist winch is also mounted on the underside of the fixed section. The wire rope is guided by sheaves mounted on both the telescoping as well as the fixed section to ensure that the telescoping motion of the gangway will not affect the hook level. In figure 1.8 the telescoping section is shown.

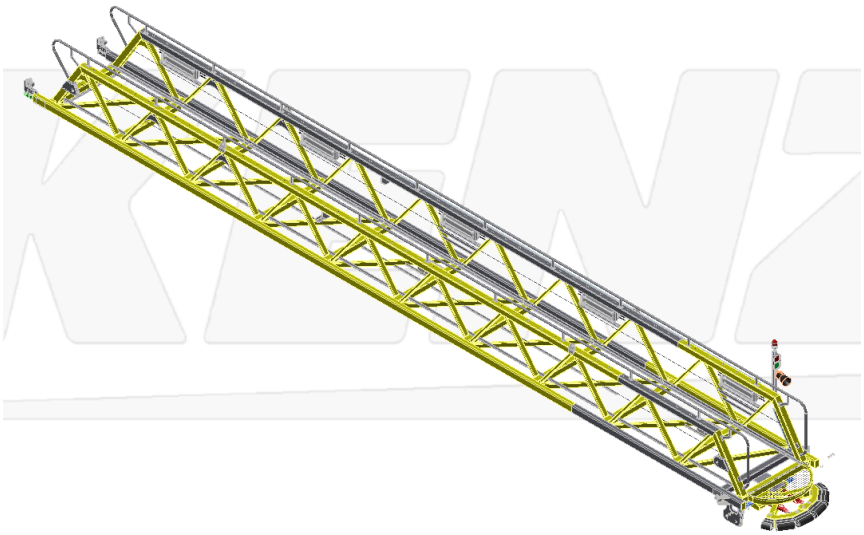

Figure 1.8 - Telescoping section of the gangway with the flexible bumper connected at the end

The flexible bumper at the end of the telescoping section provides the required connection force during personnel transfer and prevents overload in all directions. Before connection with the platform, the bumper is kept in its unloaded shape by means of two hydraulic cylinders. When connected, the bumper is deformed against the cylinder force. Hydraulic pressure in the cylinders, and thus the connection force, can be adjusted by the gangway operator. Rubber fenders provide friction and protect the bumper frame. The shape and position of the bumper are continuously monitored, together with the hydraulic cylinder pressure. The feedback is used to assist the Active Motion Compensation (AMC) system to optimize connection. A warning is given on the HMI display in the operator's cabin when approaching an overload. When an alarm limit is exceeded, the Automatic Protection System (APS) is activated. When losing any bumper position sensor, the operator will be advised to manually retract the gangway as soon as possible.

Telescoping winch

The telescoping motion of the gangway is driven by the telescoping winch, which is mounted on the underside of the fixed section of the gangway (see figure 1.7). A hydraulic motor drives the winch. The winch drum is provided with helical grooving on both sides. Two wire ropes are spooled on each side of the drum as shown in figure 1.9, one of which is attached to the front end of the telescoping section, the other to the rear end. The wire ropes are anchored to the winch drum by means of rope clamps. They are provided with a tensioner near the attachment to the gangway.
The output of the winch drum rotation encoder is used by the PLC to determine the position of the telescoping section and to guard the working limits. In combination with the input from the luffing and slewing encoders, the PLC can calculate the position of the tip of the gangway. Hardwired pre-limit and final limit sensors for the telescoping motion are mounted on the fixed section of the gangway. When a pre-limit is activated, the PLC will reduce the telescoping speed for a smooth stop.

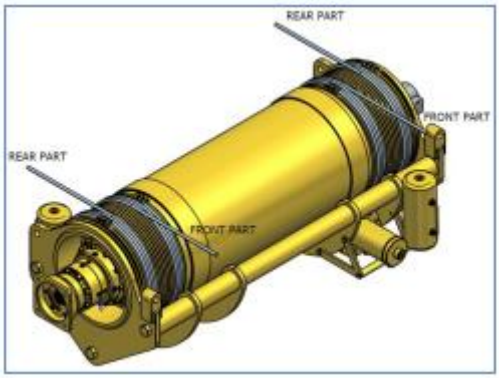

Figure 1.9 - Telescoping Winch

The winch is equipped with a built in powerful spring loaded, hydraulically released multi-disc parking brake of the wet type on the input shaft, which engages automatically in case of pressure fall. The brake therefore engages as soon as the control levers are put in the neutral position and also in case of line or hose rupture. Brake torque is at least 180% of the maximum operating torque (excluding factors). A back-up hydraulically released band brake is installed directly on the winch drum. A secondary independently hydraulically released band brake is installed on the drum. In case of a control system failure, the telescoping winch can be operated at low speed by means of the emergency control switch in the operator's cabin.

Luffing System

Two heavy-duty double acting hydraulic cylinders are provided for the luffing system. The luffing motion is limited by the end stops of the hydraulic cylinders. The signals of the linear position sensors in the cylinders are used by the PLC to calculate the angle of the gangway and to guard the working limits. Before reaching the working limits, the PLC will reduce the luffing speed for a smooth stop. When failure of the primary position sensor signal is detected, the system automatically utilizes the secondary sensor signal. In case of control system failure, the luffing function can be operated at low speed by means of the emergency control switch in the operator's cabin. In the event of a black out situation, the emergency hand pump can be connected to the luffing circuit to bring the gangway to a safe position.

Slewing System

The slewing system comprises two slewing gears being rated to withstand the combined force of wind, pedestal inclination and slewing acceleration. Setting of the pressure relief valves is based on the maximum permissible side lead forces that may occur under the given environmental conditions. The use of a slip ring unit allows for unlimited slewing through 360 [deg]. The slewing envelope in Personnel transfer mode and hoisting mode is restricted by means of encoder derived limits set in control system. Before reaching the programmed working limits, the PLC will reduce the slewing speed for a smooth step. When failure of the primary encoder signal is detected, the system automatically utilizes the secondary encoder signals. Hardwired limit sensors are installed to determine when the gangway moves over the side of the vessel.

In case of control system failure, the slewing function can be operated at low speed by means of the emergency control switch in the operator's cabin. In the event of a black power situation, the emergency hand pump can be connected to the slewing circuit to bring the gangway to a safe position.

Power Pack and Power Transmission

Each power pack consists of an electric motor, directly driving the hydraulic pumps through a flexible coupling. The gangway operator chooses which power pack is started at the beginning of operations. It is highly recommended to alternate the use of the power packs to equalize their utilization.
The power transmission to all functions is entirely hydraulic via independent open-loop circuits. Pressure transmitters are installed in all hydraulic circuits to monitor the pump pressures and also give feedback signals to the PLC for smooth control purpose. Motions will be stopped in case of low line pressure- e.g. causes by a hose burst – to prevent damage to the hydraulic system and excessive oil spill to the environment.

Hydraulic fluid Tank

The stainless steel hydraulic fuel tank with a capacity of approx. 1680 liters is mounted inside the machinery house on the left-hand side (looking forward towards the gangway). It is equipped with level and temperature gauges, level and temperature transmitters, a hydraulic fluid heater and return and breather filters. The filling connection is located in the return line at the top of the hydraulic tank. Additionally, approx. 400 liters of fluid will be present in the hydraulic system.
The level transmitter enables the fluid in the tank to be monitored by the PLC. When the fluid level drops to a low level, a warning is generated on the HMI display in the operator's cabin. When this warning is ignored and the fluid level reaches a critical level an alarm is generated on the HMI display and a shut-down is initiated to protect the hydraulic systems from damage. When the low level warning is activated and the gangway operator stops the main driver, it cannot be re-started; this can only be resolved by topping up the hydraulic fluid to correct level. A high level alarm is generated when the tank is filled above the maximum level, as the fluid needs room for expansion in the tank.

Butterfly valves are mounted in the suction lines at the bottom of the hydraulic tank to enable isolation of the hydraulic circuits for maintenance. The position of the butterfly valves is not monitored by the control system. Before operating the gangway, it must be ensured that the butterfly valves are in the fully open position, as starting the power pack with the butterfly valves closed will destroy the pumps in a few seconds.

Control system
The gangway functions are controlled by the main PLC, with a secondary PLC acting as back-up for the most critical functions. In case of failure of the main PLC, the secondary PLC can execute the automatic retract functions, the emergency functions and MOPS. The main drivers can be started by means of the secondary PLC. The PLC translates signals from the electrically operated control levers, which are integrated in the control consoles on both sides of the operator's seat, to control inputs for the hydraulic system. This allows for smooth operation and optimum 'inching' performance, whilst offering extremely light operation and quick response time.
The control levers are arranged as follows:

- Control lever for hoisting and telescoping on the right-hand side
- Control lever for luffing and slewing on the left-hand side

The control levers automatically return to their neutral position when released. All brakes are automatically engaged in this situation, unless AMC is active. Each function can be controlled infinitely from minimum to maximum speed and vice versa. The motion's limits are guarded by the PLC using position and limit sensor and Motion Reference Units (MRU) inputs. Before reaching an end limit, the PLC will reduce the speed for a smooth stop. The motion envelopes are displayed on the information plate attached to the cabin side wall for easy reference. Further operating controls are arranged on the control consoles on both sides of the operator's seat and on panels mounted on the left-hand side wall of the cabin, within easy reach of the operator. In figure 1.10 an overview of the performance data is displayed. The working envelopes of the three motions are shown. When connecting to the platform in personnel transfer mode, the laser crosshair can be used to virtually extend the gangway tip position for increased AMC accuracy. This field displays the virtual extension of the gangway in meters

Telescoping	
Minimum radius gangway tip (gangway horizontal, retracted)	16.2 m
Maximum radius gangway tip (gangway horizontal, extended)	26.2 m
Low speed zone	1 m
Storage position	16.2 m
Telescoping speed (-0% / +5%)*	30 m/min

* Infinitely variable speeds, zero to max.

Slewing	
Slewing range	unrestricted
Operational slewing range (overboard starboard side)*	-18° to +18°
Maximum operational slewing range (overboard starboard side)*	-20° to +20°
Low speed zone	2.5°
Storage position	6.1°
Slewing speed (-0% / +5%)**	0.5 rpm

* Slewing range mirrored for port side
** Infinitely variable speeds, zero to max.

Luffing	
Operational luffing range in PERSONNEL TRANSFER mode	-18° to +18°
Operational luffing range in HOISTING mode	-18° to +48°
Maximum luffing range (mechanical limits)	-20° to +50°
Low speed zone	2.5°
Storage position	0°
Luffing speed (-0% / +5%)*	3.84 m/min

* Infinitely variable speeds, zero to max.

Figure 1.10 - Working Envelopes of the luffing, slewing and telescoping motions in personnel transfer mode

1.3 Regulations regarding the AMC Gangway

To get more understanding of the AMC Gangway, the relevant standard is investigated. The standard which Kenz-Figee takes into consideration in the design of an active motion compensated gangway is the technical approach for the structural design of a type 2 offshore gangway according Det Norske Veritas DNVGL-ST-0358 Standard 'Certification of offshore gangways for personnel transfer', December 2015 [1] for certification purposes. Moreover, a hoisting device installed on the gangway, designed per DNV Standard No. 2.22 'Lifting Appliances' [1]. The gangway is to be placed on a hull interface structure, designed per DNV rules for classification: Ships. The design and engineering of this structure, hereafter referred to as the 'X-Wing' is also within KENZ scope.

A clear overview of the criteria and guidance for certification and verification of the design, following from the abovementioned standards, are adopted in this section for informational purposes.

1.3.1 Scope

All criteria and guidelines regarding the structural design of a type 2 offshore gangway for personnel transfer and an offshore crane for lifting purposes according the abovementioned standard are covered. Topics such as materials, fabrication, welding, production, testing and operational procedures are not part of the scope covered by this section

1.3.2 Client Project

KENZ is to design an offshore motion compensated gangway for Siem Offshore, to be placed on the Siddis Mariner offshore support vessel. The gangway is electrically/hydraulically driven and is able to perform slewing motions by means of a slewing bearing, driven by two slewing gears, single stage telescopic motion by means of a winch that pulls the telescopic gangway back and forth and luffing motions by means of two hydraulic cylinders. A hoisting winch, mounted on the fixed gangway, allows cargo transfer up to 1000[kg] in 2-Fall configuration including vessel induced motion compensation up to H_s = 3.0[m].

The gangway will be used to perform operation and maintenance activities at the BARD Offshore 1 (BO1) wind farm, located in the German Bight. This entails the following required operations:

- 'Walk to Work' from vessel to fixed offshore platform, 1 person (with cargo trolley), representing a maximum live load of 500[kg] at a time allowed, with motion compensation up to H_s = 3.0[m].
- Cargo transfer up to 1000[kg] by means of a hoisting winch
  - Deck lifts up to H_s = 3.0[m].
  - Floating to fixed lifts (from deck of vessel to fixed platform or vice versa), with motion compensation up to H_s of 3.0[m]

1.3.3 Gangway type

The offshore is designed for type 2 operations:

- Controlled flow of people with 'everyday' routine personnel transfer, without specific supporting documentation (i.e. DNVGL approved personnel transfer procedure).
- People do not move freely between the connected units; the flow of people is controlled/regulated by means of manual (i.e. the gangway operator) or automatic control.
- Connection time: less than 24 hours; the control of the flow of people will be ensured throughout the entire connection time.
- At least one end of the gangway is supported in the X, Y and Z axis directions (cantilever operation with bumper mode).
- Gangway will contain means to self-detach at one end and move away in a safe manner and short time.

1.3.4 Norms and standards

Unless otherwise mentioned, the latest revision of the following referenced standards are used in the design consideration of the Active Motion Compensated offshore gangway:

Main Design Code	DNVGL-ST-0358 - Certification of offshore gangways for personnel transfer (December 2015), Type 2 gangway [1] DNV No. 2.22 - Standard for certification - Lifting Appliances (April 2015)
Structural design guidelines	EN 10025 (Hot-rolled products of structural steels) ISO 898-1 (Stud bolts), ISO 898-2 (Nuts) DNV-2.9 TAP 5-778 / DNVGL-CG-0194 (hydraulic cylinders) DNVGL-RP-0005 (fatigue design of offshore steel structures) DNVGL-OS-C101 (design fatigue factor) EN 1993-1 (Design of steel structures, Eurocode 3) DNVGL-CG-0127 (Finite Element Analysis) DNVGL-OS-C102 (Structural design of offshore ships)

2 Scope of work

In the previous chapter the working principle of the AMC system is described thoroughly. The purpose, operating principle and behavior of the AMC System is known. This chapter will give the reader understanding of the problem regarding the AMC System which is addressed in this thesis.

2.1 Problem background

Access tools plays a very important role in the efficiency of a wind turbine. Transfer of technicians to the wind turbines through access systems such as motion compensated gangways on service operation vessels is the most important factor of weather downtime during maintenance activities. As an indication, the current industry standard of maximum significant wave height of 3.0 meters for accessing through walk-to-work solutions restricts the accessibility to 80% in a typical North Sea location during winter months. This makes clear the importance of improvements of offshore access systems (Offshore Wind Access, 2017). Due to global demand for safe and cost-effective offshore personnel transfers, several vessel-mounted motion compensated offshore transfer systems are developed. The active motion compensated offshore gangway is strongly developed by Kenz Group. This system allows for safe and comfortable access from vessels onto offshore structures.

2.2 Problem Definition

During offshore installations in harsh sea conditions, the involved gangway must satisfy rigorous requirements in terms of safety and efficiency. The forces resulting from the motion of the vessel have an extensive effect on the overall gangway structure and its lifetime. Moreover, vessel motion handicaps the operator during fine positioning of the gangway during connection to a platform. Hence, an active motion compensation system for the gangway is used. An important point to consider for such a system is the (electric/hydraulic) power required in order to compensate the gangway tip. Another important point to consider is the time delay of the actuators reacting on the sensors, affecting the performance of the overall system. To determine the actual control system response accuracy a detailed simulation model is necessary. Since no model is available on short notice, a calculated value cannot be presented.

So the main problem is the absence of a model of the Active Motion Compensation system. The industry has a demand for a simulation study on the AMC gangway system. By means of such study one would like to gain knowledge about the behavior of this system in different sea states and investigate the influence of much more parameters.

Currently, the AMC is designed based on hand calculations only. The system is tested by means of quayside tests on a pedestal or conducting offshore tests after installation on a vessel. In chapter 9 the difference between these two types of test will be explained. The offshore tests and experiments are costly, risky and time consuming. Moreover, in order to make the certification of the gangway possible the system have to be tested in the various sea states in which the gangway system is designed to operate. Therefore, a simulation model makes it possible that specific weather windows can be simulated (by adjusting the applied ship motions). This gives the possibility to test the gangway with the simulation model, even when the weather does not allow offshore tests (because of too small wave heights for example). This weather-dependency can cause a lot of time delay and decrease the economic profit of the company.

2.2.1 Proposed Solution and its advantages

The aim of this study is to develop a simulation model for the gangway system to simulate the AMC required to compensate wave induced vessel motions. It is proposed to develop a simulation model using software Matlab Simscape. The simulation study includes modelling the AMC system and all aspects of the gangway which influences the performance of the AMC. This model should be able to determine the power required by the gangway system, needed to compensate the motions in order to minimize the movements of the connection point during personnel transfer. Since Kenz Figee has performed several offshore tests with the real gangway, validation of the model can be done with the logged data recorded during these experiments. If the simulation model is validated, the gangway model can be subjected to different conditions (sea states, loads, design parameters etc.) which represent a real situation. The result of this simulation will represent the AMC of the gangway and the corresponding power. The development of such a model for the AMC system is of big interest to Kenz Figee because it will give the following advantages:

- A better insight in the behavior of the gangway system can be obtained
- The gangway system can be already tested in the design phase by simulation tests which will give an expectation of the behavior and makes cost savings possible
- The model enables to perform simulations in a wide range of the input parameters (ship motions). Different tests are possible and the influence of more design parameters on the performance of the AMC system can be investigated. Perhaps these insights indicate that it is more beneficial to adjust certain elements of the AMC or gangway design
- The current testing program is very confined by its feasibility, risk and duration. A simulation environment does generally not suffer from these restrictions. In the aspect of feasibility, simulation is very flexible
- The model can be used to gain more insight on improving the accuracy of the motion compensation. In the end this leads to a more efficient and safe personal transfer
- With the available model the company will be less weather-dependent
- If the model is accurate enough, less offshore tests will be required in order to certificate the gangway system which are time and costs demanding. So in the final end the model should save costs.

2.2.2 Conclusion and summary of problem and solution

In conclusion, the identified problem is the absence of a simulation model to predict the behavior of the active motion compensated gangway. This simulation model should also provide a good estimation of the required power for the AMC. Due to this missing model, designers are uncertain about the capability of the gangway to pass the tests, which are conducted after complete assembly of the gangway. So the biggest consequence of the missing model are the time and cost demanding offshore tests which have to be conducted after the design phase. It should also be noticed that during a test, a company is strong dependent on the weather which decides the sea state. Sometimes it could happen that the test cannot be conducted due to the missing waves. This means that certain working envelopes in which the gangway is design to perform are not present and the gangway cannot be certified. Therefore, a simulation model could save a lot of time and costs.

The simulation model should provide a better insight in the behavior and performance of the AMC gangway. The expectation is that this information can be obtained by simulation. In a simulation study the AMC and aspects of the gangway, which affect the overall performance, are modelled. This model can be validated by the logged data of the tests conducted in the past. Besides a solution to the main problem, simulation should also several additional benefits:

- Simulation would supply the designers with an extended insight on the AMC and its parameters with which the performance of the system could be improved.
- Simulation enables additional tests, even tests which would not be physically possible. Furthermore, is simulating less cost- and time-consuming than performing real tests.

2.3 Thesis Goal

Summarizing the previous section, we can reduce the thesis goal:

Development of a simulation (numerical) model of the gangway system, with which the required power for the active motion compensation can be estimated.

Based on this goal the research question is formulated:

How can the required power and accuracy for the active motion compensation system be determined in order to minimize the movement of the gangway tip?

To find an answer for above question, the following sub-questions help to reach the goal:

- In which sub-systems should the gangway system be decomposed?
- How should these sub-systems be integrated in the final model in order to control the two degrees of freedom (luffing and telescoping)?
- How much power does the hydraulic cylinders require to perform a luffing motion of 5 degrees (clockwise or counterclockwise)?
- How much power is required for the telescoping function in order to perform the motion compensation?
- How much oil is required for the hydraulic pumps to perform the motion compensation?
- How many accumulators are required for the power demand?
- How can the required amount of flow required for the luffing motion be determined and regulated by the PLC in order to compensate the gangway tip?

2.4 Thesis Approach

The approach used in this master thesis has the purpose to answer the main question and reach the thesis goal. The study is divided in five stages A, B, C, D and E. This five different stages include the following activities:

Stage A: Literatures Study, System Decomposition and Software Comprehension

Before starting with modelling of the gangway system a literature research has to be completed. First the current access systems in the offshore industry for wind turbine installation or oil- and gas platforms are reviewed. A comparison is made with the motion compensated gangway of Kenz Figee. In this stage a thorough study of the AMC has to be conducted and all sub-systems and main components have to be analyzed. After the literature study, a better understanding of the system (described in the previous chapter) is obtained and the research question (and sub-questions) and the thesis goals can be formulated which can be found in the previous sector. With the problem formulated, a system decomposition is made in chapter 4. The advantages and the disadvantages of the chosen solution, a simulation study, will be elaborated and examined in chapter 3. Final step in this stage is getting familiar with the software Matlab Simulink. A good software comprehension can be realized by watching tutorials, doing exercises and start with modeling of simple systems.

Stage B: Analyses and modelling of the structural/mechanical sub-system

In this stage a structural, static and dynamic analyses of the gangway system has to be conducted. A multibody model of the mechanical system is made and the corresponding equations of motion are determined. Based on this equations of motion the movements (displacements), velocities and acceleration of the gangway system relative to its mass and center of gravity are determined. In a later stage, these results will give a better insight in how the ship motions are translated to the motion of gangway tip, based on the RAO's of the vessel. The RAO's will be the input for the final model and will be provided by an external company. The mechanical sub-system is verified and validated by simple hand-calculations, static checks, analyses of the dynamic behavior by running the simulation etc. After the verification and validation, stage C can be started.

Stage C: Analyses and modelling of the hydraulic sub-system

After completion of the structural/mechanical sub-system, the actuation of this system has to be modeled. As described before, the AMC gangway system is an electrically/hydraulically system and the three degrees of freedom are performed by hydraulic actuators. Literature study has revealed that there are significant differences in power consumption of the three systems. The luffing system takes 56% of the total power for its account where the telescoping system consumes 36% and the slewing system only 8%. Because of this, the luffing system will be modelled as a detailed hydraulic model in contrast to the telescoping system which will be modeled as theoretical actuator only. During the modeling of the luffing system, the hydraulic diagram of the hydraulic cylinders will be analyzed carefully and all relevant hydraulic components such as directional (control) valves, pressure relief valves, compensators, accumulators, pumps will be modeled. As in stage B, the differential equations for the pressure and flow through the hydraulic components have to be determined. The hydraulic model will be based on these equations. At the end, the coupling of the dynamics of the hydraulics with the structural dynamics will play an essential role in obtaining an accurate simulation model.

Stage D: Analyses and modelling of the control sub-system

After completion of the hydraulic sub-system, the control sub-system will be considered. The system is PLC controlled which means that the actuators, responsible for the motion in the three degrees of freedom, are in connection with the PLC and receives signals from the encoders and sensors. The control of the gangway will be realized by a feedback loop on the position and a feedforward on the velocity of the gangway tip. The MRU measures the ship motion (displacement, rotation and

velocities) and will translate this into the motion of the gangway tip. Based on this signal the PLC will calculate the required compensation and convert this to the required actuator forces (pressures), displacements and velocities. Since control is a large field of technology and is a research field in itself, in this thesis the application of the control will be limited to a basic P-control.

Stage E: Integrating the sub-systems, estimation of the required powers and Validation of the model

After completion of the four stages, in the final stage the three sub-systems will be integrated in order to create an accurate simulation model. This is done in several steps, going from simplified to more complex. After each step the model is validated qualitatively and quantitatively. The validation is performed by comparing the predictions from the simulation with observations from experimental logged data. Based on this validation, points of improvements are addressed. A brief discussion indicates which points are implemented in the next stage of the model.

2.5 Thesis Outline

With the problem formulated, a solution is proposed. The advantages and the disadvantages of this solution will be elaborated. The chosen solution, a simulation study, is examined in chapter 3. Literature on how to perform a simulation study is reviewed. The result of the review is a stepwise plan to achieve an adequate simulation model. An approach is presented which is taken as guidance for the remainder of the research.
The subject of interest, a gangway system including the AMC system, is defined as a system and divided into subsystem in chapter 4. This is done to obtain a clear description and get a better understanding of the system and its sub-systems.

The described approach can be considered as an engineering design process which is an iterative decision making process. Basically, this thesis consists of two of such iterative processes in which the whole approach with the five described stages is completed: The initial 2D simplified gangway model which will be described in chapter 5 and the improved AMC gangway model including the hydraulic sub-system (luffing cylinders) which will be elaborated in chapter 6. In chapter 7 the coupling of the hydraulic sub-system with the mechanical sub-system in the simulation model will be elaborated on. In chapter 8, the control-sub system will be thoroughly discussed. The simulation model has to be subjected to given data of the ship motions to determine the power required by the gangway system. Boundaries are determined under the condition that the system is safe to operate. This will be discussed in chapter 9. In this chapter the constructed simulation model in which all three sub-systems are integrated will be validated with the logged experimental data.

The credibility of the model and its result is dependent on its sensitivity to parameter uncertainty. Based on the results of this analyses statements of the modelled credibility are done in chapter 10. Also the accuracy of the modelled system is determined using graphs, calculations and real data. In this chapter the research will be concluded with the conclusions and recommendations.

2.6 Coordinate Systems

In this thesis, three coordinate systems are used in order to describe the kinematics and dynamics appropriately. To distinguish all four of them, they are described separately in this section.

2.6.1 Global coordinate system

All local coordinate systems are implemented in one global earthbound coordinate system (XYZ). The local coordinate system of the gangway is placed in XYZ in a way that the origin of the gangway and XYZ are the same. The gangway is simulated as to be positioned on the vessel pedestal with the origin at the cross point of the vertical centerline and the horizontal USB line. Note in figure 2.1 that gravity is directed in negative Z-direction and the waterline is parallel to the X-direction and Y-direction.

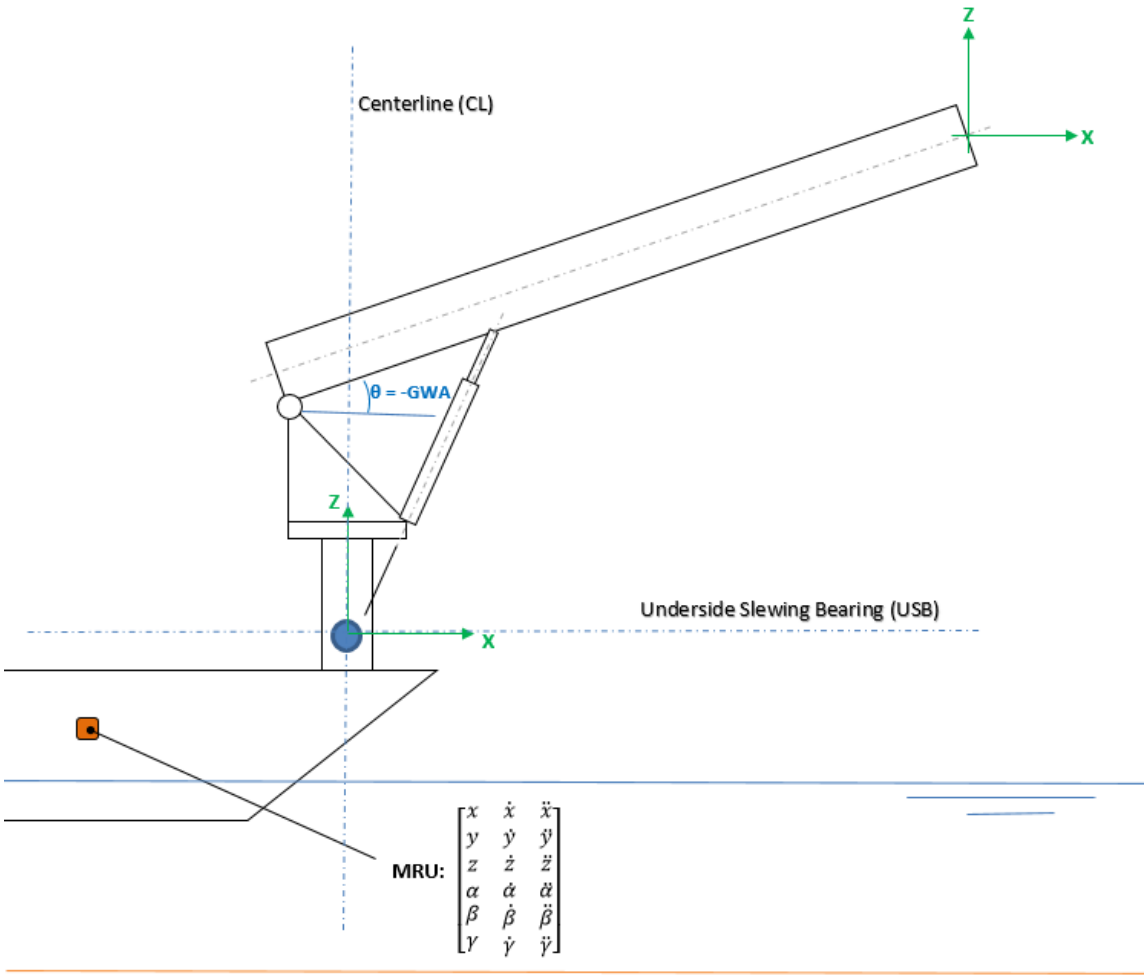

Figure 2.1 – 2D Representation (ZX-plane) of the gangway system in the global XYZ-coordinate system

2.6.2 Local coordinate system for the vessel

The origin in the local Cartesian coordinate system (xyz) of the vessel is at its After Perpendicular (AP). AP is defined as the intersection between the water line with the after-side from the straight portion of the vessel's rudder post (McGraw-Hill, 2002). The vessel motions are parallel to the axis of the coordinate system. The forward motion of the vessel (surge) is parallel to the x-axis. The motion directed to the port side (sway) is parallel to the y-axis and the motion lifting the vessel upwards (heave) is parallel to the z-axis. Besides the three translational degrees of freedom (DOF) also three

rotational vessel motions occur. Roll rotates about the x-axis, pitch rotates about y-axis and yaw rotates about the z-axis. In figure 2.2 the vessel motions at the center of gravity (COG) of the vessel are presented.

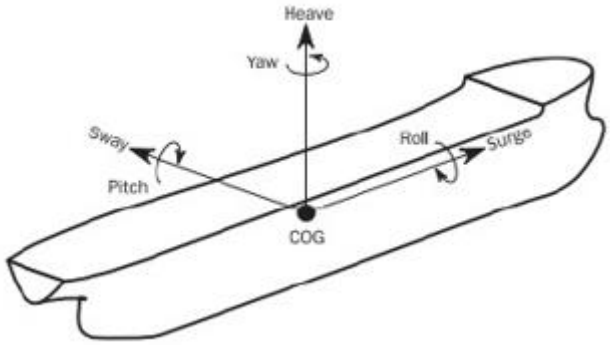

Figure 2.2 - Vessel Motions in six degrees of freedom at the center of gravity of the vessel

2.6.3 Local coordinate system for the gangway: Walkway frame

Because the gangway has always a certain luffing angle, the coordinate system for the gangway is described in a local walkway frame $X_WY_WZ_W$ which is a rotating coordinate system (figure 2.3). Since the numerical model is restricted to a 2D simulation, only the X_WZ_W – plane will be used. The positive X_W is always directed in the telescoping direction while the positive Z_{GW} is directed in the vertical upwards direction perpendicular to the telescoping gangway. Basically we have the following motions wich are actuated by the hydraulic actuators and controlled by the PLC:

- **Telescoping**: This is a translational motion (extension and retraction) in x-direction. With this motion only a displacement in the horizontal X_W-direction can be performed
- **Luffing**: rotation of the gangway around the pivot points on top of the mainframe. This is a motion in the XZ-plane and displacements in the global vertical Z-direction and horizontal X-direction can be performed
- **Slewing (not considered in this thesis)**: rotation around the centerline of the gangway. This is a motion in the XY-plane and displacements in the global X - and Y-direction can be performed.

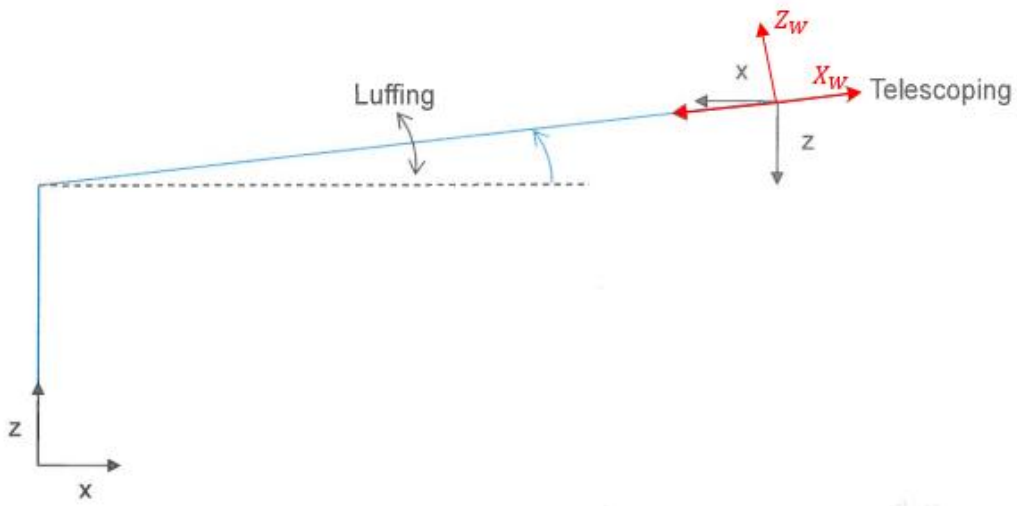

Figure 2.3 – Local $X_WY_WZ_W$ – coordinate system for the gangway: the Walkway frame

2.7 Scope of research and domain definition

The problem as defined in section 2.2 covers the P340 EH 16-26/1800 O.S. Retractable gangway, built for Siem Offshore Contractors GmbH for installation on service operations vessel Siddis Mariner. The load cases described by the DNVGL certification are not unambiguous since all kinds of environmental loads, off-and side lead angles are possible. For the full motion compensation, the bumper system is attached at the end of the telescoping gangway in order to reach a geostationary gangway tip when connection to the platform is made. This means that also the extra degrees of freedom of the bumper should be taken into account for simulating the full motion compensation. The problem thus covers a very large domain and is limited for this research based on two reasons. The first reason is to confine the time needed for the research. The total problem is considered to be too comprehensive to tackle within the regular timespan of a master thesis. The second reason is based on the availability of data. A simulation and its result are only of value if the model is validated. For the validation of a model, comparative data is required. The model can be considered valid within the domain it is validated in. Outside the domain it is not possible to validate the model. However, this does not mean that the model might not be of value outside the domain. When the model is found to be credible on certain areas outside the domain, useful information can be obtained from it. Later in this report, model validation will be explained more extensively (section 3.3.7)

Prior to this research a lot of offshore test were conducted at Kenz Figee regarding the performance of the AMC system. These tests and the recorded (logged) data determine the domain, for which the model can be validated in this research. An extended description of the tests can be found in Appendix A. In chapter 9, a comparison of the created numerical model with the experimental logged date will be provided.

The scope of this research is adapted to the available data and time. For simplicity the relevant components (mainframe, fixed- and telescoping gangway) are considered as rigid bodies and deflections of the structure will be ignored. The input of the system will be the ship motions induced by the waves. The numerical model is restricted to a 2D simulation. This means that there are 3 degrees of freedom which are the sway, roll and heave motion of the vessel (two translations and one rotation). Other possible inputs like wind, ice loads will not be considered. Since the bumper is also not part of this research, the thesis focus on the AMC system before the gangway tip is connected to the platform or wind turbine. So, in case the AMC is activated a certain reference point will be taken and the AMC will compensate the gangway to a certain range around this point. In the next sextion the value of the research, with the applied scope, is assessed.

Value of the research

In this section the value of this work is explained. By building the simulation program as proposed, it becomes possible to simulate the AMC system and estimate the required power for the actuators in order to minimize the motion of the gangway tip. Especially the required power for the luffing system will be of important interest since the amount of required accumulators can be deducted from this result.

Alongside this primary objective, the research will acquire more valuable information. After the simulation model is proven to be valid, a sensitivity analysis is performed on the model. With the outcome of this analysis insights are gained on the influence on the performance of the AMC system. By knowing the influence of important parameters, designers are given a handle to improve the AMC or gangway design.

This work might lay the foundations for an extensive research to the gangway's behavior in the different sea states and the influence on the response time. The model could be subjected to situations which simulate actual ship motions. One might also investigate the influence of the noise of the MRU on the performance of the gangway.

The simulation model of this research can also be taken as the basis for a more complex model in which more structural/mechanical, hydraulic and control components are taken into account. The model could also be extended with the bumper system. Such model can also be used to investigate the AMC in the hoisting mode or after positioning of the gangway tip against the platform.

3 Defining (Sub-) Systems

As the previous chapter explained, defining the system and its sub-systems is a task requiring some consideration. Well-made choices on the determination of each (sub-) system will improve the understanding of the whole. Also, with improved insight in the system, verification becomes more practicable. Therefore this chapter elaborates the total system and the sub-systems it incorporates. To adopt a systematic way of defining the (sub-) systems, they are described by the following respects:

- **Boundary** A way to distinguish the system from its environment. Only in- and outputs traverse this boundary.
- **Elements** The smallest parts considered by the modeler in view of its goal.
- **Behaviour** The way system reacts (changes its output) given a certain state and input.
- **Function** That what is brought about by an element to contribute to the goal of the total system
- **Tasks** That what needs to happen in order to realize the contribution such that the function is fulfilled

In the analysis performed in this research, no distinction is made between sub-systems and aspect systems. Looking at the gangway these two would have too much resemblance. The hydraulic system for example can be separated from the total with a physical boundary (sub-system). However, consists the hydraulic system also of all 'hydraulic' components of the total. The same goes for other sub-systems.

3.1 Defining Total System

3.1.1 Boundary

In figure 4.1 a schematic representation of the total system is shown. For the simulation model only the systems and the sensors are relevant to take into account. For the structural sub-system, a separation with the environment is made at the underside of the mainframe. The reason for this boundary is that for this simulation only the motion of the gangway is relevant. The transaction of the gangway with the ship will be modeled as an imposed motion due to the seat state at the underside of the pedestal at the MRU. This motion will be translated to the gangway tip. Another boundary is drawn at the Main Control Center. The user of the simulation can give input signals to the simulation through the boundary of the gangway control. The boundary at the gangway tip is an interaction point with the environment. The user of the simulation can define at which position in the global coordinate system this point is located. The output is data collected from all the sensors in the gangway by the PLC. The measured error and the calculated compensation signals in time are the most valuable of this data set.

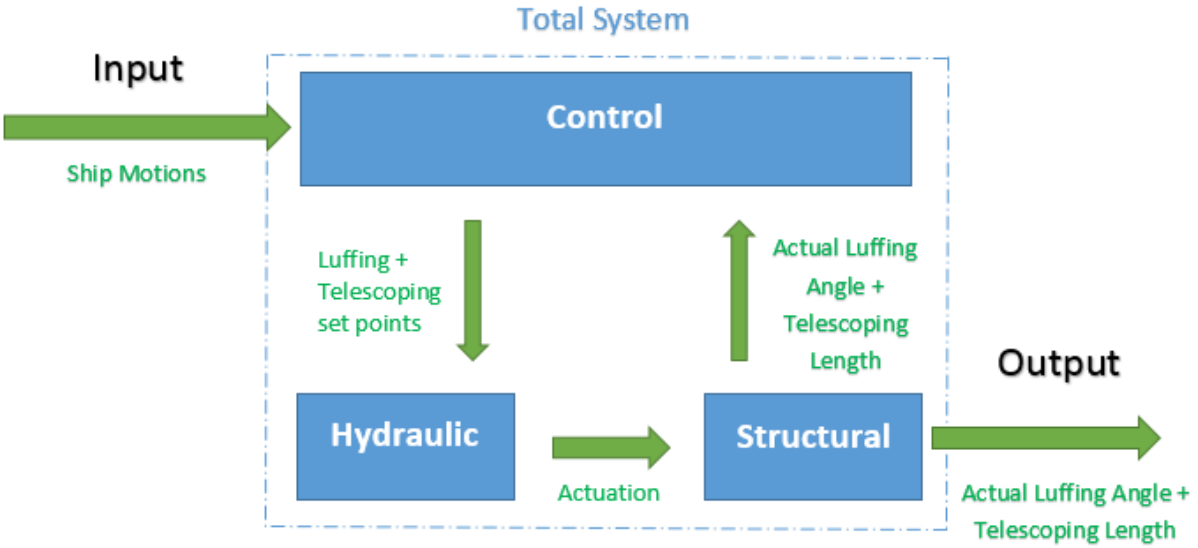

Figure 4.1 – Schematic representation of the total system and its sub-systems

3.1.2 Elements

A gangway includes many components, but of course not all have to be modelled. Since the behavior during AMC is studied, only the components, which have influence on this behavior, need to be considered. These elements are clustered such that sub-systems are formed. The separate sub-systems are discussed in sections 4.2 - 4.5. The coherence between the different components in the sub-systems is schematically depicted in figure 4.2

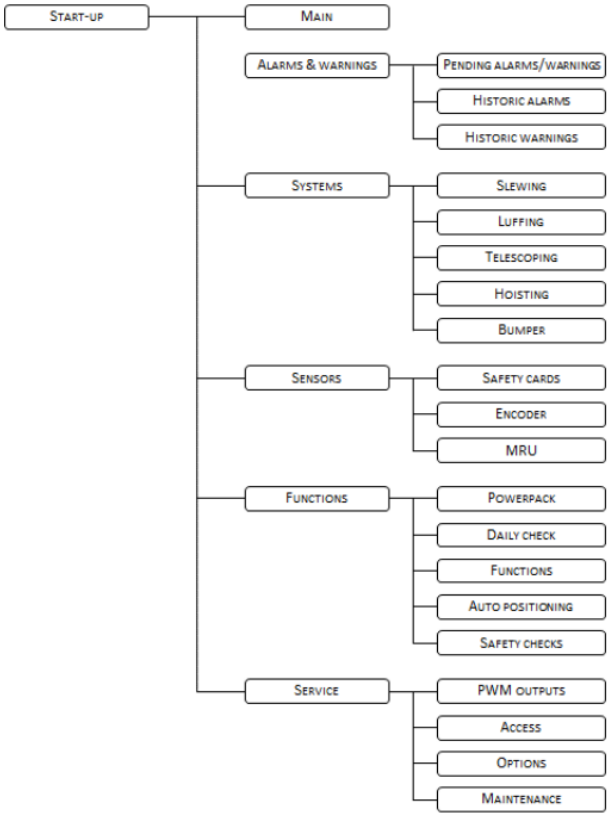

Figure 4.2 - Functional Description of the Total System

3.1.3 Behavior

Without actually specifying the inputs, the behavior of the gangway can be described. If the inputs are such the gangway is displaced (due to the ship motions), the gangway tip also displaces from its original (reference) position. With the AMC activated all sub-systems are put into operation such that the motion can be compensated. The dynamic response of the gangway to the motion compensation depends on the inputs which are the MRU signals. During operation the pressure and flow in the hydraulic actuators are controlled. The system outputs data from several sensors included in the system.

3.1.4 Function

The system is defined as the gangway with an activated AMC. In this analyses the function of the system can be described as follows: Mimic the behavior of the gangway when the AMC is activated.

3.1.5 Tasks

The tasks required to achieve the function are listed below:

- Continuously measuring the error and velocities of the gangway tip relative to its reference point and calculate the setpoint values for compensation
- In case the setpoint values are calculated, these signals actuates the luffing, telescoping and slewing functions in order to perform the required compensation motions.

3.2. Defining Structural Sub-System

3.2.1 Boundary

The structural sub-system is bounded such that it contains all structural components of the total system. The choice is made to cluster all the components that relate force to displacement, e.g. stiffness related parts. In the modelling stage of this research it will be beneficial to have these components grouped together. The boundary is drawn at the gangway tip like was described in 4.2. The boundary is also present in the interface between the mainframe and pedestal. Outputs of the structural sub-system are the displacements and velocities of the components.

3.2.2 Elements

The elements of the structural sub-system are depicted in figure 4.4. The structural system covers the mainframe, the cylinder which is divided in two sections, the fixed section and telescopic section of the gangway. The connection between the fixed section and telescoping section is at the winch.

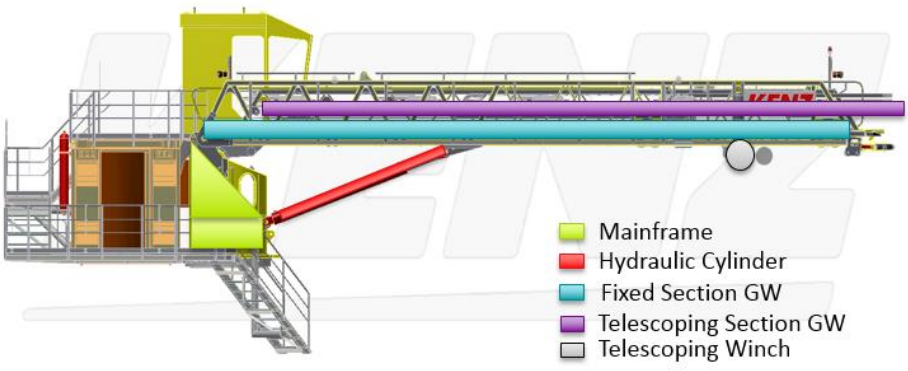

Figure 4.3 - Components of the Mechanical Sub-system

3.2.3 Behavior

The behavior of the structural sub-system is all about the relation between forces and displacements. An applied force on one of the elements will result in a movement and velocity of the element.

3.2.4. Function

The Function of the structural sub-system within the simulation is to mimic the forces and motions within the structural components of the actual gangway structure. The system should forward the correct forces/displacements to the driveline subsystem and load measurement to the control system. With the term 'driveline' the mechanical transition from the shaft of the hydraulic motor up to the rope leaving the telescoping winch is indicated. This sub-system will not be modeled explicitly but embodies all components which are involved with this transition. Inputs to this system are actuators which are controlled by the PLC. Outputs to this system are sensoring feeding information to the PLC. Examples of components which are belonging to the drive-line are the ideal rotational hydraulic actuators, gearboxes and splitter boxes. The function of the driveline sub-system is to transmit energy from the hydraulic system to the mechanical elements. A secondary function is to lock the drive line such that rotation of the winch is not possible.

3.3. Defining Hydraulic Sub-System

3.3.1. Boundary

The hydraulic sub-system is defined to contain all hydraulic components in the gangway. The boundary can thus be drawn around the collection of all the hydraulic components. Again, the clustering of the components by sort will benefit the modeling later on.

Transition to other sub-systems can be found on places with conversion to other physical quantities (mechanical or electrical). One of the conversion takes place at the shaft of the hydraulic motor. At that place there is interaction between the driveline and hydraulics. Another output of the hydraulic sub-system is the actuation of the parking and safety brakes, since these brakes are hydraulically powered. Pressure sensors are installed on several positions inside the hydraulic system. The readings of these sensors are considered outputs to the control sub-system.

For convenience, the main drive and the splitter box are added to the hydraulic sub-system. These two components drive the hydraulic pumps. Creating a separate sub-system for these mechanical elements would be unnecessary, while classifying them in the driveline sub-system would be illogical since they are not physically connected.

3.3.2. Elements

As said above, the hydraulic sub-system is composed of all hydraulic components. Like other sub-systems should the set of elements be limited to all elements which (significantly) effect the behavior of the gangway in the active motion compensation mode. To figure out which elements meet these requirements, the hydraulic-diagram of the gangway are referred to (figure 4.5). From these complex schemes important lines and components are addressed. Secondary lines serving for example the luffing system emergency cycles and auxiliaries are neglected.

The luffing movement of the gangway is actuated by two hydraulic cylinders, controlled by a servo control valve to control the speed and direction of rotation. The servo control valve works as a throttle valve, limiting the ingoing flow by luffing up and limiting the outgoing flow by luffing down.

The hydraulic parts that are included, are listed below and depicted in figure 4.5

- Luffing Pump
- Bladder Accumulators
- Hydraulic valves
- Pressure compensators
- Hydraulic pressure sensors
- Hydraulic lines
- Hydraulic Cylinders

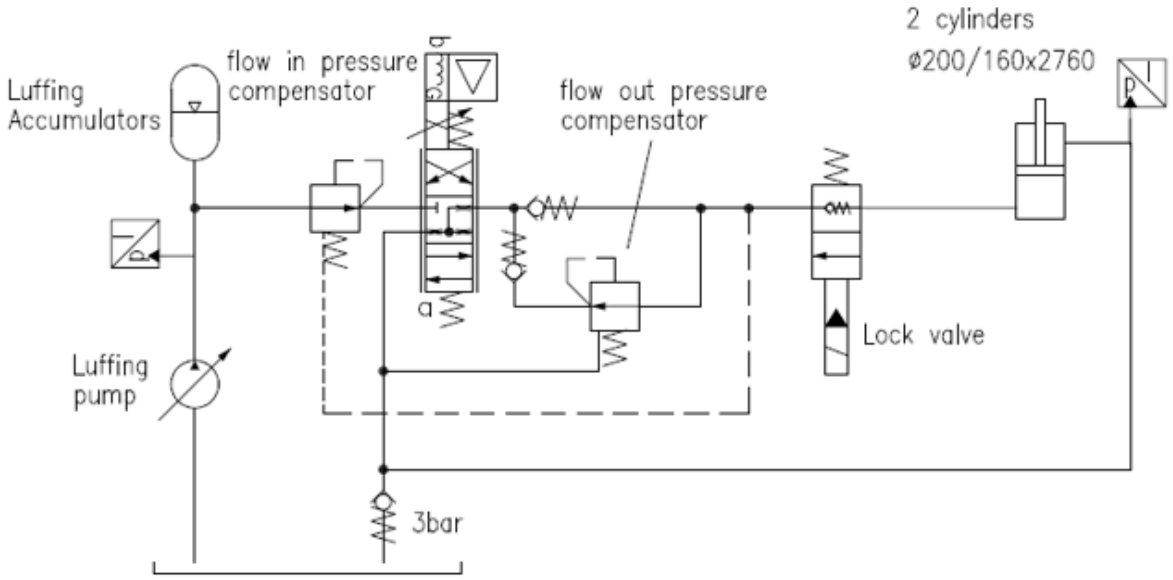

Figure 4.4 - Hydraulic Diagram, including the main hydraulic components for the Hydraulic Sub-System

3.3.3. Behavior

The main drive has a constant engine speed and is driving the hydraulic luffing pump. Since the input speed of the pumps remain constant, the displacement setting on the pumps determine what the flow rate of oil through the hydraulic system is. Given the flow rate the displacement setting on the motors determine the output speed of their motor shaft. Eventually, the output speed of the motor shafts depends on the displacement setting of both the pump and motor. The larger the pump displacement the higher the motor shaft speed. The larger the motor displacement the lower the motor shaft speed. The behavior of the rest of the system is determined by the proportional directional valve (servo valve), which is controlled by the PLC.

3.3.4. Function

The function of the hydraulic sub-system is to drive the hydraulic cylinder performing a luffing motion. For the hydraulic luffing system, all relevant hydraulic components are modeled.

3.3.5 Tasks

In normal operation, the hydraulic system should be controlled such that the desired transfer ratio from main drive to hydraulic motor is achieved. This is done by controlling the displacements of the pumps and the motors by means of joystick input. After the AMC is activated the pumps should be controlled by the PLC which translates the recorded displacements of the MRU sensors and encoders into the required pump displacements. In chapter 6 the hydraulic sub-system will be discussed extensively.

3.4 Defining Control Sub-System

3.4.1. Boundary

The boundary of the control system is determined to be at the transition layer between electrical to mechanical/hydraulic. All sensors and actuators in the system incorporate a mechanical/hydraulic and electrical part. The electrical part then belongs to the control system, while the mechanical/hydraulic part belongs to either the driveline-, structural- or hydraulic sub-system. One can say that through the boundary different physical quantities (displacement, force, pressure etc.) are converted to electrical signals containing information. The list of sensors thus represents the inputs to the system:

- MRU at the pedestal (measures the ship motion)
- MRU sensor at the gangway tip (measuring the displacement in 3 DOF)
- Encoder at the telescoping winch
- Encoders at the hydraulic cylinders (measuring the luffing angle)

The actuators represent the outputs of the system

- Pump solenoid (controlling the pump displacement)
- Motor Solenoid (controlling the motor displacement)
- AMC Valve (short-circuiting the hydraulic system)
- Pressure relief valve

3.4.2. Elements

The control system consists of all the sensors, actuators and PLC in the gangway. The control sub-system also includes all means of communication between the different sensors/actuators and the PLC, which are all hard wired.

3.4.3. Behavior

The behavior of the control system is equal to the gangway control software uploaded to the PLC. In the investigated gangway this is a lot of rather complex coding. These simplified logic rules, on which the AMC-part of the PLC is generally based on, will be discussed in detail in chapter 8.

3.4.4. Function

Controlling a set of actuators based on the information obtained from a set of sensors, such that the gangway compensates the wave induced vessel motion.

3.4.5. Tasks

A PLC works according standard method. It operates in cycles with constant cycle times. Each cycle is composed of the following steps:

- Scan all inputs, meaning that the values of all sensors are read out and stored in an array
- The program is executed, meaning that the sensor readings (inputs) are processed and outputs values are calculated with them.
- After the complete program is executed the outputs are set, meaning that the actuators are adjusted.

4 Initial Simplified Gangway Model

This chapter describes the first stage of modelling the gangway system. In chapter 4 the division of sub-systems was explained. From chapter 3 it is known that one can best start out with a simple model. Therefore, the initial model is strongly simplified. In this initial model the focus is mainly on the structural sub-system. Main objective of this model is to obtain more insight in the dynamic behavior of the structure. For the sake of simplicity the hydraulic cylinder is replaced by a torsional spring which is attached to the pivot point at the left side of the fixed section. This results in the following multi-body diagram:

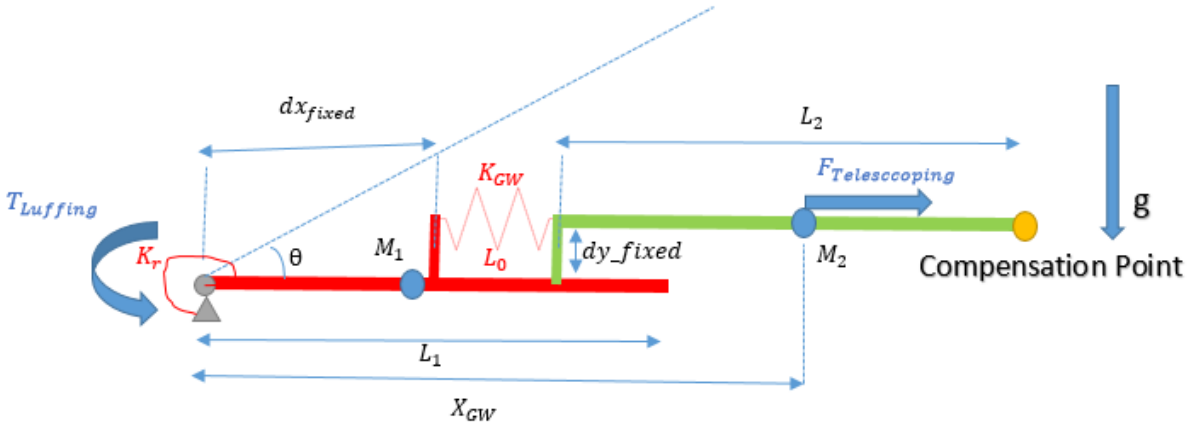

Figure 5.1 - Multibody analyses of the initial simplified gangway model

In this system the generalized coordinates are x_{GW} and θ. The first coordinate x_{GW} is the distance from the pivot point to the COG of the green telescoping part of the gangway. This coordinate is rotating with the gangway and points always in the direction of the telescoping gangway. The second coordinate θ is the luffing angle which indicates the rotating of the fixed section (red part) around the pivot point.

4.1 Dynamic Analyses

4.1.1. Derivation of the Equations of Motion

From Newton's law, and the Lagrangian Method the equations of motion of the simplified 2D system are determined. The system consists of two rigid bodies which mimics the fixed part (red) and the telescoping part (green) of the gangway. The telescoping section is connected to the fixed section through a rotational spring which is attached to the fixed section at a certain distance dx_{fixed} from the pivot point. By pulling this spring back or forth it performs the motion in the direction of the extending and retracting telescoping gangway. At the pivot point there is a rotational spring attached which replaces the hydraulic cylinders. At this point we put also a moment T_{Luff} as external load to perform the luffing (rotation around the pivot point). The rope stiffness is modelled as a translational spring which is attached to a fixed point of the fixed part of the gangway and constraints the telescoping gangway. After determining the potential energy and kinetic energy of the system the equations of motion of this system are derived according the Lagrange Method. The expressions for the potential and kinetic energy are:

$$V = \frac{1}{2}k_{GW}\left(x_{GW} - dx_{fixed} - L_0 - \frac{L_2}{2}\right)^2 + M_1 g\frac{L_1}{2}\sin(\theta) + M_2 g x_{GW}\sin(\theta) + M_2 g\, dy_{fixed}\cos(\theta) + \frac{1}{2}K_r\theta^2 \quad (5.1)$$

$$\mathrm{T} = \frac{1}{2}(I_{zz1} + I_{zz2})\dot{\theta}^2 + \frac{1}{2}M_2(\dot{x}_{GW}^2 + x_{GW}^2\dot{\theta}^2) \quad (5.2)$$

Where:

- M_1= Mass of Fixed section [kg]
- M_2= Mass of Telescoping section [kg]
- L_1= Length of Fixed section [m]
- L_2= Length of Telescoping section [m]
- L_0=unstretched spring length [m]
- k_{GW}= Translational Spring Stiffness (equivalent rope stiffness) $[\frac{N}{m}]$
- K_r= Rotational Spring Stifness $[\frac{Nm}{rad}]$
- I_{zz1}= moment of inertia of the fixed section around the pivot point $[\frac{kg\,m}{s}]$
- I_{zz2}= moment of inertia of the telescoping section around its COG $[\frac{kg\,m}{s}]$
- dx_{fixed}= horizontal distance from the pivot point at which the spring is attached [m]
- dy_{fixed}= vertical distance from the pivot point at which the spring is attached [m]

After substituting the expressions (5.1) and (5.2) in the Lagrange equations, the following equations of motion are obtained:

$$M_2\ddot{x}_{GW} - M_2 x_{GW}\dot{\theta}^2 + k_{GW}\left(x_{GW} - dx_{fixed} - L_0 - \frac{L_2}{2}\right) + M_2 g\sin(\theta) = F_{Telesc} \quad (5.3)$$

$$(I_{zz1} + I_{zz2} + M_2 {x_{GW}}^2)\ddot{\theta} + 2M_2 x_{GW}\dot{x}_{GW}\theta + M_1 g\,\frac{L_1}{2}\cos(\theta) + M_2 g\cos(\theta) - M_2 g\, dy_{fixed}\sin(\theta) \quad + K_r\theta = T_{Luff} \quad (5.4)$$

The model will be constructed simply from these expressions. In order to implement the equations of motion the blocks in the Simulink Library are used and inserted into the Simulink model.

4.1.2. Constructing the Model in Matlab Simulink

This set of system equations can now be represented graphically, without further manipulation. In figure 5.2 you can see the equations of motion presented graphically in a Simulink model. First step is to rearrange the two differential equations of motion in order to eliminate the two accelerations of the degrees of freedom. The first one is the acceleration in the direction of the telescopic gangway x_{GW}. The second the hook acceleration of the luffing angle θ. Rearranging the equations, the following equations are obtained:

$$\ddot{x}_{GW} = \frac{1}{M_2}\left(F_{Telesc} + M_2 x_{GW}\dot{\theta}^2 - k_{GW}\left(x_{GW} - dx_{fixed} - L_0 - \frac{L_2}{2}\right) - M_2 g \sin(\theta)\right) \quad (5.5)$$

$$\ddot{\theta} = \frac{1}{(I_{zz1}+I_{zz2}+M_2 x_{GW}{}^2)}\left(T_{Luff} - 2M_2 x_{GW}\dot{x}_{GW}\theta - M_1 g\,\frac{L_1}{2}\cos(\theta) - M_2 g\cos(\theta) + M_2 g\, dy_{fixed}\sin(\theta) - K_r\theta\right) \quad (5.6)$$

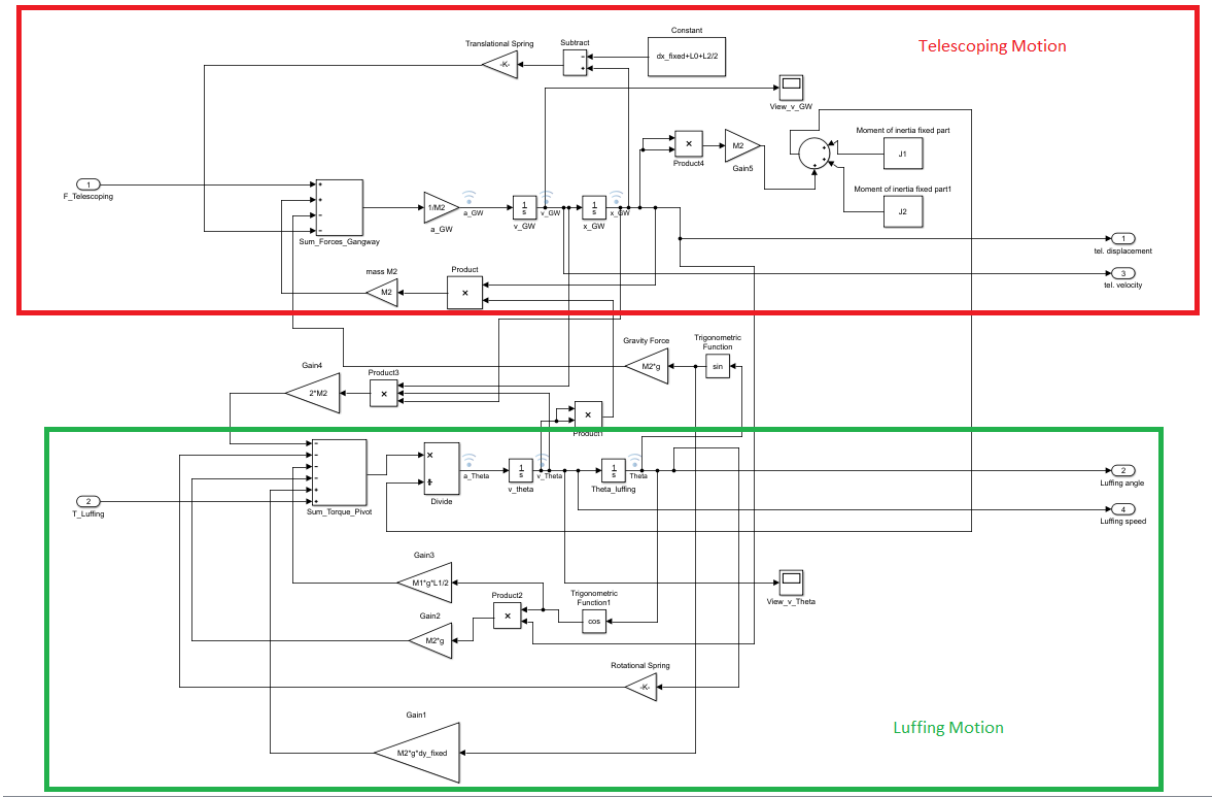

Figure 5.2 - Equations of motion modeled in Simulink

In appendix D, the construction of these two equations in Simulink is described.

4.1.3. Dynamic Analyses of the initial simplified model

After modeling the equations of motion in Simulink also an animation of the gangway motion can be made by importing the numerical solutions of these equations in the workspace and process them in a script (Appendix C). From the Simulink model also an analyses of the dynamic behavior can be realized. After linearization of the coupled non-linear second order differential equations, the eigenvalues and eigenvectors can be obtained. Analyzing this initial model we can distinguish two different modes: the 'telescoping mode' and the 'luffing mode'. Each mode has its own natural frequency. Based on the current parameters, for the telescoping mode the natural frequency is:

$$\omega = \sqrt{\frac{k}{m}} = \sqrt{\frac{k_{GW}}{M_2}} = 4.24\ [\frac{rad}{s}] \qquad (5.7)$$

In the luffing mode the natural frequency varies in the time because during the luffing (rotation around the pivot point) the telescoping section is moving (vibrating) which influences this luffing motion.

In figure 5.3 an animation of the final configuration of the initial gangway model is shown. Also the initial conditions which are applied on this model are presented next to the configuration. In figure 5.4 the results for the luffing and telescoping motions are shown.

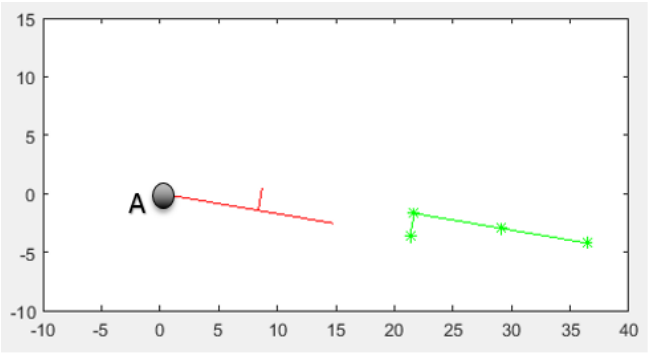

Initial conditions:
Theta0 = 15 deg
X_GW= 0
V_Theta= 0
V_X_GW= 0

Figure 5.3 - Animation plot of the simplified initial gangway mode

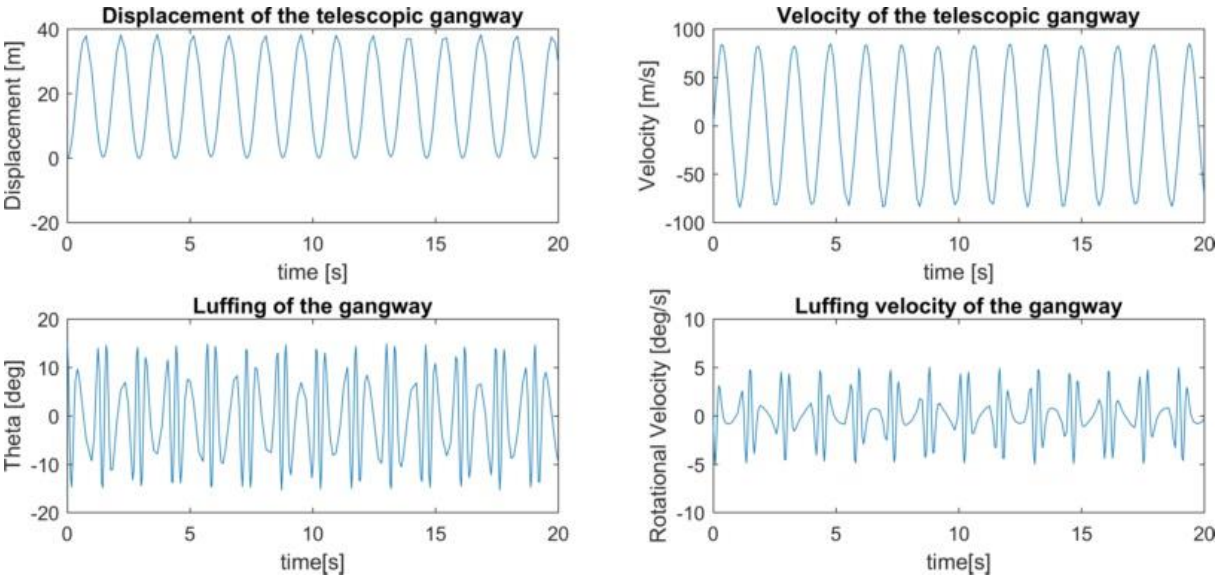

Figure 5.4 – Telescoping displacement (top left), telescoping velocity (top right), Luffing (bottom left) and luffing velocity (bottom right) of the initial simplified gangway model.

4.2 Construction of the initial model in Simscape

For the verification of this Simulink model, exact the same system is built in Simscape. The big difference between Simulink and Simscape is that in Simscape it's not required to derive the equations of motion. By connecting the different components (blocks) the system is created and the equations which describes the dynamics will automatically be developed. Each physical phenomenon can be modeled by choosing a block from the library browser which has the same physical properties and is based on the same physical equations. So when using Simscape, the equations which are required to describe the system are already included in the blocks and if the blocks are connected in the right way the model will generate automatically the right equations of motion. Furthermore, if you run the Simscape model an animation plot will automatically be generated. So, in contrary to Simulink environment, there is no specific code required for the animation of the system during the simulation. In figure 5.5, the Simscape model is shown and in figure 5.6 the automatically generated animation plot is presented

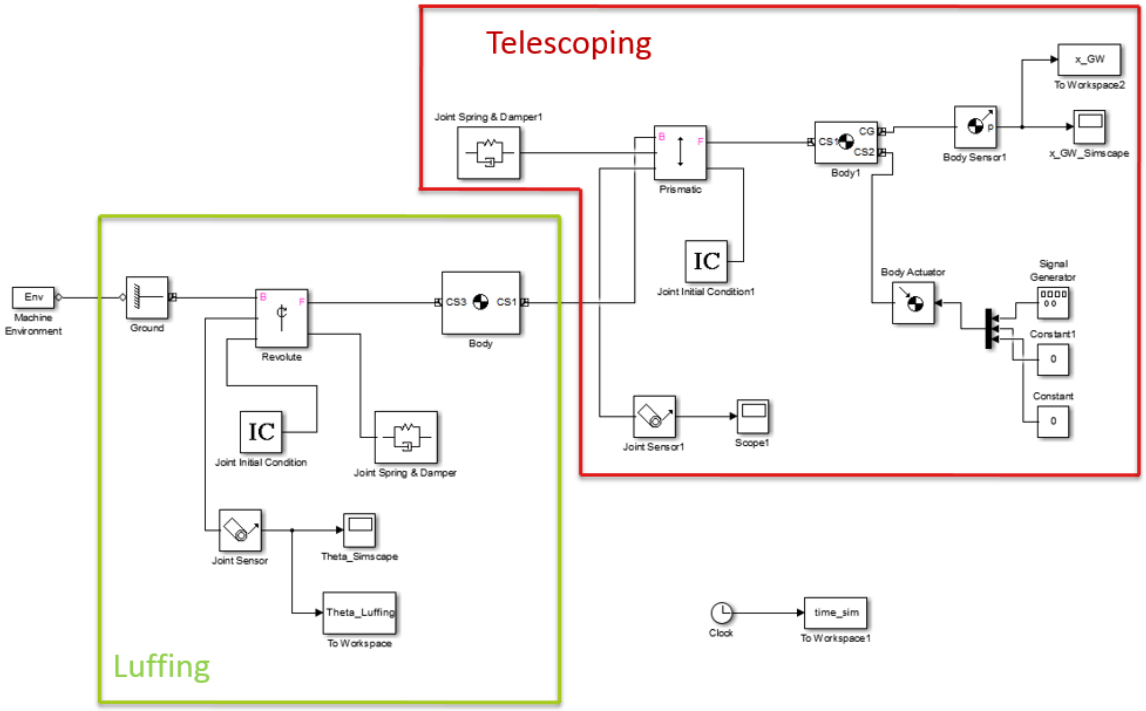

Figure 5.5 - Simscape model of the initial simplified gangway model

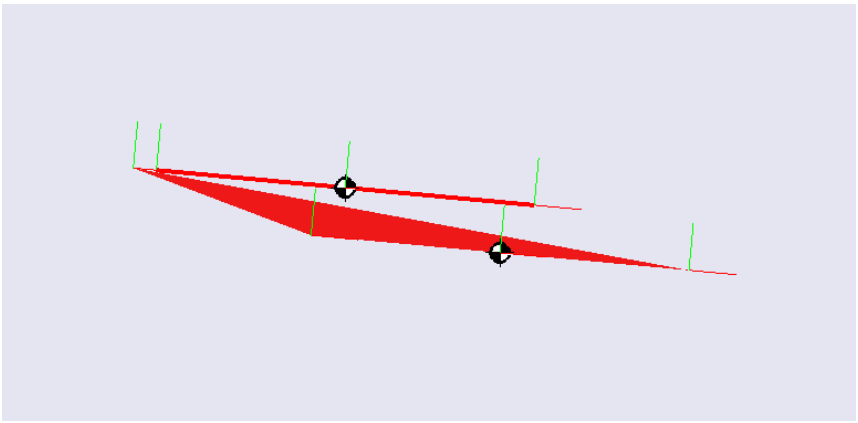

Figure 5.6 - Automatically generated animation plot of the Simscape model

4.3 Verification of the equations of motion with the Simscape Results

After completion of the Simscape model the results are compared with the Simulink results. The telescoping motion and the luffing motion are considered separately. In figure 5.7 below you can see that for the telescoping motion the graphs corresponds quite well. For the Luffing motion the behavior also corresponds well, but there is a little delay of the Simscape results with respect to the Simulink model. Based on this analyses we can assume that the derived equations of motion are correct and the structural sub-system can be used as reference model for further improvements and addition of the hydraulic and control sub-system.

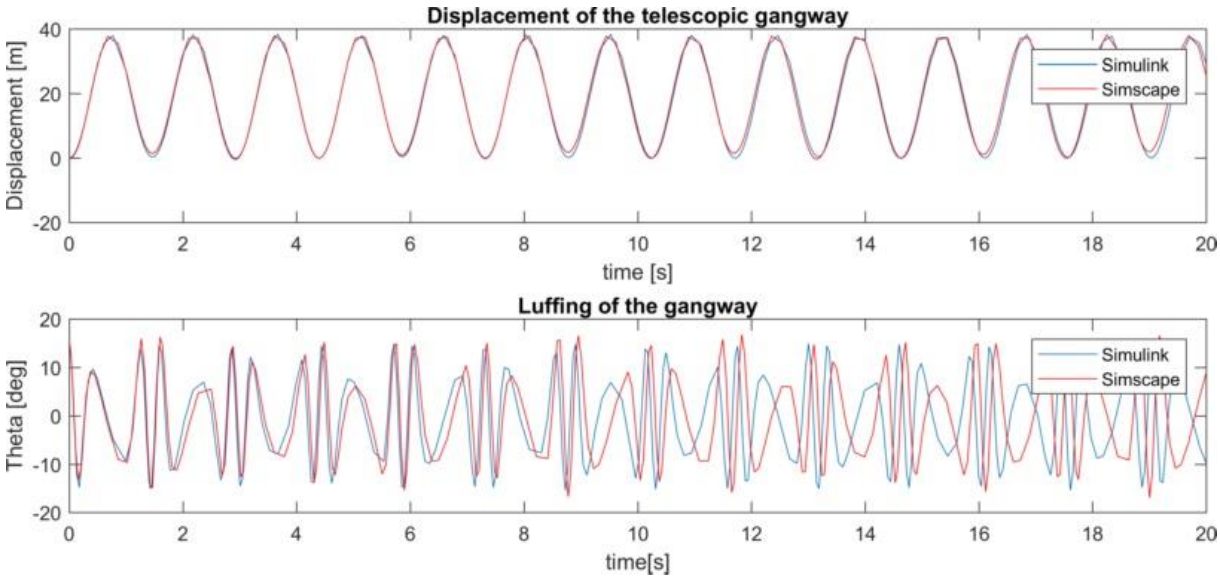

Figure 5.7 – Comparison of the telescoping and luffing motion modeled in Simulink and in Simscape

4.4 Addition of a basic control sub-system to the Simulink model

After the verification of the equations of motion a first step can be made in modelling the AMC (control sub-system). In order to build a feedback or feedforward loop which is required for the compensation of the gangway model, the excitation of the gangway itself has to be modelled. An external moment is applied from 5 – 6 seconds of the simulation time. This is a strong simplified representation of the ship motions which result in the displacements of the gangway. The short term of this 'disturbance' is just to see how the model reacts and if the compensation is performed as quick as possible. In figure 5.8 you can see how the feedback and feedforward is applied on the initial gangway model. The gangway model has in total four output variables:

- θ = The luffing angle [deg]
- $\dot{\theta}$ = Luffing velocity [deg/s]
- x_{GW} = Telescoping position [m]
- $\dot{x}_{GW}$ = Telescoping velocity [m/s]

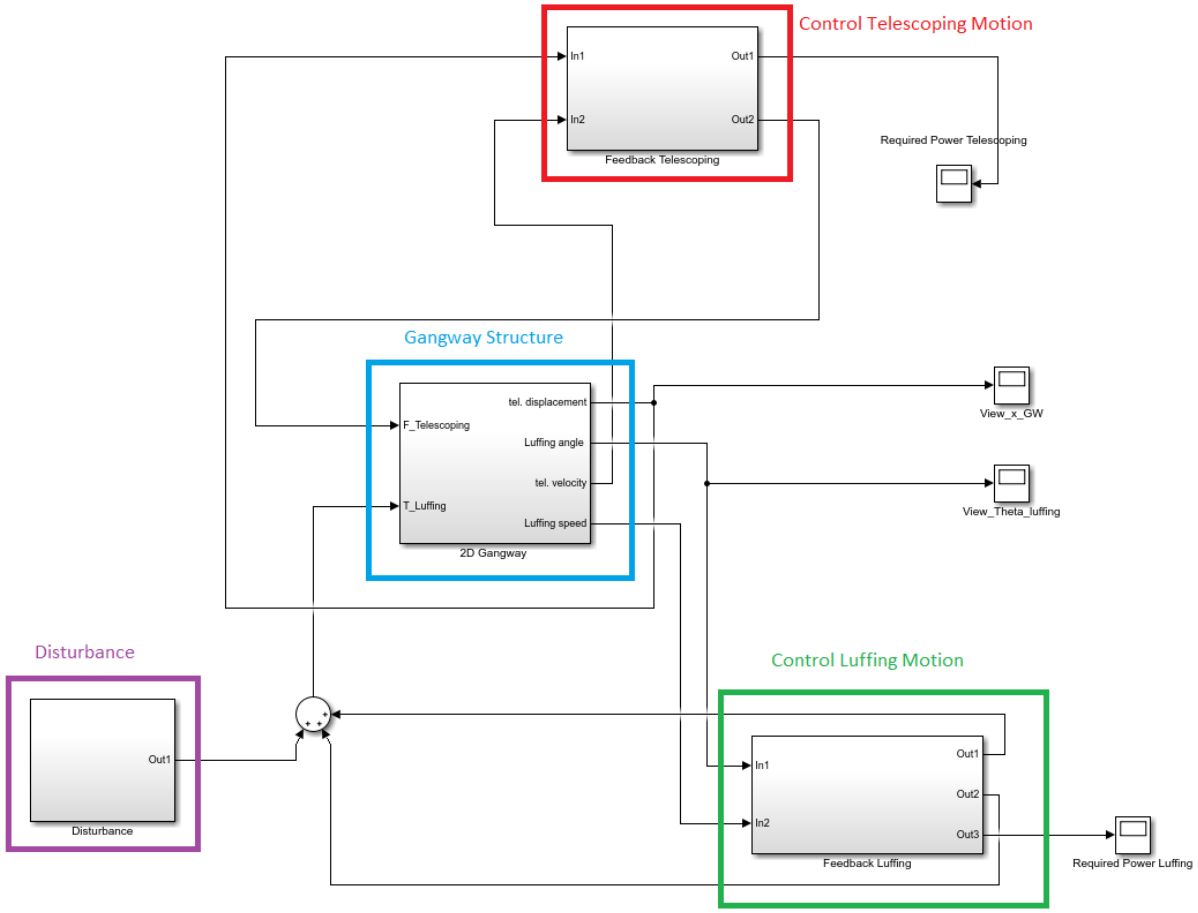

Figure 5.8 – Simulink model of the initial simplified controlled gangway model

First goal is to compensate the gangway to a reference point. For example we choose the reference point as the position of the gangway tip if the gangway is in the horizontal configuration and has a telescoping length of 17.5 m. So the reference points from which the error will be calculated by subtracting the output values are:

- $x_{GW}ref = 17.5 \quad [m]$
- $\theta_{ref} = 0 \quad [deg]$

The feedback is performed by multiplying the calculated error with a constant gain which will give the value of the actuation force that is required for the compensation motion. In this simple case of the simplified initial model this gain is equal to the translational and rotational spring coefficient. Besides the feedback, also a feedforward on the output velocities is essential for the motion compensation. This has to do with the kinematic forwards which has to be included in the control sub-system. The kinematic forwards can be considered as a prediction of the new position of the gangway tip. This is required information because if this signal lacks, the compensation will always have a delay. This is due to the fact that the feedback only compensates the position at the specific time step if it's in rest but is not able to compensate the position if the gangway is in motion with certain velocity. In figure 5.9 the results of this feedback and feedforward are shown.

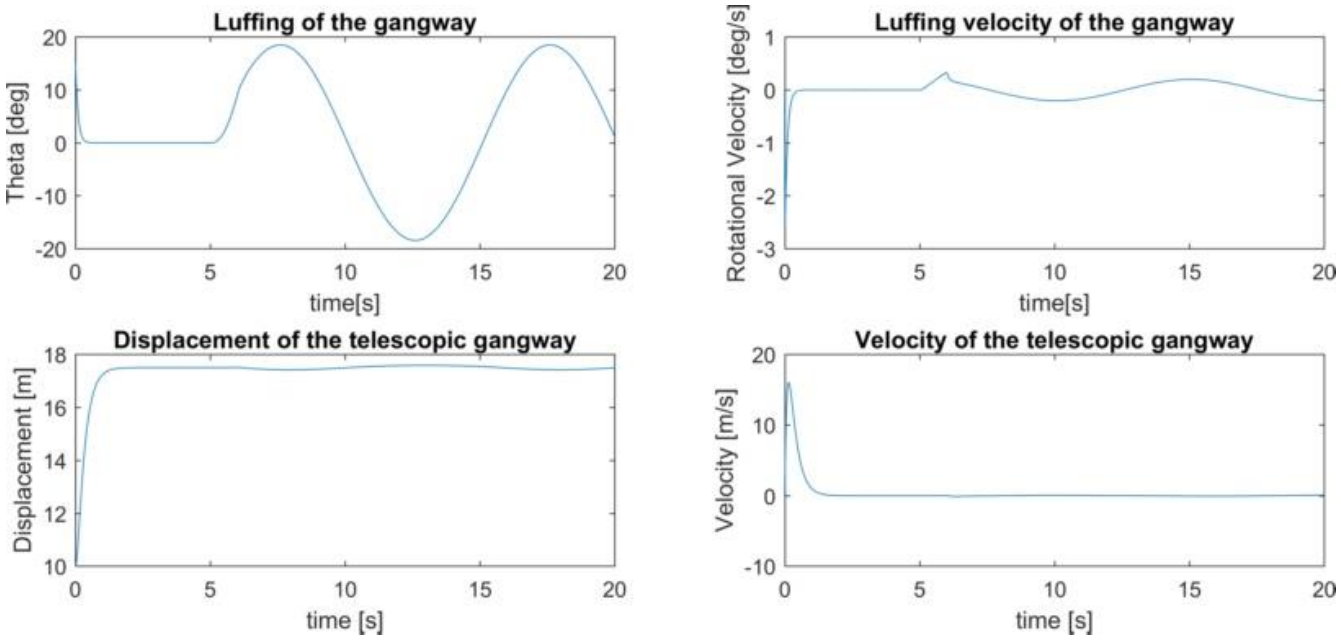

Figure 5.9 – Luffing (top left), Luffing velocity (top right), telescoping displacement (bottom left) and telescoping velocity (bottom right) after applying the feedback and feedforward loop in order to compensate the gangway to the reference configuration.

A first conclusion we can make is that the applied control seems to compensate the gangway and makes sure the gangway tip will always be moved to the reference point. From the graph of the luffing angle, the disturbance at 5 seconds is obviously visible but after a few seconds the gangway tip moves back to the reference point. If we consider the telescoping motion we don't see a big disturbance which means that this function has a smaller response time.

With the obtained results also a first estimation of the required power can be done. The two basic equations which can be used to calculate the required power for the described compensation are:

- $P_{telesc} = F_{telesc} \cdot \dot{x}_{GW}$ (5.8)
- $P_{Luff} = T_{Luff} \cdot \dot{\theta}$ (5.9)

4.5 Conclusion initial simplified model

In this chapter we went through the process of conceptual modelling of the system and a better insight in the mechanical behavior of the gangway is obtained. An important outcome is that the two degrees of freedom luffing and telescoping are not independent. From the equation of motion we can see that the dynamics of the total system is a result of the coupling of this two motions. They influence each other and this coupling make the system more complex than a usual dynamic system. The basic equations for the structural and control sub-system are treated. Also a better feeling of how the feedback and feedforward can be applied on the gangway which is motion induced through an external moment. In the next chapter this initial model will be extended by adding the detailed hydraulic luffing sub-system.

5 Modeling the Hydraulic Luffing Sub-System

In the process of modelling the hydraulic luffing sub-system a simplified hydraulic diagram as shown in figure 6.1 is proposed as the basic model. This diagram will be discussed extensively in section 6.2. In this chapter all relevant hydraulic components will be discussed. The function, the physical theory behind its behavior, physical explanation of its task will be covered. Also the settings for all the block parameters will be given and the source where it comes from. Often these settings have to be calculated, deduced from characteristic charts, or searched for in the documentation. All relevant hydraulic blocks will be modeled and connected in the right way such that the hydraulic sub-system is able to perform its function: actuating and controlling the piston of the hydraulic cylinder in order to reach the desired luffing motions.

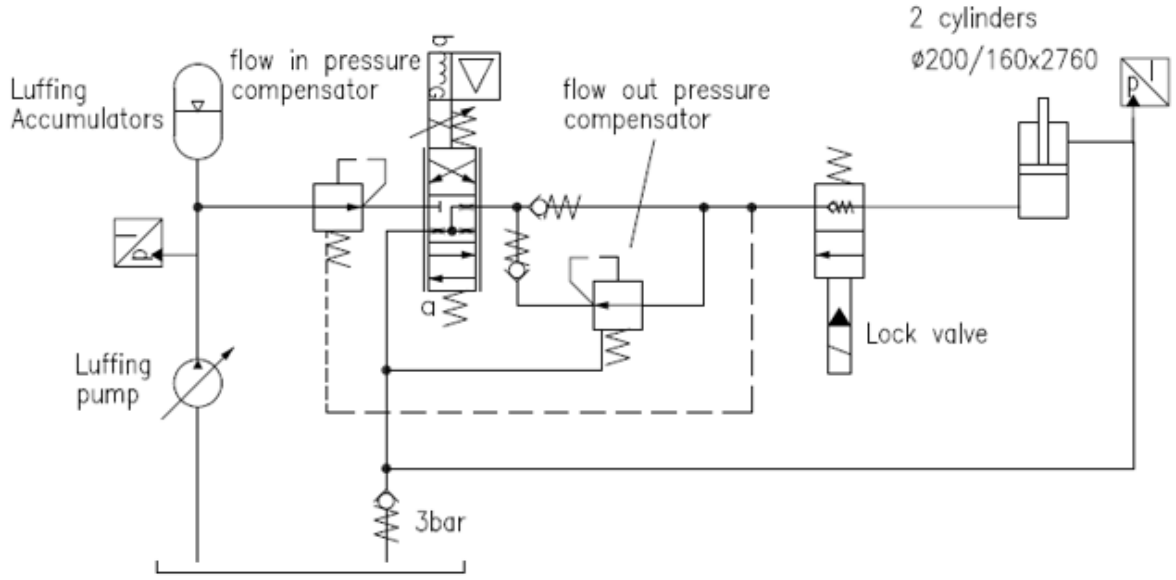

Figure 6.1 - Simplified Hydraulic Luffing diagram

5.1 Hydraulic model conventions

Before starting with the process of modelling, first some key parameters in the hydraulic domain are highlighted:

- Q = Flow through the hydraulic components [m^3/s]
- P = Pressure/Pressure drop in/over the hydraulic components [bar]
- X = Position of the piston of the cylinder [m]
- V = Velocity of the piston of the cylinder [m/s]
- ω = Rotational speed of the luffing pump [rad/s]
- A = Passage Areas of the valves/orifices [m^2]

The output of the hydraulic sub-system is the displacement X and velocity V of the piston. In order to get the right output values which are required for the motion compensation, it's essential to control the flow through and pressure in the cylinder. The component which controls these parameters is the proportional directional (servo) valve. This component is also the connective part of the hydraulic sub-system with the control sub-system. The servo valve regulates the amount of flow through the system while the pressure is kept constant. The constant pressure network is realized by the two pressure compensators: one pressure compensator for the luffing-up motion and the other for luffing-downwards motion.

5.2 Process of modelling the hydraulic luffing sub-system

Main challenge in the process of modelling the luffing components is choosing the corresponding block for each hydraulic component in the toolbox of the Simscape Library and give them the right settings for the parameters. After choosing the right tool it's task to give this block the settings which will result in a physical behavior which comes as close as possible to the real used components in the gangway design. Sometimes the setting can be simply copied from the manual but verification checks by doing simple hand calculations and filling in the basic equations are necessary in order to build a model that is accurate. In figure 6.2 for each hydraulic component the corresponding block from the toolbox which is used for the model is indicated. In figure 6.3 the construction of the hydraulic luffing system in the Simscape environment is shown. The lock valve will not be considered because it has no influence on the motion compensation.

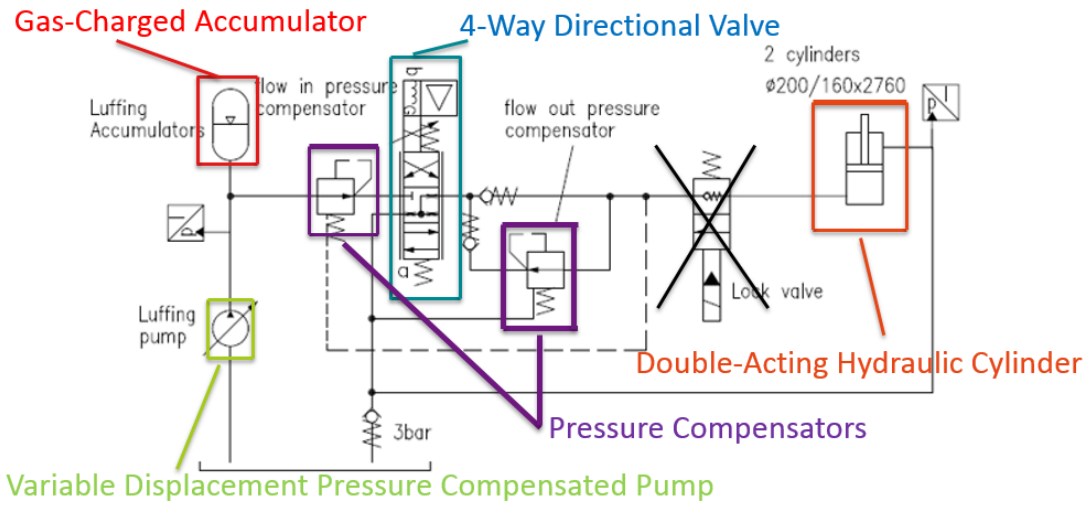

Figure 6.2 - Indication of the chosen blocks for modeling the corresponding component

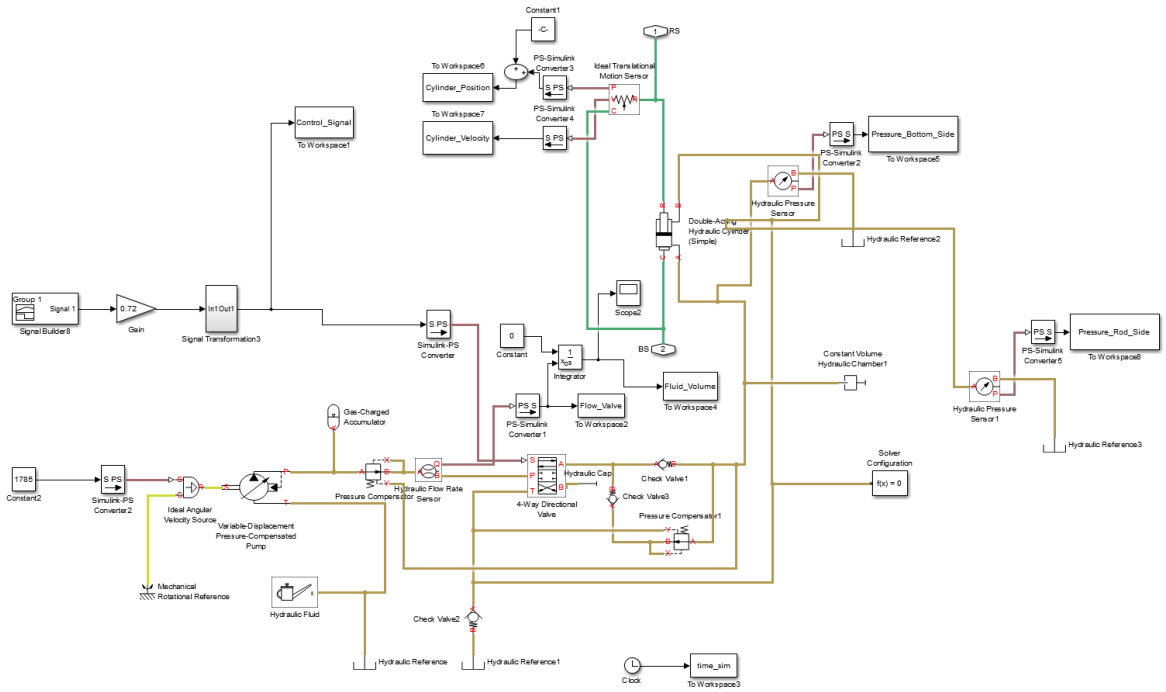

Figure 6.3 - Created Simscape model of the hydraulic luffing sub-system

5.2.1. Assumptions and starting conditions

The main physical behavior which has to be modelled is a constant pressure network. This is required in order to be able to regulate the flow. To realize this constant pressure we will assume a variable displacement pump which will keep the pressure in the system at 300 bar. Furthermore, the energy losses in the ideal electromotor and variable displacement pump will be neglected. Also the leakages in the valves will be kept as small as possible to make sure that more or less all the flow from the pump and accumulators will reach the cylinder.

5.2.2. Modeling the hydraulic cylinder

In figure 6.4 you can see the hydraulic cylinder which is used in the assembly of the gangway. In the real gangway system two of this cylinders are used parallel to support the fixed section and to perform the luffing motion. To keep the simulation model as simple as possible we only model one cylinder with the total surface bottom area which equals two times the surface area of one hydraulic cylinder.

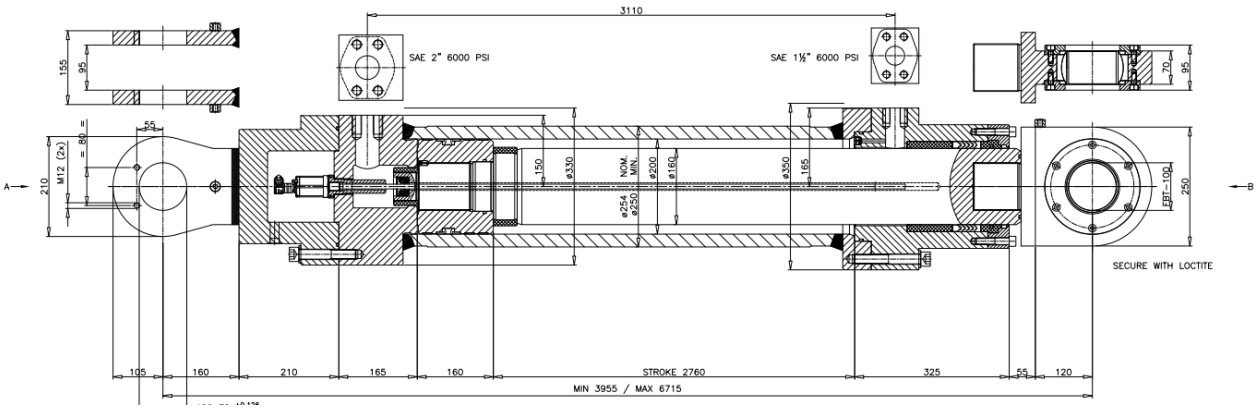

Figure 6.4 - Hydraulic cylinder used in the gangway design

Figure 6.5 - Double-Acting Hydraulic Cylinder from the Simscape Library toolbox

The hydraulic cylinder is a modeled as a Double-Acting Hydraulic Cylinder block (see figure 6.5). The Double-Acting Hydraulic Cylinder is developed for applications where only the basic cylinder functionality must be reproduced, in exchange for better numerical efficiency. For these reasons, such factors as fluid compressibility, friction, and leakages are assumed to be negligible. The hard stops are assumed to be fully inelastic, to eliminate any possible oscillations at the end of the stroke. The model is especially suitable for real-time and HIL (hardware-in-the loop simulation, if such simplifications are acceptable). The model block is described with the following equations:

$$F = A_A \cdot p_A - A_B \cdot p_B - F_c \quad (6.1)$$

$$q_A = A_A \cdot v \quad (6.2)$$

$$q_B = A_B \cdot v \quad (6.3)$$

$$\frac{dx}{dt} = v \quad (6.4)$$

$$v = v_R - v_C \quad (6.5)$$

$$F_c = (x - x_E) \cdot K_p \cdot v \qquad if\ x > x_E, \quad v > 0 \quad (6.6)$$

$$F_c = (x - x_R) \cdot K_p \cdot v \qquad if\ x > x_R,\ v > 0 \quad (6.7)$$

$$F_c = 0 \qquad otherwise \quad (6.8)$$

$$x_E = S - x_0 \quad (6.9)$$

$$x_R = -x_0 \quad (6.10)$$

Where:

F = Force developed by the cylinder	[N]
v = Cylinder rod velocity	[m/s]
v_R, v_C = Absolute velocities of cylinder rod and cylinder case, respectively	[m/s]
A_A = Piston area at port A side	$[m^2]$
A_B = Piston area at port B side	$[m^2]$
p_A = Pressure at the cylinder port A	[bar]
p_B = Pressure at the cylinder B	[bar]
q_A = Flow rate through port A into the cylinder	$[\frac{m^3}{s}]$
q_B = Flow rate through port B from the cylinder	$[\frac{m^3}{s}]$
x = Piston position	[m]
x_0 = Initial distance between piston and cap A	[m]
F_c = Hard stop force	[N]
x_E = Distance the piston can travel to fully extend from initial position	[m]
x_R = Distance the piston can travel to fully retract from initial position	[m]
K_p = Penetration coefficient	[-]
S = Piston stroke	[m]

Connections R and C are mechanical translational conserving ports corresponding to the cylinder rod and cylinder clamping structure, respectively. Connections A and B are hydraulic conserving ports. Port A is connected to chamber A an port B is connected to chamber B. In this Double-Acting Hydraulic Cylinder the friction between moving parts is not taken into account. Also the fluid compressibility and the inertia effect are not taken into account.
The hydraulic sub-system should be designed such that the design criteria of the maximum speed of the cylinder piston can be achieved. This maximum speed is set on a value of 0.24 m/s. In order to design the model we start from the following cylinder design values:

- $A_{bottom} = 0.0628$ $[m^2]$
- $v_{piston} = 0.24$ $[\frac{m}{s}]$
- $Stroke\ Length\ Piston = 2.76$ $[m]$

Given the dimensions of the cylinder the required maximum flow in case of maximum speed can be calculated:

$$Q_{bottom} = A_{bottom} \cdot v_{piston} = 0.015072 \text{ [m}^3\text{/s]} = \mathbf{905 \text{ [l/min]}} \qquad (6.11)$$

5.2.3. Modeling the Proportional Directional Servo Valve

The servo valve is the core of the hydraulic sub-system and makes sure the flow through the cylinder is exactly the amount of flow which is required for the motion compensation. In figure 6.6 the servo valve used for the luffing hydraulic system is shown. The servo valve consists of three main assemblies: the pilot valve, main stage and trigger electronics. A detailed functional description can be given but in this thesis we are only interested in the relation between the control signal on the control member displacement, which decides the passage area of the valve, and thus the flow through this valve.

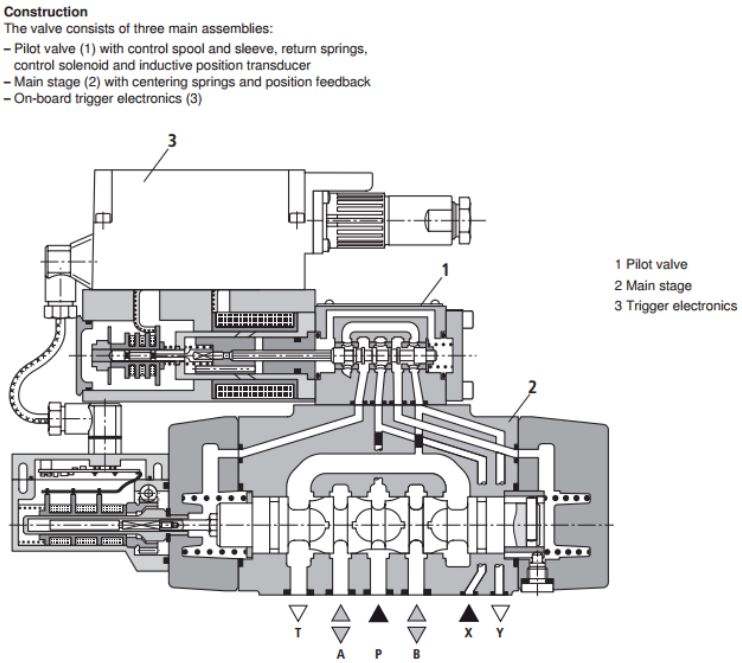

Figure 6.6 - Servo (proportional directional) valve that is used in the gangway design [Reference: Bosch Rexroth]

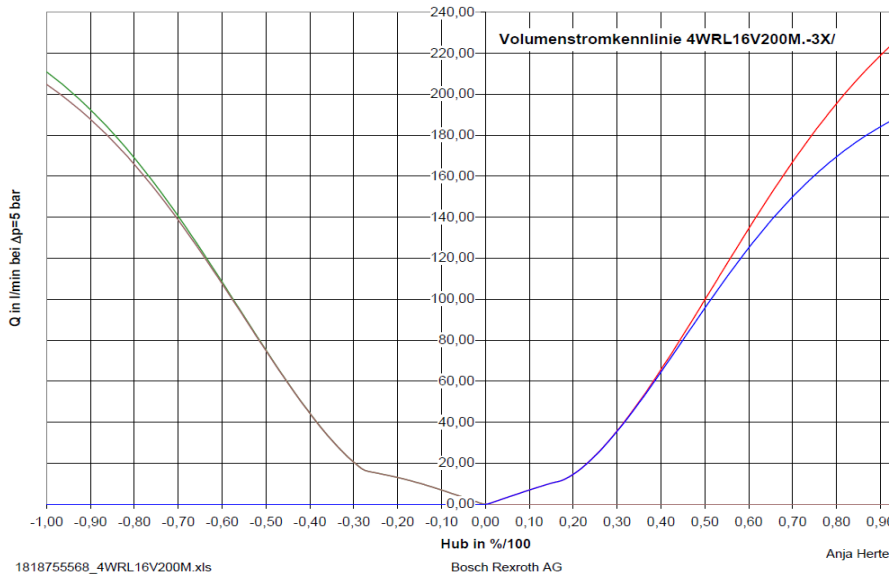

Figure 6.7 - Curve for the relationship between the flow through the servo valve and the applied control signal [Bosch Rexroth]

In figure 6.7 the curves represent the characteristic property of the servo valve. There are 4 different curves. The red curve corresponds with the flow through variable orifice P – A (see figure 6.10), the blue curve corresponds with the flow through variable orifice P – B, the green curve with B – T and the pink curve with A – T. For the luffing system only the P – A curve which is used for the luffing up motion and the A – T curve which is used for the luffing down motion are simulated for the servo valve. It's clear that there is a non-linear relationship between the set point (electrical control signal that actuates the control member displacement of the valve) and the flow through the valve. The block that is used to model the valve in the model (figure 6.8) is a linear valve. In order to obtain the same non-linear behavior of the valve, the input signal (which is the control signal) is pre-processed before it goes into the valve. In figure 6.9 you can see the transformed non-linear yellow signal against the linear pink line. This transformation is realized by dividing the domain of the control signal in four 'linear sections', each with its own slope that fits the best with the gradient of the real curvature. In this way, the physical property of the valve is modeled more accurate and a better simulation can be done. In figure 6.9 it can be noticed that the A – T curve is modeled with a negative sign since a negative control signal should result in a luffing down motion which is performed by a negative flow.

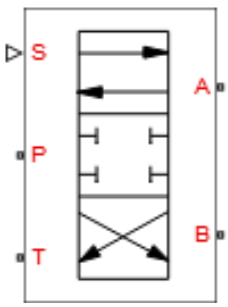

Figure 6.8 - The 4-Way Directional Valve from the Simscape Library toolbox

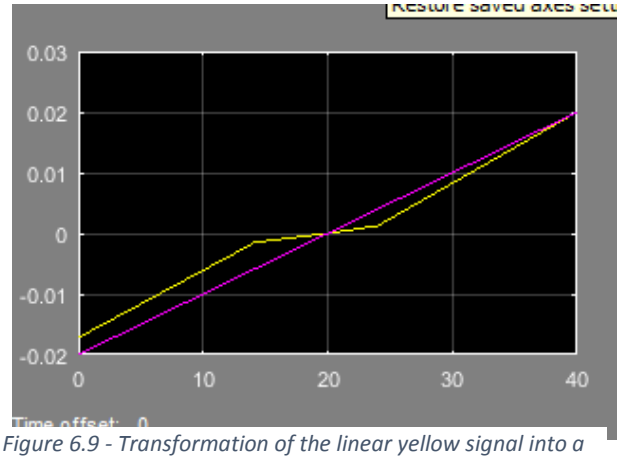

Figure 6.9 - Transformation of the linear yellow signal into a non-linear (pink) control signal

The 4-Way Directional Valve block represents a continuous 4-Way directional valve. The fluid is pumped in the valve through the inlet line P and is distributed between two outside hydraulic lines A and B (usually connected to a double-acting actuator) and the return line T. The block has four hydraulic connections, corresponding to inlet port (P), actuators ports (A and B), and return port (T), and one physical signal port connection (S), which controls the spool position.

There are multiple configurations of 4-way directional valves, depending on the port connections in three distinctive valve positions: leftmost, neutral and rightmost. This block lets you model the most popular configurations by changing the initial openings of the orifices. The 4-Way Directional Valve block is built of four Variable Orifice blocks, connected as shown in the following diagram.

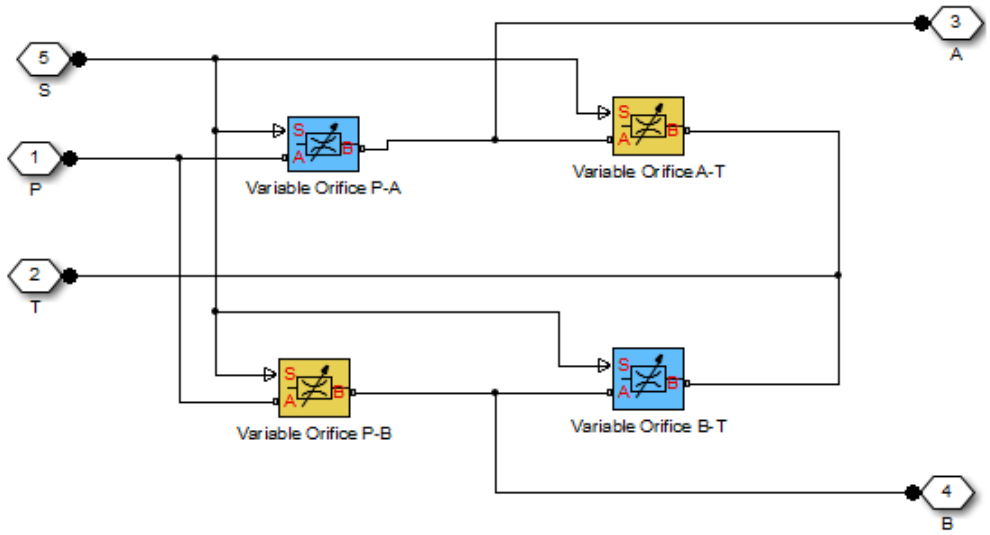

Figure 6.10 - Block diagram of the system of variable orifices of which the servo valve is composed

The Variable Orifice blocks are installed as follows: orifice P-A is in the P-A path, orifice P-B is in the P-B path and orifice B-T is in the B-T path. All blocks are controlled by the same position signal, provided through the physical signal port S, but the Orifice orientation parameter in the block instances is set in such a way that positive signal at port S opens the orifices colored blue in the block diagram (orifices P-A and B-T) and closes the orifices colored yellow (orifices P-B and A-T). As a result, the openings of the orifices are computed as follows:

$$h_{PA} = h_{PA0} + x \qquad (6.12)$$

$$h_{PB} = h_{PB0} - x \qquad (6.13)$$

$$h_{AT} = h_{PAT0} - x \qquad (6.14)$$

$$h_{BT} = h_{BT0} + x \qquad (6.15)$$

Where:

h_{PA} = Orifice opening for the Variable Orifice P-A block [m]
h_{PB} = Orifice opening for the Variable Orifice P-B block [m]
h_{AT} = Orifice opening for the Variable Orifice A-T block [m]
h_{BT} = Orifice opening for the Variable Orifice B-T block [m]
h_{PA0} = Initial opening for the Variable Orifice P-A block [m]
h_{PB0} = Initial opening for the Variable Orifice P-A block [m]

h_{PAT0} = Initial opening for the Variable Orifice P-A block [m]
h_{BT0} = Initial opening for the Variable Orifice P-A block [m]
x = Control member displacement from initial position [m]

The passage are of the variable orifices are assumed to be linearly dependent on the control member displacement, that is, the orifices is assumed to be closed at the initial position of the control member (zero displacement), and the maximum opening takes place at the maximum displacement. In this case the model accounts for the laminar and turbulent flow regimes by monitoring the Reynolds number (Re) and comparing its value with the critical Reynolds number (Re_{cr}). After the area has been determined, the flow rate is computed according to the following equations:

$$q = C_D \cdot A(h) \cdot \sqrt{\frac{2}{\rho}} \cdot \frac{p}{(p^2+p_{cr}^2)^{\frac{1}{4}}} \quad (6.16)$$

$$p = p_A - p_B \quad (6.17)$$

$$p_{cr} = \frac{\rho}{2}\left(\frac{Re_{cr}\cdot \mathrm{v}}{C_D \cdot \mathrm{D_H}}\right)^2 \quad (6.18)$$

$$h = x_0 + x \cdot \mathrm{or} \quad (6.19)$$

$$A(h) = h \cdot \frac{A_{\max}}{hmax} + A_{leak} \quad for\ h > 0 \quad (6.20)$$

$$A(h) = A_{leak} \quad for\ h \leq 0 \quad (6.21)$$

$$D_H = \sqrt{\frac{4A(h)}{\pi}} \quad (6.22)$$

Where

q = Flow rate $[\frac{m^3}{s}]$
p = Pressure differential [bar]
p_A, p_B = Gauge pressures at the block terminals [bar]
C_D = Flow discharge coefficient [-]
$A(h)$ = Instantaneous orifice passage area $[m^2]$
$A_{\max}$ = Orifice maximum area $[m^2]$
$hmax$ = Control member maximum displacement [m]
x_0 = Initial opening [m]
x = Control member displacement from initial position [m]
h = Orifice opening [m]
or = Orifice orientation indicator [-]
ρ= Fluid density $[\frac{kg}{m^3}]$
V = Fluid kinematic viscosity $[\frac{\mathrm{m}^2}{\mathrm{s}}]$
p_{cr}= Minimum pressure for turbulent flow [bar]
Re_{cr} = Critical Reynolds number [-]
D_H = Instantaneous orifice hydraulic diameter [m]
A_{leak} = Closed orifice leakage area $[m^2]$

The main parameter for the 4-Way Directional Valve that has to be set in the block parameters settings is the valve passage maximum area. This is the passage area of the valve when there is a 100% control signal applied on the control member displacement which means that the valve is fully opened. This value can be calculated with the following equation which is a simple form of the previous presented equation 6.16:

$$Q = C \cdot A \cdot \sqrt{\frac{2 \cdot \Delta p}{\rho}} \qquad (6.23)$$

In which:

- C = Flow discharge coefficient [-]
- A = Passage Area [m^2]
- Δp = pressure drop over the valve [bar]
- ρ = density of the fluid [kg/m^3]

As described before, the hydraulic sub-system is designed in order to control the flow and provide the cylinder with the required flow. This is the calculated flow Q_{bottom}. Inserting this value in the equation with a flow discharge coefficient of 0.7 [-], a constant pressure of Δp=25 bar and fluid density of $\rho = 961.446$ kg/m^3 the maximum passage area becomes:

$$A = \frac{Q_{bottom}}{C \cdot \sqrt{\frac{2 \cdot \Delta p}{\rho}}} = 3.515e-4\ m^2 \qquad (6.24)$$

5.2.4. Modelling the luffing pump

The luffing pump is modelled by a Variable – Displacement Pressure Compensated Pump. The basic equation on which the settings are based is:

$$Q_{pump} = V_{pump} \cdot \omega \cdot \eta \qquad (6.25)$$

Where:

- V_{pump} = maximum displacement (stroke volume) [m^3/rev]
- ω = rotational shaft speed [rpm]
- η = efficiency of the pump

The maximum displacement of the luffing pump is 1.4e-4 m^3/rev and the rotational speed at which the pump is driven is 1785 rpm. If the losses ($\eta = 1$) are neglected, the flow delivered by the pump can be calculated:

$$Q_{pump} = 1.4e-4 \cdot 1785 = 0.2499 \left[\frac{m^3}{min}\right] = \mathbf{250}\ [\boldsymbol{\frac{l}{min}}] \qquad (6.26)$$

The Variable-Displacement Pressure-Compensated Pump block which is used to model the luffing pump used for the gangway system is shown in figure 6.11. The Variable Displacement Pressure-Compensated Pump block represents a positive, variable-displacement, pressure-compensated pump of any type as a data-sheet based model. The key parameters required to parameterize the block are the pump maximum displacement, regulation range, volumetric and total efficiencies, nominal pressure, and angular velocity.

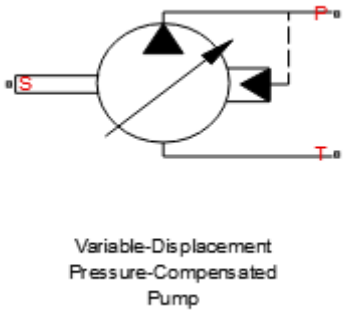

Figure 6.11 - Variable-Displacement Pressure-Compensated Pump

The luffing pump has a setting pressure of 300 [bar] and ensures this pressure can always be delivered to the system. The pump is pressure compensated which means that it contains a swash plate. This is a control mechanism which reduces the flow in order to make sure that the setting pressure of 300 [bar] cannot be exceeded.

The following figure shows the delivery-pressure characteristic of the pump.

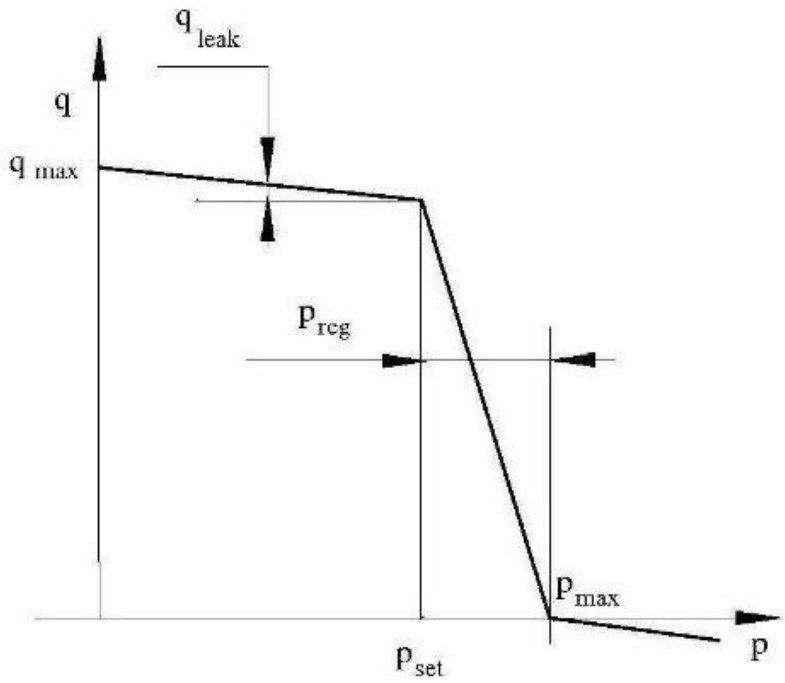

Figure 6.12 - Relationship between the pump pressure and the flow delivered by the pump

The pump tries to maintain preset pressure at its outlet by adjusting its delivery flow in accordance with the system requirements. If pressure differential across the pump is less than the setting pressure, the pump outputs its maximum delivery corrected for internal leakage. After the pressure setting has been reached, the output flow is regulated to maintain preset pressure by changing the pump's displacement. The displacement can be changed from its maximum value down to zero, depending upon system flow requirements. The pressure range between the preset pressure and the maximum pressure, at which the displacement is zero, is referred to as regulation range. The smaller the range, the higher the accuracy at which preset pressure is maintained. The range size also affects the pump stability, and decreasing the range generally causes stability to decrease.

5.2.5 Luffing Accumulators

The luffing accumulators used for the gangway are bladder accumulators. These are hydro pneumatic accumulators with a flexible bladder as separation element between compressible gas cushion and operating fluid. The physical behavior of the accumulators can be described by the following equation which is based on the theory of adiabatic expansions:

$$p1 \cdot V1^k = p2 \cdot V2^k \qquad (6.27)$$

Where:

- P1 = Maximum operating pressure of the gas volume [bar]
- P2 = Minimum operating pressure of the gas volume [bar]
- V1 = Gas volume at maximum operating pressure [m^3]
- V2 = Gas Volume at minimum operating pressure [m^3]
- K = specific heat ratio [-]

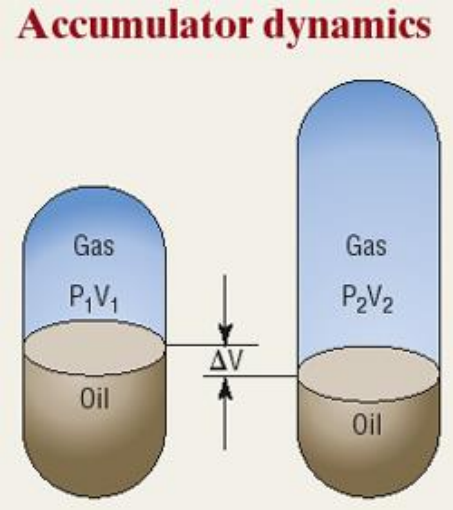

Figure 6.13 - Schematic of the accumulator [20]

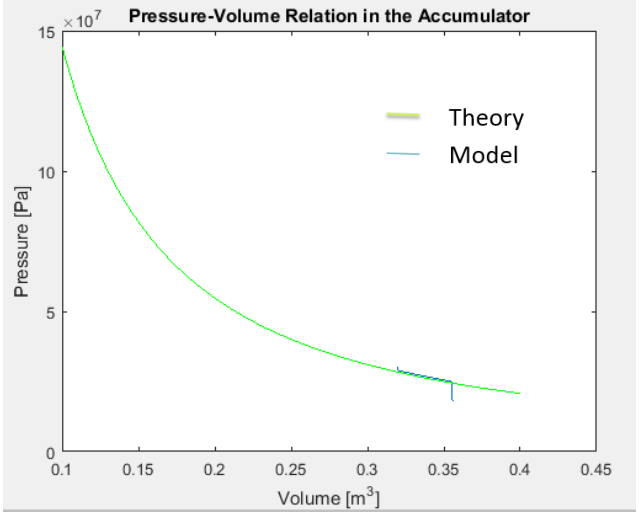

Figure 6.14 - Adiabatic expansion of the gasvolume of the accu

In figure 6.13 the accumulator dynamics is visualized. The expansion of the gas volume will result in an effective useful volume ΔV which is the amount of fluid that is delivered to the hydraulic system. After starting the luffing pumps, the luffing accumulators will be filled up to the maximum pump system pressure. A pressure sensor measure the system pressure. When the maximum pump pressure is reached, the gangway is ready for moving, the accumulators are filled. The bladder accumulators are modeled by a Gas-Charged Accumulator (figure 6.15).

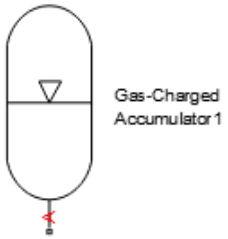

Figure 6.15 - Gas-Charged Accumulator in Simscape

The verification of the gas-charged accumulator can be done by plotting the expansion of the gas volume versus the pressure in this volume and check if it corresponds with the theoretical adiabatic expansion. In figure 6.14, the blue line is more or less on top of the green (theory) which confirms that the luffing accumulators are modeled in the right way. In case the AMC requires more flow than the pump delivers, the luffing accumulators provide the extra flow. For the down movement of the gangway there is pump flow needed, the pump is used to refill the accumulators. The Gas-Charged Accumulator block models the bladder accumulators used in the hydraulic system of the gangway. The accumulator consists of a precharged gas chamber and a fluid chamber. The fluid chamber is connected to a hydraulic system. The chambers are separated by a bladder, a piston or any kind of a diaphragm.

As the fluid pressure at the accumulator inlet becomes greater than the precharge pressure, fluid enters the accumulator and compresses the gas, storing energy. A decrease in the fluid pressure causes the gas to decompress and discharge the stored fluid into the system. During typical operations, the pressure in the gas chamber is equal to the pressure in the fluid chamber. However, if the pressure at the accumulator inlet drops below the precharge pressure, the gas chamber becomes isolated from the system. In this situation, the fluid chamber is empty and the pressure in the gas chamber remains constant and equal to the precharge pressure. The pressure at the accumulator inlet depends on the hydraulic system to which the accumulator is connected. If the pressure at the accumulator inlet builds up to the precharge pressure or higher, fluid enters the accumulator again. The motion of the separator between the fluid chamber and the gas chamber is restricted by two hard stops that limit the expansion and contraction of the fluid volume. The fluid volume is limited when the fluid chamber is at capacity and when the fluid chamber is empty. The hard stops are modeled with the finite stiffness and damping. This means that it is possible for the fluid volume to become negative or greater than the fluid chamber capacity, depending on the values of the hard-stop stiffness coefficient and the accumulator inlet pressure.

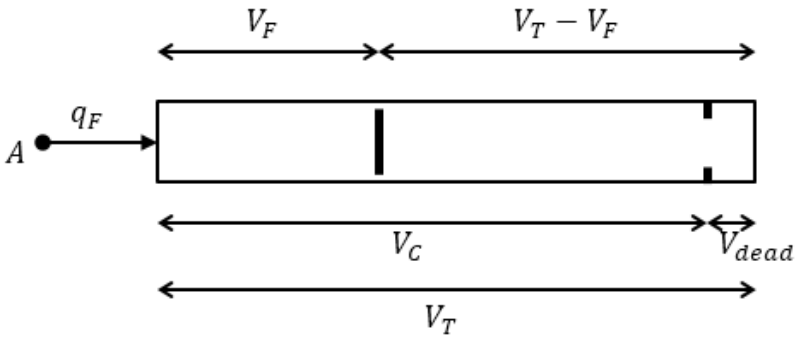

Figure 6.16 - Schematic diagram of the Gas-Charged Accumulator

The diagram represents a gas-charged accumulator. The total accumulator volume (V_T) is divided into the fluid chamber on the left and the gas chamber on the right by the vertical separator. The distance between the left side and the separator defines the fluid volume (V_F). The distance between the right side and the separator defines the gas volume (V_T - V_F). The fluid chamber capacity (V_C) is less than the total accumulator volume so that the gas volume never becomes zero. The flow rate into the accumulator is the rate of change of the fluid volume:

$$q_F = \frac{dV_F}{dt} \qquad (6.28)$$

At t=0, the initial condition is V_F=V_{init} , where V_{init} is the value you assign to the initial fluid volume parameter.

5.2.6 Pressure Compensators

Two pressure compensators are mounted to ensure load independent flow through the servo control valve which means that the pressure drop over the control valve is kept constant. One pressure compensator is used for the ingoing flow and one pressure compensator is used for the outgoing flow. Pressure compensators are used to maintain preset pressure differential across hydraulic components to minimize the influence of pressure variation on a flow rate passing through the component.

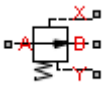

Figure 6.17 - Pressure Compensator Block

In figure 6.17 the Pressure Compensator block is shown. The Pressure Compensator block represents a hydraulic pressure compensating valve, or pressure compensator. Pressure compensator is a normally open valve. Its opening is proportional to the pressure difference between ports X and Y and the spring force. The following illustration shows typical relationship between the valve passage area A and the pressure difference p_{xy}.

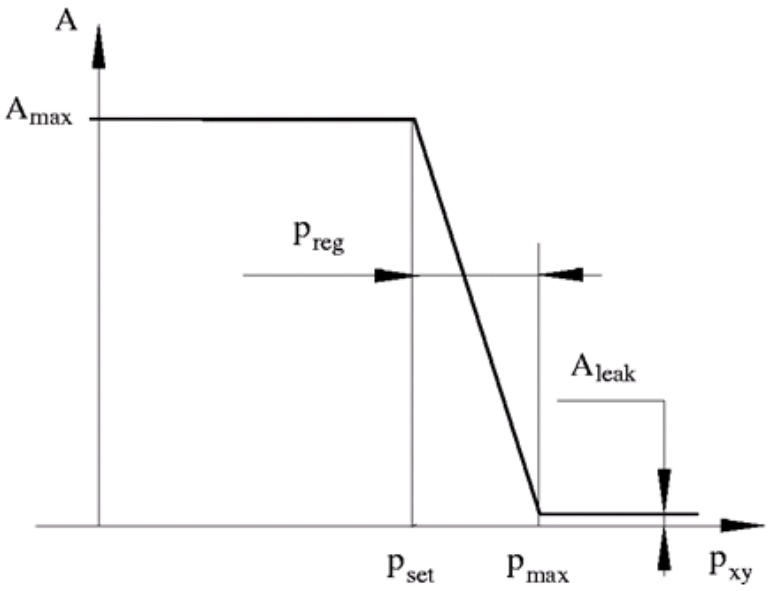

Figure 6.18 - Relationship between the valve passage area A and the pressure difference Pxy

The orifice remains fully open until the pressure difference is lower than the valve preset pressure determined by the spring preload. When the preset pressure is reached, the valve control member is forced off its stop and starts closing the orifice, thus trying to maintain pressure differential at preset level. Any further increase in the pressure difference causes the control member to close the orifice even more, until the point when the orifice is fully closed. The pressure increase that is necessary to close the valve is referred to as regulation range, or pressure compensator static error, and usually is provided in manufacturer's catalog or data sheets. The flow rate through the valve is determined according to the equations 6.16 – 6.22.

The following two illustrations with numerical examples (figure 6.19), give a better insight in the working principle and the typical application of the pressure compensators, where it is used in combination with the orifice (servo control valve).

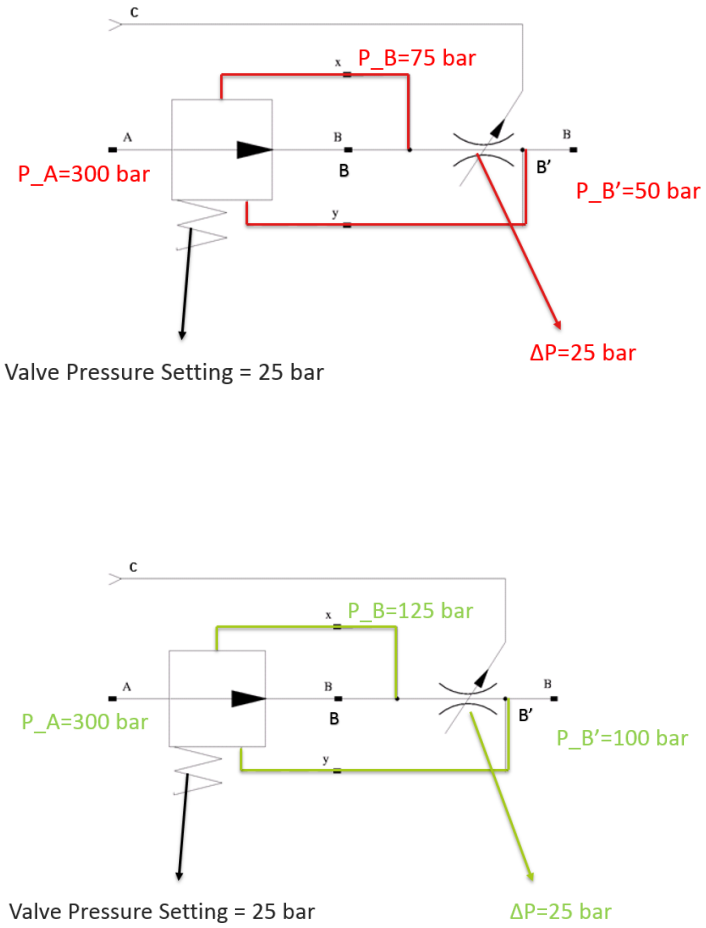

Figure 6.19 - Working principle of the pressure compensator

The pressure compensator can be considered as a pressure reducer. If we analyze the first illustration we can see that the pressure compensator contains a spring which can be set according to a certain Valve Pressure Setting. This setting also decides the value of the constant pressure which will always be maintained in the system. We assume a pump pressure P_A= 300 bar on the left side and a cylinder pressure due to the weight of P_B'= 50 bar. The orifice between the pressure compensator and the cylinder causes always a pressure drop Δp= P_B – P_B'. The pressure P_B' at the cylinder side is fed back to the pressure compensator by a return line (marked as the red line y). This pressure is summed up to the valve pressure setting. This makes sure that the pressure after the pressure compensator can increase to a total value of 75 bar. From a physical point of view this means that pressure P_B has to exceed the equilibrium pressure of 75 bar to overcome the valve pressure setting (spring force) and the cylinder pressure (feedback) to disconnect flow from the pump with the flow through the orifice. This results in a pressure drop of Δp= P_B – P_B'= 25 bar.

In the second illustration (figure 6.19 bottom) we can see that if the cylinder load is increased to 100 bar this means that also the reduced pressure which is equal to the equilibrium pressure in the pressure compensator is increased. This results that pressure drop over the valve remains constant and the goal of keeping the pressure constant is achieved.

5.2.7 Check Valves

Three check valves are used for the hydraulic luffing system. Two check valves to let the flow pass in the right direction through the pressure compensators and servo valve. One check valve is located at the hydraulic thank to prevent that the total amount of fluid returns back in the tank which will cause a pressure drop at the rod side of the hydraulic cylinder. The check valve block is shown in the figure below.

Figure 6.20 - Check Valve

The Check Valve block represents a hydraulic check valve as a data-based model. The purpose of the check valve is to permit flow in one direction and block it in the opposite direction. The following figure shows the typical dependency between the valve passage area A and the pressure differential across the valve:

$$p = p_A - p_B \qquad (6.29)$$

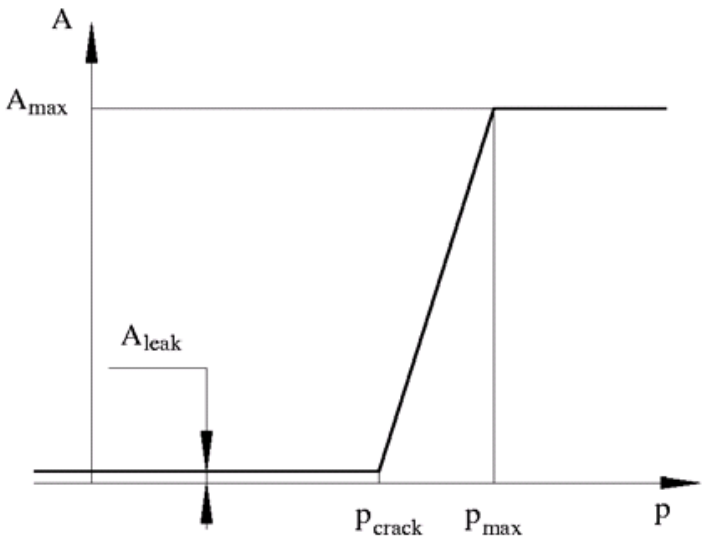

Figure 6.21 - Relationship between the passage area A of the check valve and the pressure in the check valve

5.3 Verification of the luffing hydraulic cylinder

For the verification of the hydraulic luffing sub-system a simple test is done. A control signal is generated by a signal builder which is put on the control servo valve. This control signal is shown in the upper diagram of figure 6.22. When starting the simulation the control signal remains zero until the signal starts to increase at t=6 s. The signal reaches a certain maximum value and remains constant till t=80 s. At this moment the signal will switch from positive in to a negative signal which means that the direction of the movement is switched from luffing up into luffing down. Important to notice is that increasing the control signal also the flow rate increase. In the middle diagram of figure

6.22 the flow in the orifice P-A of the servo valve is shown. This is the orifice which is opened when the oil has to be delivered from the pump into the bottom chamber of the cylinder. If the maximum control signal is reached also the maximum flow rate is reached and from this point the pressure is kept constant on Δp = 25 bar. The constant pressure line is visible in the lower diagram. In figure 6.23 the resulting displacement of the piston stroke is shown. If the piston starts from the bottom side, the piston displaces to a stroke length of approximate 1.1 m. At the moment the sign of the signal is changed into negative value, the piston moves back in the direction of the bottom till the end of the. So the simulated motion is a luffing up and luffing down motion of the gangway.

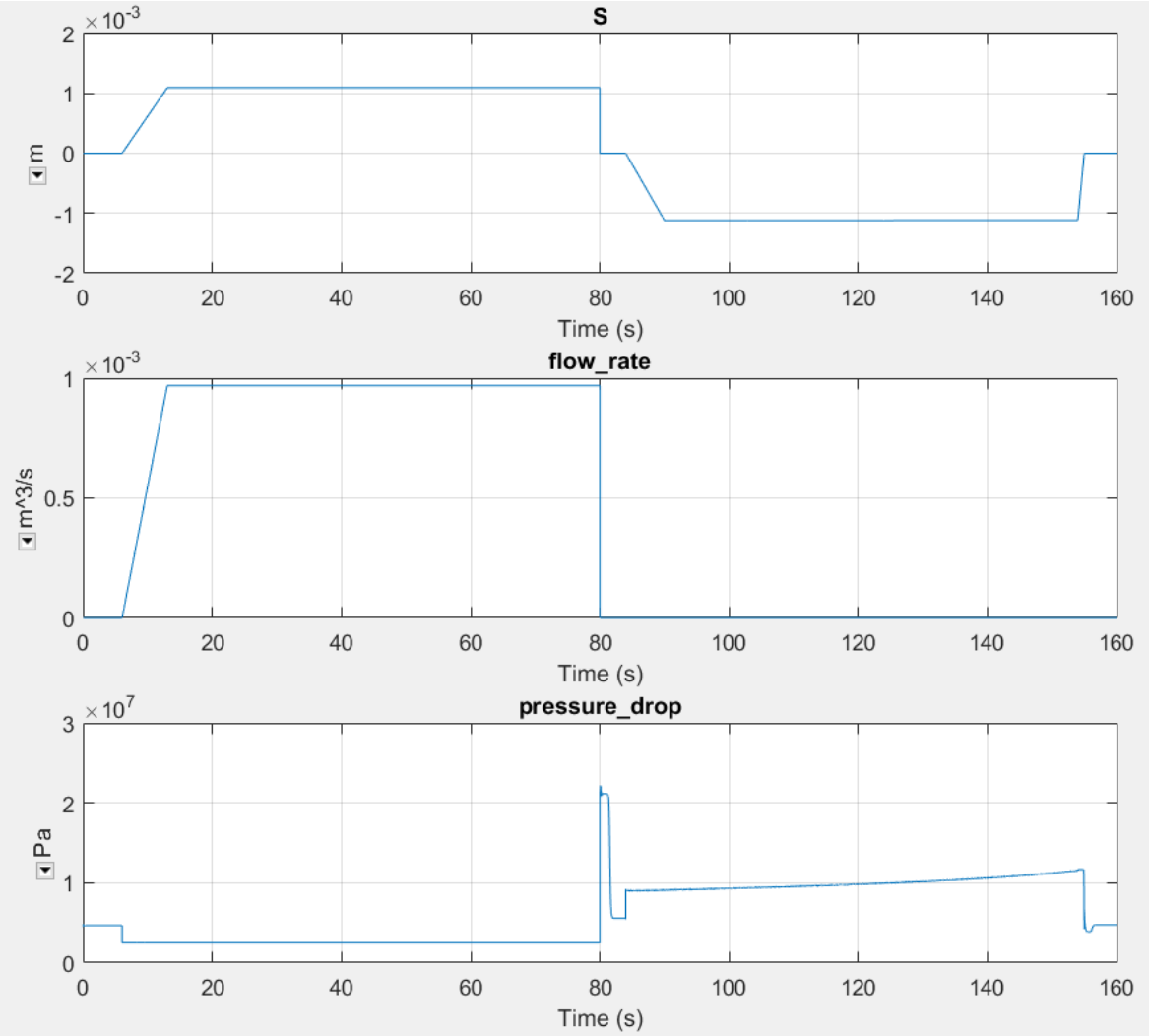

Figure 6.22 - Verification results of the hydraulic sub-system: control signal applied on the servo valve (top), flow (middle) and pressure in the orifice P-A of the servo valve (bottom)

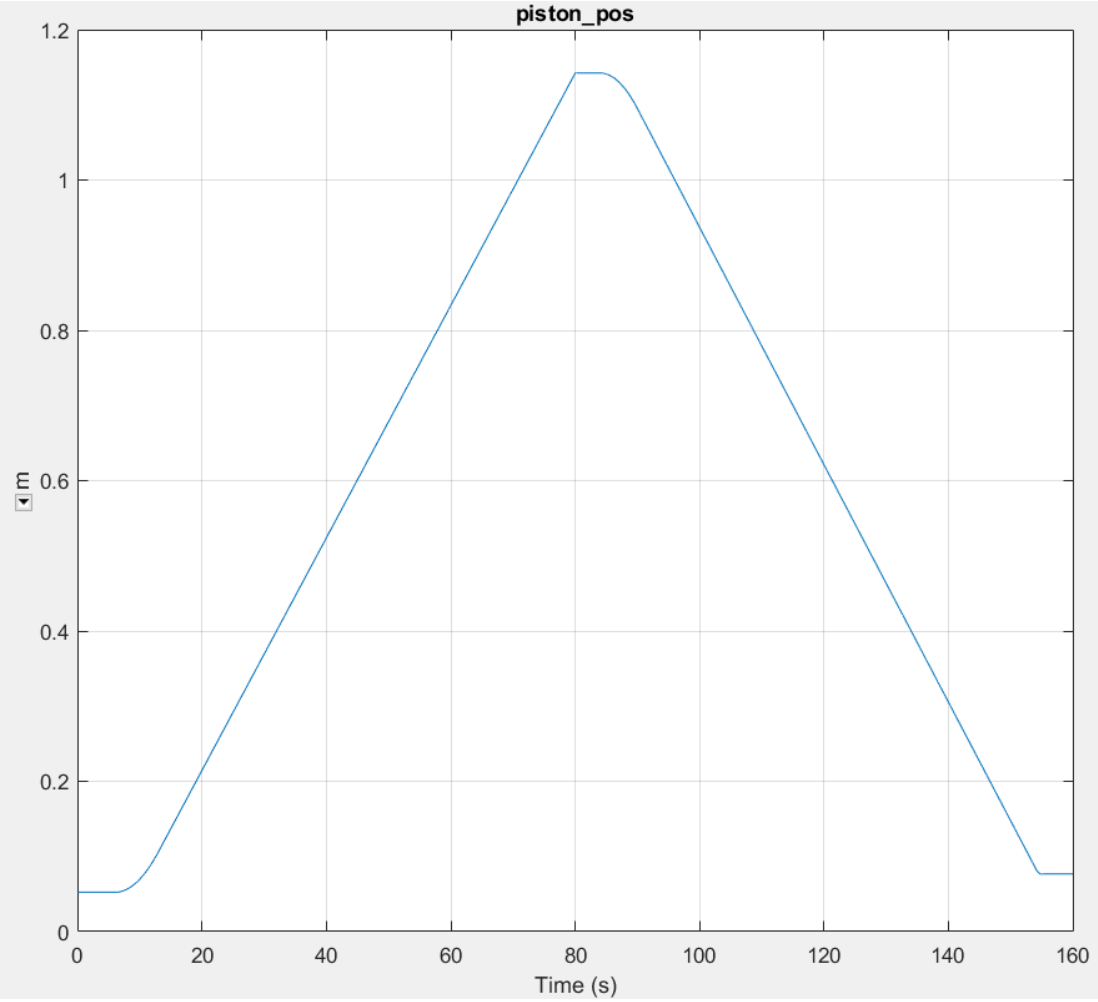

Figure 6.23 - Piston position during the verification step

As shown in the plot of figure 6.23 the cylinder displaces from nearly zero till a piston position of approximate 1.1 m from the bottom and returns back to its initial position. This motion is simulated to make sure that the hydraulic sub-system works well in the whole working envelope. That means that the luffing up as well as the luffing down motion work as they should work. Conclusion from this simple test is that the hydraulic sub-system functions as it should function according the real hydraulic system and the tasks of all components are fulfilled.

6 Coupling the hydraulic and mechanical sub-system.

After finishing the hydraulic sub-system it's task to integrate this model in the mechanical model of the offshore gangway. The structural sub-system that is modeled for the initial simplified model (chapter 5) is taken as the basic model. This model is extended with more bodies and configuration settings which result in an improved simulation and visualization of the gangway system. In figure 7.1 the included bodies of the mechanical sub-system are presented.

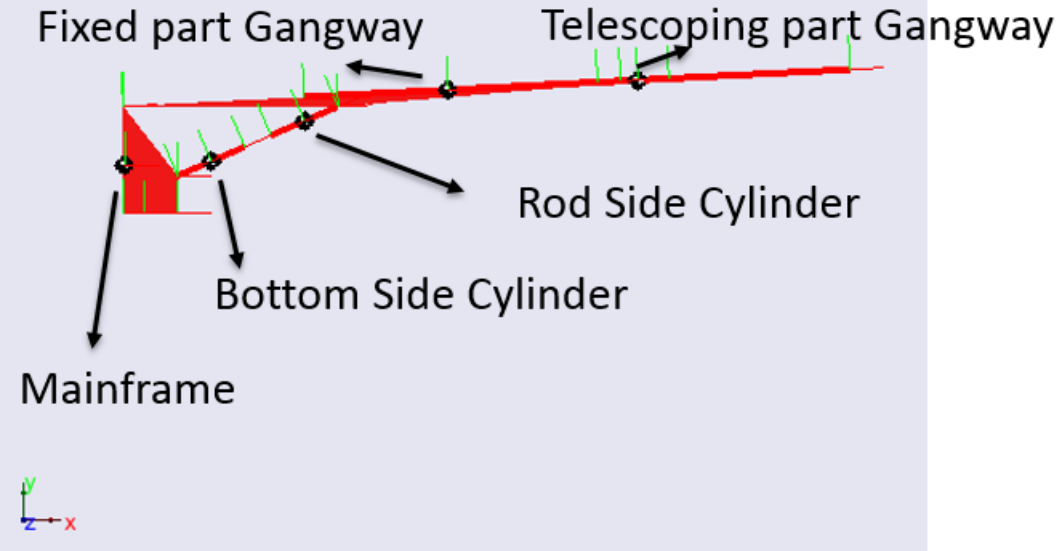

Figure 7.1 - Overview of the mechanical sub-system

The mechanical sub-system consists of the following five components:

1. Mainframe
2. Bottom Side Cylinder
3. Rod Side Cylinder
4. Fixed Part Gangway
5. Telescoping Part Gangway

Every component is modeled as rigid body with a center of gravity and dimensions which are fixed or dependent on the changing gangway geometry due to the luffing and telescoping motion.

6.1 Gangway geometry and variable parameters

In figure 7.2 an illustration of the geometry of the gangway in a horizontal configuration (luffing angle = 0 deg) is shown. A displacement of the hydraulic cylinder (extension or retraction) will lead to a rotation (luffing motion) upward or downwards.

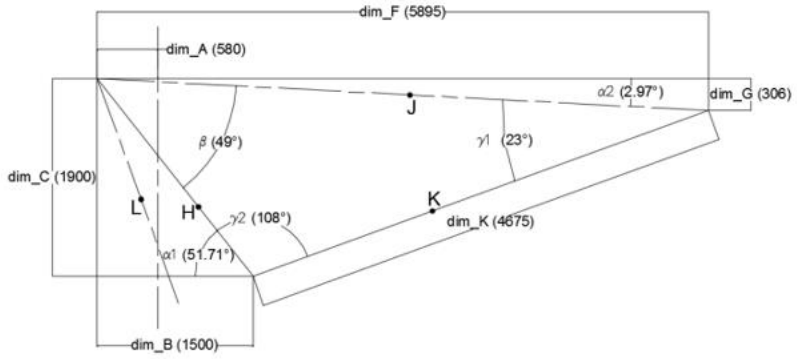

Figure 7.2 - Gangway geometry in a horizontal configuration of the fixed part

The relationship between the luffing angle and cylinder dimension (dim_K) can be given by the use of cosine rule, which result in the following equation:

$$\dim\_\mathrm{K} = \sqrt{\dim\_H^2 + \dim\_J^2 - 2 \cdot \dim\_H \cdot \dim\_J \cdot \cos(\beta - \theta)} \qquad (7.1)$$

Where

β = Starting configuration angle (49 [deg]) in horizontal configuration [deg]
θ = Luffing Angle [deg]

In Simscape it's possible to import data from the Matlab workspace by calling the parameters back in the parameter setting blocks. Some coding was needed to implement the described geometry dependency of some dimensions and parameters to implement variable parameters. The script for the implementation of the luffing angle dependent configuration of the gangway can be found in Appendix E. In case the cylinder is fully retracted (piston pushing against the bottom, the corresponding dim_K and luffing angle are 3.955 [m] and -20 [deg] respectively. In case the piston is displaced over its total stroke length of 2.76 [m], the corresponding dim_K and luffing angle are 6.715 [m] and 50 [deg] respectively.

6.2 Kinematic Analyses

In order to connect the mechanical bodies in such a way that the motions can be performed as expected, the type of connection of the bodies is essential. A kinematic analyses is a good support in finding the right joint which can be chosen from the Simscape toolbox. In figure 7.3 the conducted kinematic analyses is shown.

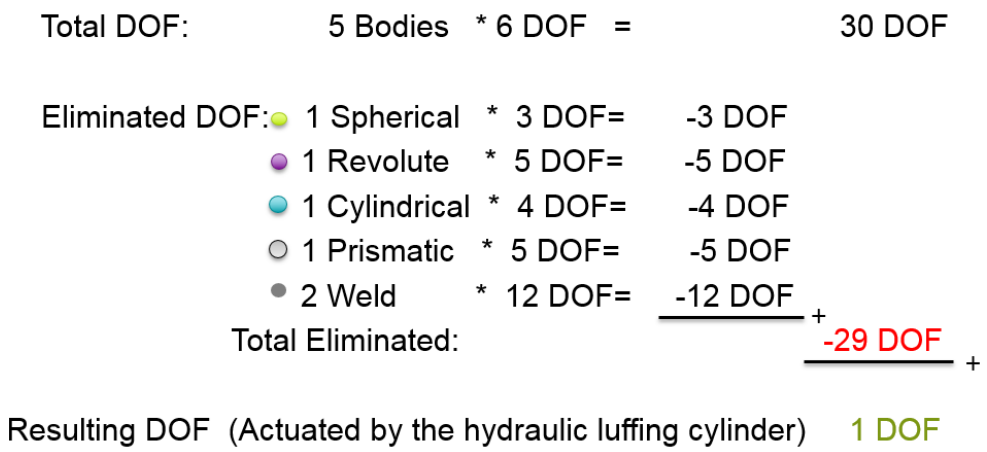

Figure 7.3 - Kinematic analysis of the degrees of freedom in the model

The bodies deliver in total 30 degrees of freedom from which finally one degree of freedom remains which is the expansion/retraction of the luffing cylinder. In the model there are in total 6 joints used for the connection of the bodies. In figure 7.4 the location of the different connection points are indicated with the corresponding joints.

Figure 7.4 - Joints used in the structural model

The spherical joint connects the bottom side of the cylinder with the mainframe and allows only the three rotations and eliminates the three translations. The prismatic joint allows only the translation in the longitudinal direction which is the actuated motion. The cylindrical joint connects the rod side of the cylinder with the fixed section of the gangway. It allows one translation and one rotation. The rotation is around the axis in the direction of the allowed translation. The revolute joint connects the fixed section with the mainframe which allows only the rotation around this hinge, this is the luffing motion. The two welds eliminates all degrees of freedom. One weld is used to pin the gangway in the global word coordinate system and the second weld is initially used to constrain the telescoping motion. The location of the first weld, at the bottom of the mainframe, is also chosen as the origin (0,0,0) of the coordinate system and is the reference point for this coupled model. The dimensions and motions of the gangway tip will always be measured relative to this origin point. This is also the point which intersects the vertical centerline. In a later stage the two welds will be replaced by other joints which will make it possible that the gangway can move free in the 2D plane and telescope back and forth.

In figure 7.5 the constructed mechanical model with all the components, the incorporated geometry dependent configuration and the joints is shown.

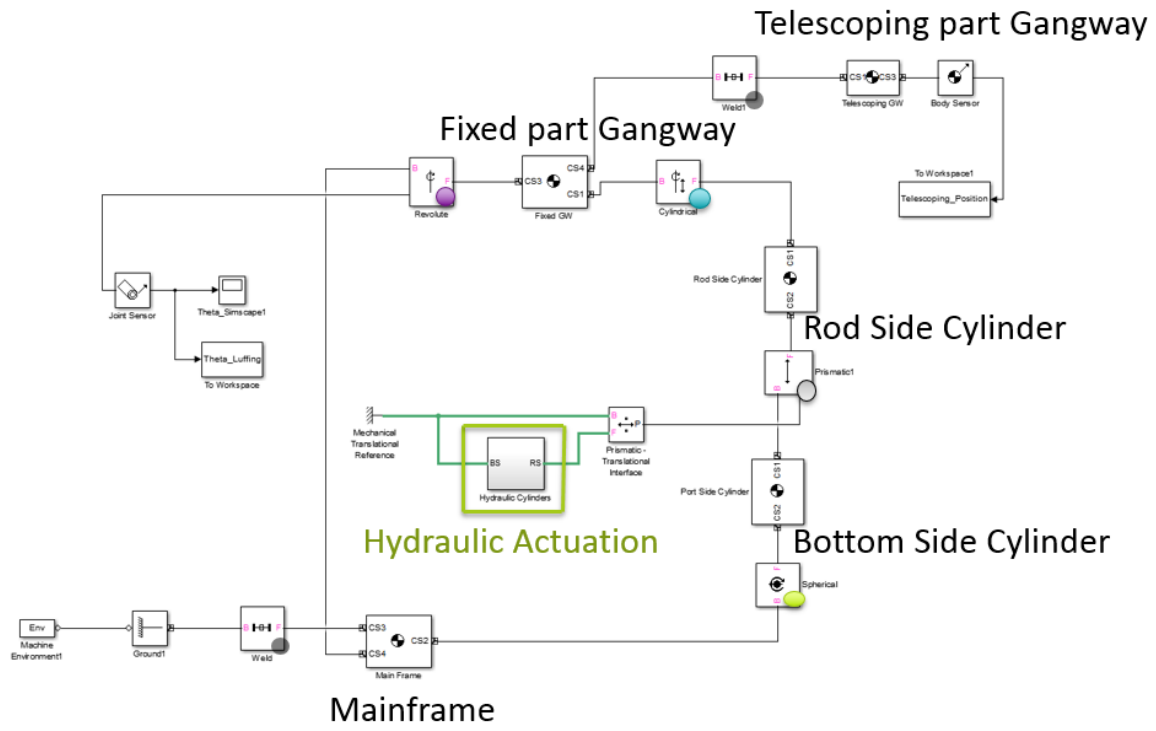

Figure 7.5 - Simscape model of the coupled mechanical-hydraulic system

In the figure above the integration of the hydraulic sub-system in the mechanical system is presented. The interaction of the hydraulic sub-system with the mechanical sub-system is visualized by the green boarder which is the boundary for the output signal (displacement/velocity of the piston) and the input signal (the control valve signal).

6.3 Validation of the coupled mechanical-hydraulic model

In order to validate the coupled mechanical/hydraulic model, experimental data from the company are used. These are logged data from experimental tests which are executed with the gangway. The data are recorded in excel files. After importing these data in Matlab (Appendix X), they are further processed, analyzed and visualized in diagrams. From these data several information about the motion and hydraulic sub-system can be provided. First of all, it's important to know what the starting conditions were during the experiments. What was the starting configuration? This can be found out by analyzing the applied control signal on the servo valve. The signal looks like the green line in the figure below. In order to compare the simulation result of the model with the experimental data, a signal is generated which corresponds as much as possible with the green line. The gangway model should reacts more or less the same as in the experimental tests.

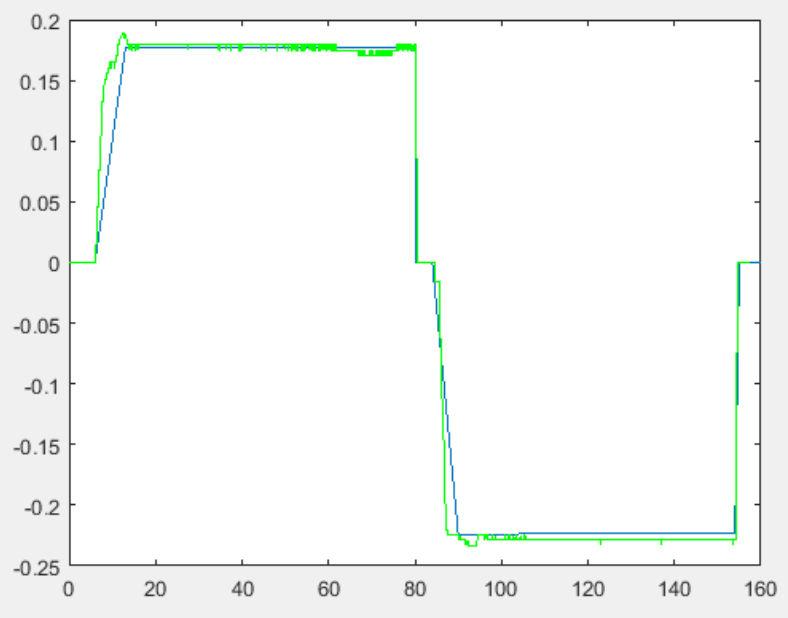

Figure 7.6 - Control Signal applied during the tests (green) vs the generated control signal used in the simulation model (blue)

This applied signal has the same shape as the signal that is used for the verification of the hydraulic sub-system in section 6.3. This signal implies a luffing motion which start from t=6 s and is upwards till t=80 s. Then the signal drops immediately to zero and at t=84 s the signal decreases and reaches negative values which means that the orifice P-A is closed and the orifice A-T is opened. The gangway will start to move downwards. From the experimental data the starting configuration can be decided. The gangway starts at an inclined angle of -18.328 [deg]. This is the configuration in which the walkway has almost reached its maximum downwards luffing angle of 20 [deg]. This is the case when the hydraulic cylinder is fully retracted and the piston pushes against the bottom of the cylinder (piston position= 0 [m]). In this configuration dimension K is also at its minimum value of 3.955 m. In figure 7.7, the initial configuration of the gangway is presented from which the experiments and the simulation will start.

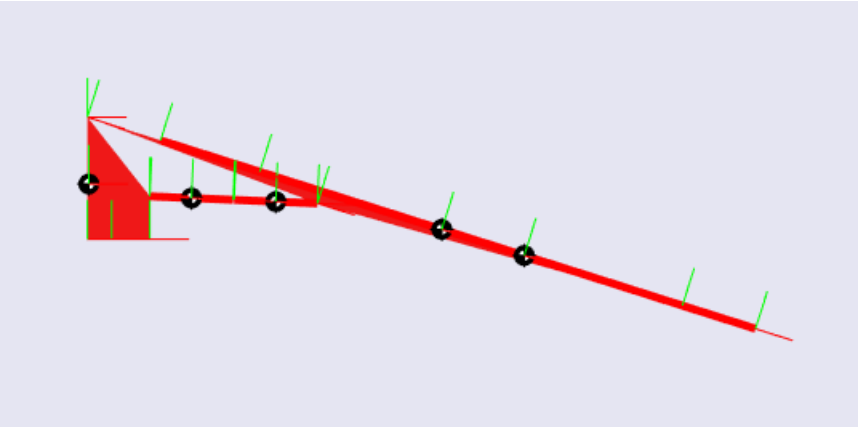

Figure 7.7 - Initial configuration of the gangway: Luffing angle=-18.328 [deg], dim_K=4.007 [m]

In figure 7.8 you can see the luffing angle of the gangway during the simulation and experiments. The two lines corresponds quite well which tells us that the motion that we simulate is more or less as the motion during the experiments. So the motion which will be analyzed is a luffing up motion starting from -18.328 [deg]. The gangway will move from its initial configuration upwards a positive luffing angle of approximate 5.1 [deg]. After a few seconds this maximum is reached the gangway will move back downwards to its initial position.

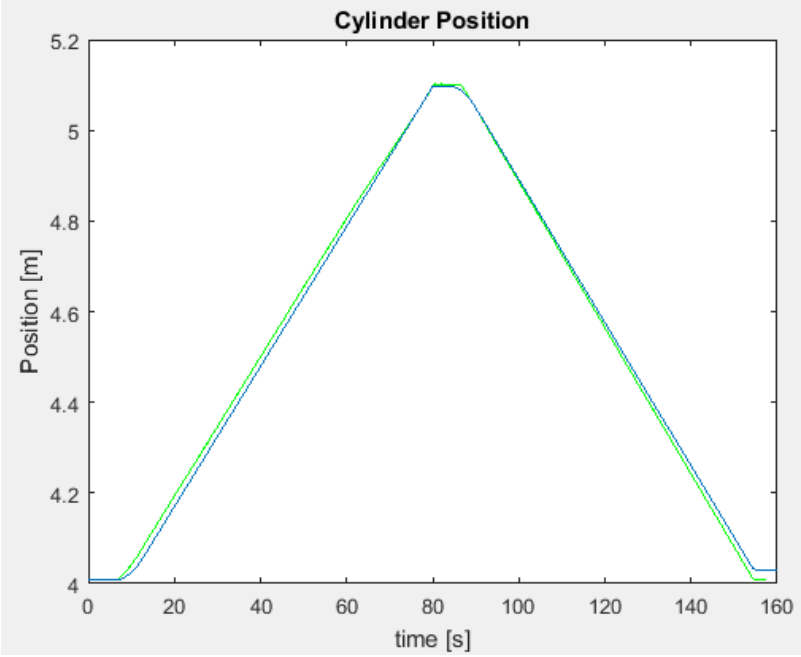

Figure 7.8 - Luffing angle of the gangway as function of the time (green=experiment, blue=simulation)

Also the cylinder velocity is compared. In figure 7.9 this comparison is shown. We can see that the cylinder velocity which is reached with the simulation is more or less equal to the mean of the strong fluctuating cylinder velocity from the experimental test.

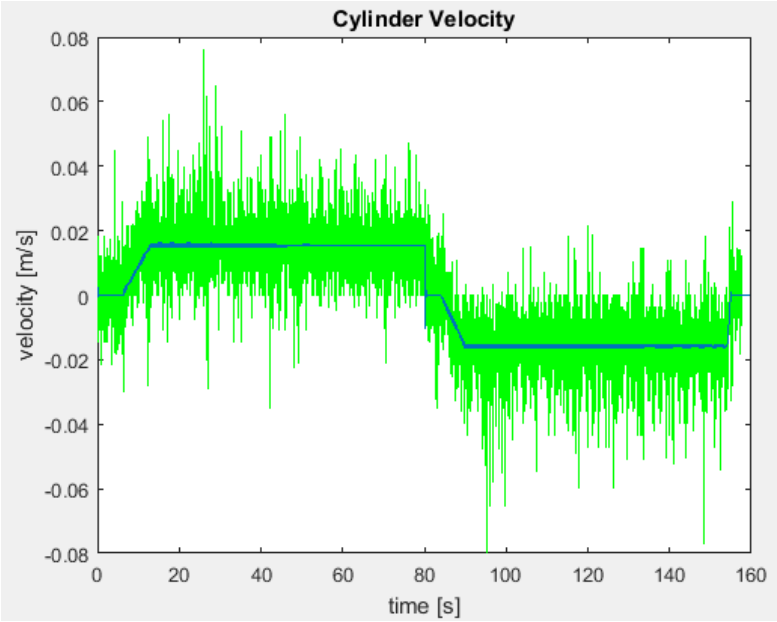

Figure 7.9 - Cylinder velocity (green=experiment, blue=simulation)

After comparison of the motion (displacement and velocity) of the gangway, the hydraulic pressure in the cylinder will be analyzed. The outcome is shown in figure 7.10. We can see that the shape of the pressure diagram of the experiments (green line) corresponds well with that of the simulation but the pressure in the simulation model are higher. It's also remarkable that in the luffing down motion, there is a bigger difference between the simulation and experiments. It seems that in the experiments there is some pressure drop at the turning point of the luffing motion (from upwards to downwards luffing). This pressure drop is much smaller in the simulation model which implies that there is a certain phenomenon, which is most probably a force, which is not included in the model but is present in the real world.

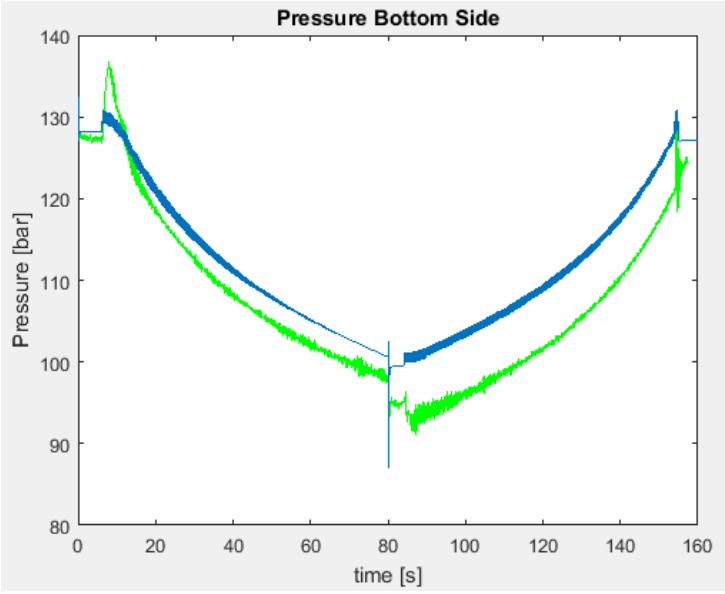

Figure 7.10 - Hydraulic pressure on the bottom side of the hydraulic cylinder

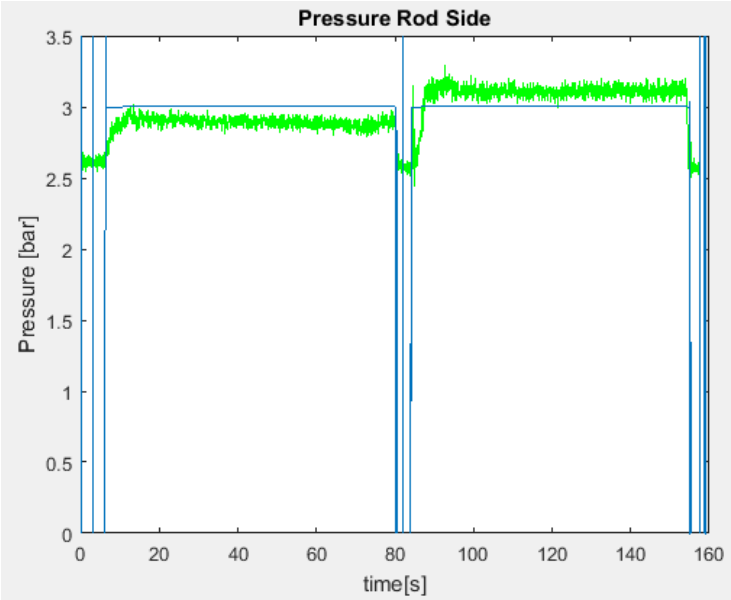

Figure 7.11 - Hydraulic pressure in the rod side of the hydraulic cylinder

Conclusion from previous verification/validation steps is that model seems to work quite well but there is still an obvious difference in the hydraulic pressure in the bottom size (pressure drop). This will be further investigated in the next section

6.4 Adding a telescoping function to the mechanical/hydraulic model

In the previous section an attempt is made to validate the mechanical/hydraulic model. The pressure drop which occurs around t=80 [s] is an important point to investigate. It's important to note that the pressure is directly influenced by the cylinder force which is decided by the weight of the fixed and telescoping gangway. Since the gangway can perform telescoping motion this force depends on the telescoping length. The bigger the telescoping length the larger the force is exerted on the hydraulic cylinder and thus the larger the hydraulic pressure. Since, the information about the telescoping motion lacks in the experimental data we cannot denote this pressure drop to this telescoping behavior. But a telescoping motion should give at least give a transition of the pressure line, so that difference which is observed in the first comparison could be minimized. So the telescoping function will be added to the model. In the figure below the telescoping winch and the cables which are shown with the pink color are shown.

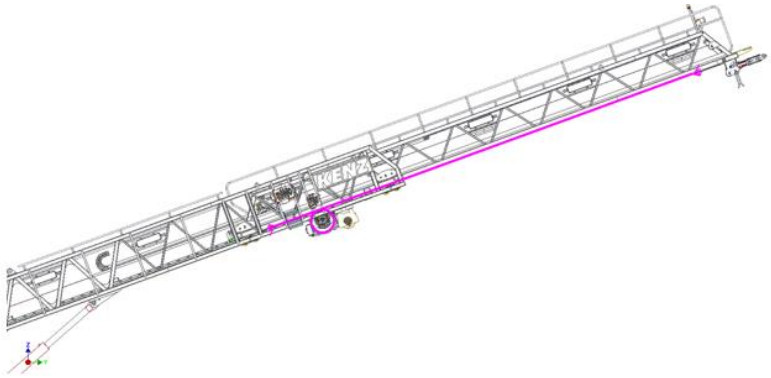

Figure 7.12 - Telescoping winch with the two cables, one attached to the front end and the other to the rear end

As discussed in chapter 1, the telescoping motion of the gangway is driven by the telescoping winch, which is mounted on the underside of the fixed section of the gangway. Two wire ropes are spooled on each side of the drum, one of which is attached to the front end of the telescoping section, the other to the rear end. In the figure below, the telescopic winch and the cables are presented more specifically.

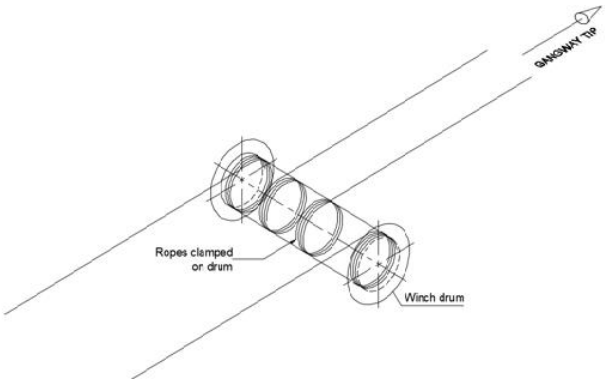

Figure 7.13 - Configuration of the wire ropes that are spooled on each side of the drum

The wire ropes has a certain stiffness which affects the dynamics of the telescoping motion. The cables are modeled as springs, one attached to the front and the other attached to the rear end of the telescoping section. An important aspect in modeling the telescoping motion is determining the equivalent cable stiffness which will be the spring constant value that is used for the spring. In reality the axial length of the wire ropes are changing during telescoping motion which means also the cable stiffness will not be constant. For the sake of simplicity we assume a constant axial length of 7.5 [m] (the case when the telescoping winch is exact at the middle of the telescoping gangway). In this analyses the stiffness is decided through equation 7.2, meaning that the stiffness is constant:

$$k_{eq} = \frac{E \cdot A}{l} \qquad (7.2)$$

Where:

E= E-modulus of the material $[\frac{N}{m^2}]$
A= Cross sectional area of the component $[m^2]$
l = Axial length of the cable [m]

In order to perform a telescoping motion the weld which is used in the model as connection of the fixed and telescoping section will be replaced by a prismatic joint which allows the motion in the longitudinal direction (x-direction) of the gangway. The prismatic joint is located at the location of the telescoping winch. The distance from the main hinge to this point is 13.038 [m]. As decided before, the hydraulic telescoping system which drives the hydraulic motor will not be modeled. The telescoping function will simply be actuated by a joint actuator. The rotational speed of the hydraulic motor will be the input for the telescoping function. After multiplying with the gearbox ratio and the radius of the drum, the translational speed for the telescoping motion is obtained. After integrating this speed, the telescoping displacement is obtained which tells the prismatic joint how much telescoping displacement has to be performed.

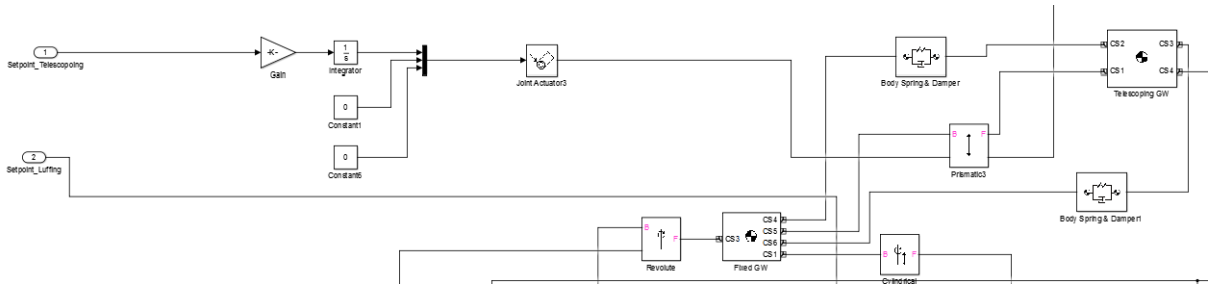

Figure 7.14 - Simscape model of the telescoping system, which is added to the coupled mechanical-hydraulic model

6.5 Additional validation step of the mechanical/hydraulic model

Now the telescoping function is included, the differences in the hydraulic pressure can be further investigated. During the validation in section 7.3, the model was built in such a way that the telescoping section is extracted 4 [m] from its minimum telescoping length (approximate 15.5 [m]). The first simple check is to investigate what happens if the telescoping section is retracted 2.5 m with respect to the previous telescoping length, so the extraction is now 1.5 [m] instead of 4 [m]. The result is shown with the red line in the right diagram of figure 7.15. It's obvious that the pressure is pushed down. This is a logic consequence because, as discussed in the previous section, when telescoping back the telescoping section will cause a smaller moment around the pivot point which means that the force exerted on the hydraulic cylinder will also smaller.

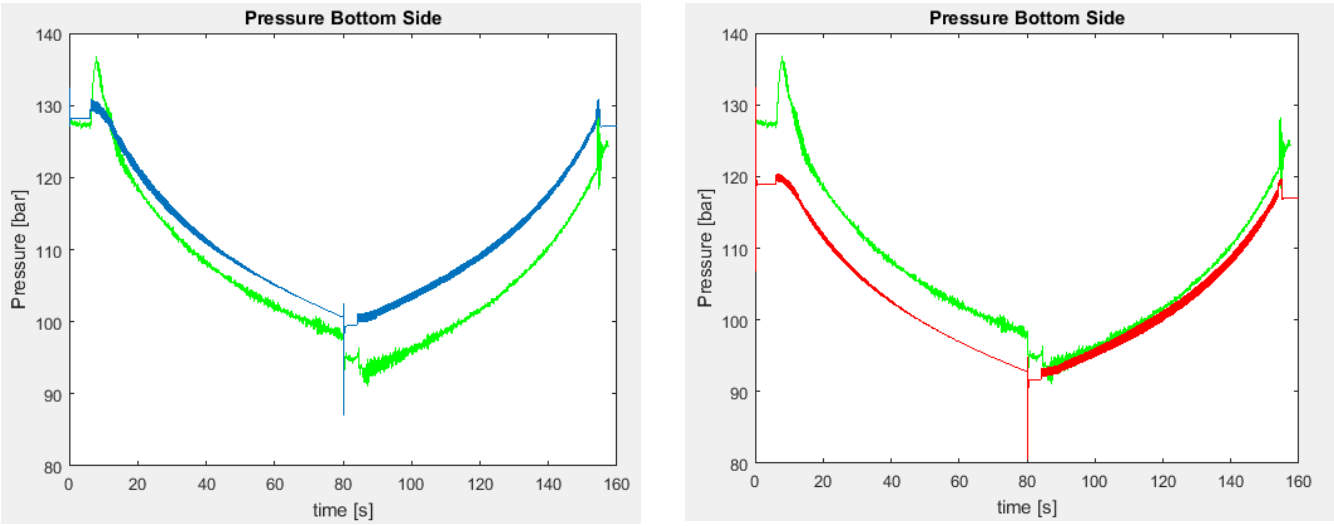

Figure 7.15 - The hydraulic pressure in the bottom side in the case the telescoping is extracted 4 [m] (left) and 1.5 [m] (right). Green line is pressure during the experiments (where no information about the telescoping length is available)

We can see that the pressure on the right half of the diagram (luffing down motion) is overlapping now but there is still a significant difference in the pressure on the left half of the diagram (luffing up motion). A third check is conducted. Now the pressure will be monitored while telescoping function is actuated from t=20 [s] till t=80 [s], with the signal as shown in figure 7.16 which will cause a retraction of 2.5 [m]. So we start at a configuration in which the telescoping section is extracted 4m, and we will end with a 2.5 [m] retracted gangway.

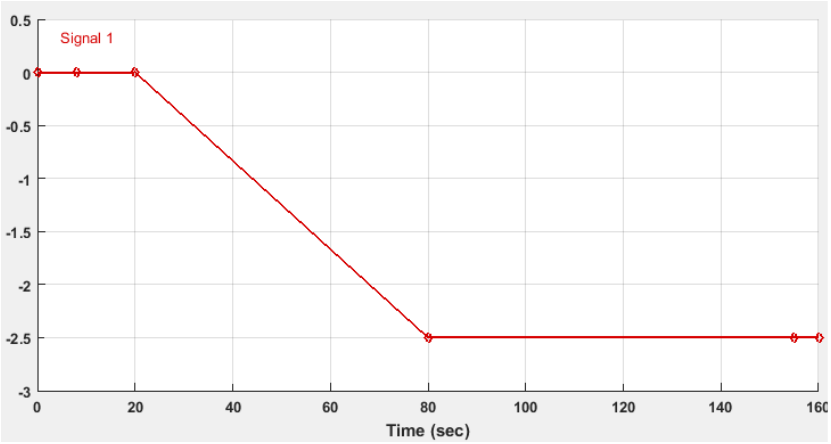

Figure 7.16 - Actuation signal for the telescoping motion

In figure 7.17 the result is shown of this simulation model. We can see that that pressure lines corresponds now much better which indicated that during the experiments also a telescoping motion (retraction) was performed. However, there is still a significant difference round t=80 [s] which is due to the pressure drip which is still present at the experiment but absent in the simulation model.

This can be caused by an external force which is not included in the simulation model for example friction, fluid compressibility or the mass of the cylinder itself.

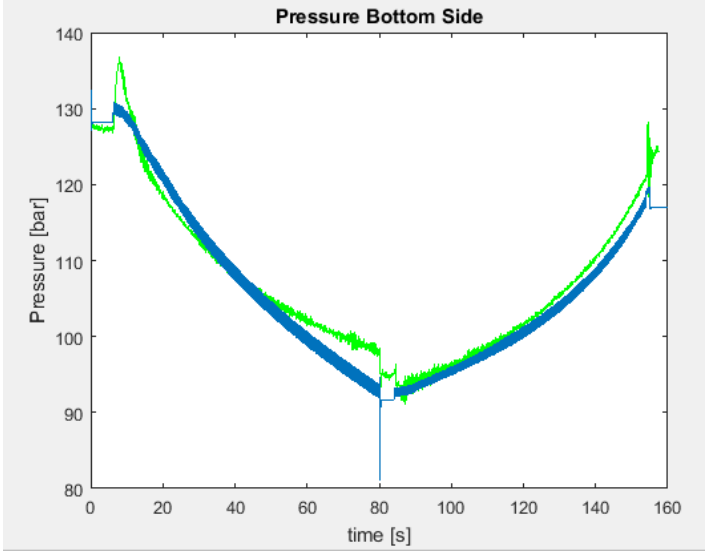

Figure 7.17 - Comparison of the hydraulic pressure in case the gangway will be retracted 2.5 [m] from t=20 [s] to t=80 [s].

7 Modeling the Control Sub-System

In this section the control sub-system will be discussed extensively. Goal of the control sub-system is to compensate the ship motions in order to minimize the displacement of the compensation point: the tip of the gangway. In figure 8.1 below a schematic representation of the control system is shown. From previous chapters is known that motion compensation is achieved by the actuators which receives feedback and feedforward signals from the PLC. These actuators are the luffing cylinders which cause the gangway luffing up and down (rotation around the main hinge), the hydraulic motor which drives the telescoping winch for telescoping back and forth and the hydraulic motor which drives the slewing gearbox. The last one is not considered in this thesis due to the restricted time and scope of the master thesis. This means that the motion compensation will be applied on a 2D system with two degrees of freedom. In this 2D model there are 3 possible ship motions which can be applied: heave, sway and roll. In section 8.2 this will be explained.

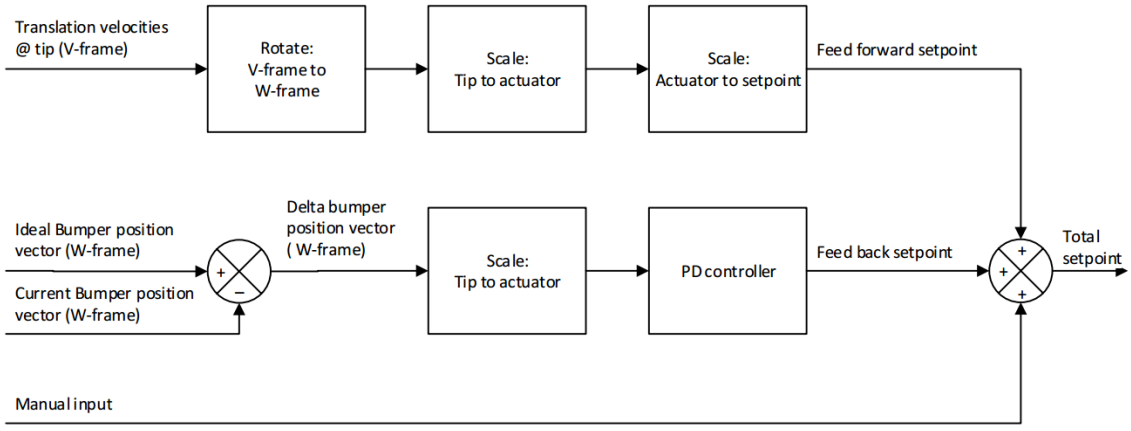

Figure 8.1 – Diagram of the control system for the active motion compensation, as applied at the company

7.1 Used Controller: P-Controller

In this thesis a P-controller is used to control the compensation point. A P-controller is a basic type of control which is applied on the measured error of a system, with respect to a certain reference set point. For a more accurate control, often a PID-controller is used. In the diagram of 8.2 the working principle of this control is shown. The PID-controller consists of a Proportional element, an Integral element and a Derivative element, all three connected parallel. All of them take the error as input. Kp, Ki and Kd are the gains of the P, I and D elements respectively. The type of control applied in the simulation model is a basic P-controller which means that the control system consists of the Proportional element, which is applied on the error of the gangway tip. Practically, this means that the measured error (displacement of the gangway tip) will be multiplied by a gain (Kp) where after the signal will be fed back to the system. At KENZ a PD-Controller is applied which also contains the derivative element and causes a more accurate control. Normally, the proportional gain can be determined using systems and control theory. However, in the construction of the control sub-system in the simulation model this Kp-value will be determined empirically (section 8.3). Besides the P-Control which is applied in the feedback, there is also a feedforward loop required for the control sub-system. This feedforward is applied on the velocities of the compensation point and can be considered as a prediction of the motion of the gangway top caused by the wave induced vessel motions. In section 8.3 the feedback and feedforward loop will be discussed extensively.

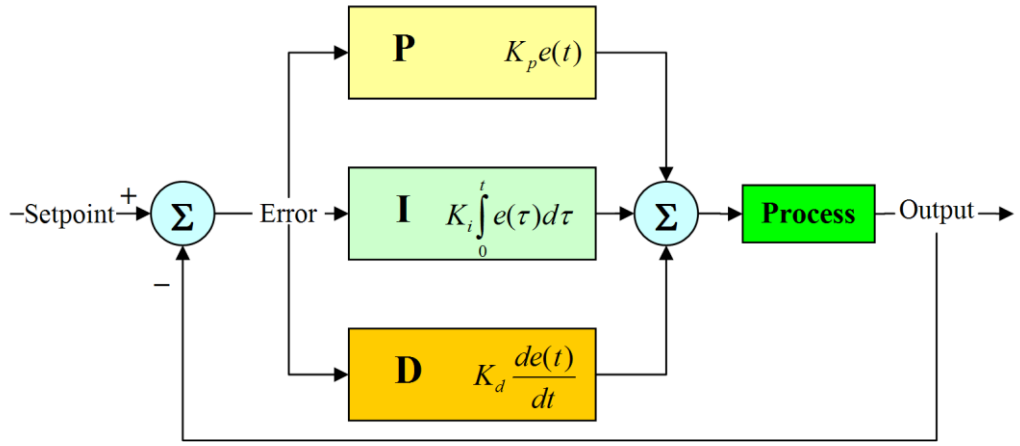

Figure 8.2 - Schematic representation of the working principle of a PID Controller

7.2 Considered ship motions, configuration parameters and sign conventions

Since a 2D model is considered, the applied ship motions are reduced from 6 to 3 motions: heave, sway and roll. These 3 motions will be applied on the COG as a translation in the z-direction (heave), translation in x-direction (sway) and a rotation of the COG around the y-axis (Roll) which represents the roll motion. In figure 8.3 a schematic overview of the gangway configuration and the relevant parameters are shown.

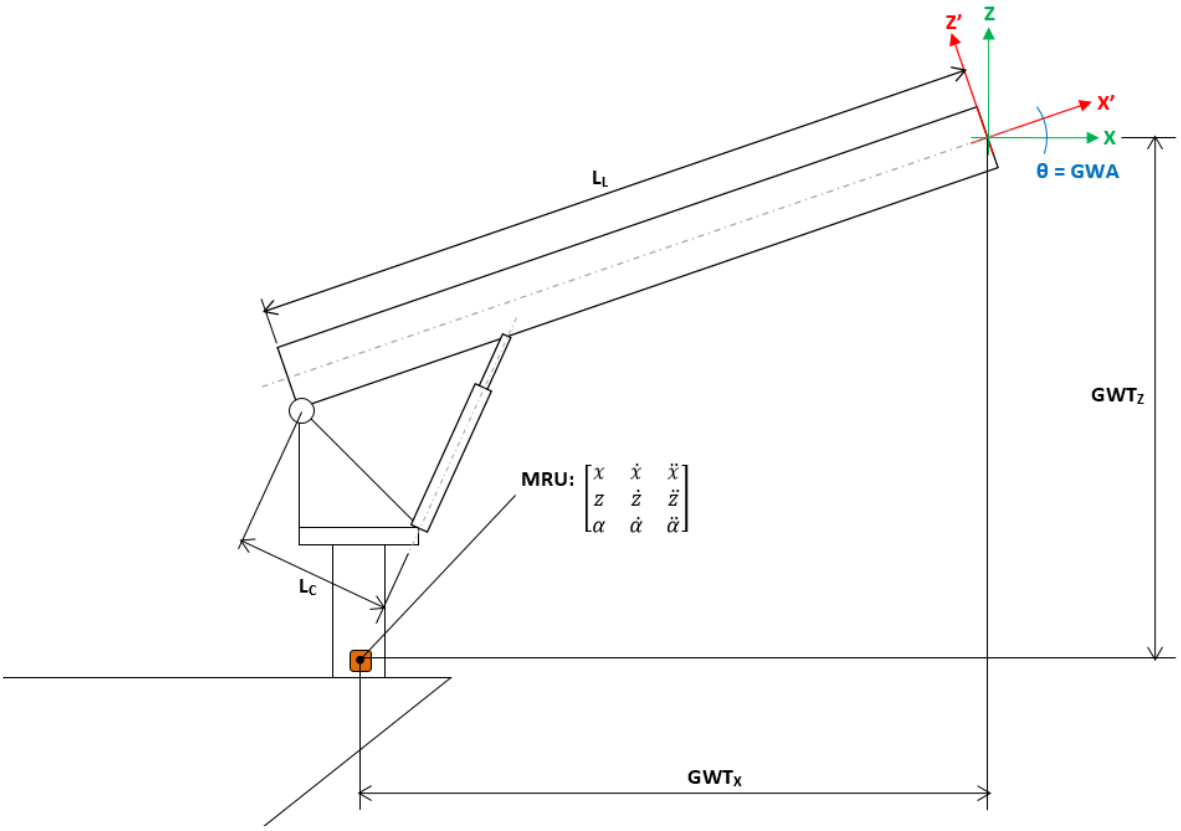

Figure 8.3 - Important configuration parameters and conventions for the control sub-system

The ship motions are measured at a certain point of the vessel. In the configuration as shown in figure 8.3 the MRU is placed at the pedestal. For the sake of simplicity, in the simulation model the COG of the ship is assumed to be on the cross section of the Underside Slewing Bearing and the centerline. This point is located at the bottom of the mainframe. An important parameter for the control sub-system is the vector from the MRU towards the compensation point. This is called the 'lever arm' and in figure 8.3 this vector is decomposed in the global coordinates GWT_X and GWT_Z. The parameter L_L is the distance from the main hinge till the compensation point. This will also be indicated as the telescoping length. The parameter L_C is the perpendicular distance from the main hinge to the actuation direction of the hydraulic cylinder. Furthermore at the gangway tip (compensation point), the rotation is shown from the global coordinate system (XYZ) to the walkway frame (x'y'z'). The required angle for the rotation matrix is the luffing angle θ. In the next section all these parameters will be used for the calculation of the required compensation as consequence of the applied MRU Motions.

7.3 Modeling the feedforward and the feedback loop of the control sub-system

For the motion compensation, feedforward and feedback on the motion of the compensation point has to be applied. First, the feedforward has to be applied in order to predict the new position and counteract this predicted motion. The feedforward will be applied on the velocity of the gangway tip. The feedforward gains will be determined theoretically by using the characteristics of the proportional servo valve (figure xx). After the feedforward is applied on the signals from the MRU, feedback will be applied on the error of the gangway tip. The feedback gains will be decided empirically as stated in section 8.1. The feedback and feedforward set point signals will be summed up before they will be applied on the actuators of the gangway. So the most important task in the control sub-system is the determination of the velocity and displacement of the gangway tip, given a certain ship motion.

This will be done in several steps which will be explained in detail:

Step 1: Determine the lever arm coordinates: GWTX and GWTZ

The lever arm is the vector from the MRU towards the compensation point. This vector is required for the transformation of MRU Motions to the compensation point. This operation has to be done for the feedforward as for the feedback control as well. The lever arm depends on the actual luffing angle and telescoping length of the gangway (configuration at every time step). If the MRU is located on the bottom of the mainframe the lever arm can be de decided using the following equations:

$$\mathrm{GWT_X} = L_L \cdot \cos(\theta) - dimA \qquad (8.1)$$

$$\mathrm{GWT_Z} = L_L \cdot \sin(\theta) + dimC + dimD \qquad (8.2)$$

Where

θ = Luffing Angle	[deg]
L_L= Telescoping Length	[m]
dim_A = 0.58	[m]
dim_C=1.9	[m]
dim_D = 1.032	[m]

Step 2.1: Transformation of the measured MRU velocities to the corresponding velocities at the gangway tip: Velocity at MRU → Velocity at Compensation Point

The feedforward will be applied on the velocity of the compensation point. In order to get the right velocities (in the global coordinate system) at the compensation point, the ship motions have to be transformed. This is done through the following formulas:

$$\dot{x}_{CP\_Global} = \dot{x}_{MRU} + \dot{\alpha}_{MRU} \cdot GWT_Z \qquad (8.3)$$

$$\dot{z}_{CP\_Global} = \dot{z}_{MRU} - \dot{\alpha}_{MRU} \cdot GWT_X \qquad (8.4)$$

Where

$\dot{x}_{CP\_Global}$ = the velocity in the global x-direction of the compensation point	[m/s]
$\dot{z}_{CP\_Global}$ = the velocity in the global z-direction of the compensation point	[m/s]
$\dot{x}_{MRU}$ = the measured translational speed of the ship in the global x-direction (sway)	[m/s]
$\dot{z}_{MRU}$ = the measured translational speed of the ship in the global z-direction (heave)	[m/s]
$\dot{\alpha}_{MRU}$= the measured rotational speed of the ship around the COG (Roll)	[deg/s]

Analyzing the equations 8.xx , the velocities at the compensation point $\dot{x}_{CP\_Global}$ and $\dot{z}_{CP\_Global}$ are a result of the summation of two types of motion, generated by the ship: translation and rotation, of

which the last one has to be multiplied by the concerning lever arm. This is required for converting a rotational speed into a translational speed.

Step 2.2: Transformation of the measured MRU displacements to the corresponding displacements at the gangway tip: Displacement at MRU → Displacement at the gangway tip

Similar to step 2.1 in this step, the displacements measured at the MRU are transformed into displacements at the gangway tip. This step is part of the feedback process which is applied. In this step the error, which is the calculated displacement from a chosen reference point, can be calculated. This error is required for the next step in the feedback process. The error in the global coordinate system will be calculated through the next formulas:

$$\varepsilon_{X\_Global} = x_{MRU} + GWT_X \cdot \cos\alpha_{MRU} - GWT_Z \cdot \sin\alpha_{MRU} - x_{Reff} \quad (8.5)$$

$$\varepsilon_{Z\_Global} = z_{MRU} + GWT_X \cdot \sin\alpha_{MRU} + GWT_Z \cdot \cos\alpha_{MRU} - z_{Reff} \quad (8.6)$$

Where

ε_{X_Global} = the global error in x-direction [m]
ε_{Z_Global} = the global error in z-direction [m]
x_{MRU} = the measured displacement of the ship in the global x-direction (sway) [m]
z_{MRU} = the measured displacement of the ship in the global z-direction (heave) [m]
α_{MRU} = the measured rotation of the ship around the y-axis in the global x-direction (roll) [deg]
x_{Reff} = global x-coordinate of the reference point [m]
z_{Reff} = global z-coordinate of the reference point [m]

In the equation it can be noticed that the error is calculated by subtracting the reference coordinate from the actual gangway tip. The actual gangway tip is calculated by applying the rotation matrix on the actual lever arm of the gangway tip.

Step 3.1: Rotation of the gangway tip velocities from the vessel coordinate system to the gangway coordinates system (walkway frame)

After the velocities in global coordinate system are calculated during step 2.1, this velocities has to be rotated to the walkway frame in order to obtain the required velocities that has to be performed by the actuators (telescoping winch and hydraulic cylinder). This rotation is simply realized by applying the rotation matrix on the calculated velocities $\dot{x}_{CP\_Global}$ and $\dot{z}_{CP\_Global}$:

$$\begin{bmatrix} \dot{x}_{WW} \\ \\ \dot{z}_{WW} \end{bmatrix}_{GWT} = \begin{bmatrix} cos\,\theta & sin\,\theta \\ -sin\,\theta & cos\,\theta \end{bmatrix} \begin{bmatrix} \dot{x}_{CP\_Global} \\ \\ \dot{z}_{CP\_Global} \end{bmatrix} \quad (8.7)$$

Where

$\dot{x}_{WW\_GWT}$= the velocity of the gangway tip in the x'-direction of the walkway frame [m/s]
$\dot{z}_{WW\_GWT}$ = the velocity of the gangway tip in the z'-direction of the walkway frame [m/s]
θ = Luffing Angle [deg]

Step 3.2: Rotation of the calculated errors of the gangway tip from the vessel coordinate system to the gangway coordinates system

Similar to step 3.1, the calculated errors from step 2.2 will be rotated to the walkway frame (see figure 2.3 in section 2.6) using the same rotation matrix:

$$\begin{bmatrix} \varepsilon_{X\_WW} \\ \\ \varepsilon_{Z\_WW} \end{bmatrix}_{GWT} = \begin{bmatrix} cos\ \theta & sin\ \theta \\ -sin\ \theta & cos\ \theta \end{bmatrix} \begin{bmatrix} \varepsilon_{X\_Global} \\ \\ \varepsilon_{Z\_Global} \end{bmatrix} \tag{8.8}$$

Where

ε_{X_WW} = the error of the gangway tip in the x'-direction of the walkway frame [m]
ε_{Z_WW} = the velocity of the gangway tip in the z'-direction of the walkway frame [m/s]
θ = Luffing Angle [deg]

Step 4: determine the ratio between the telescoping length and perpendicular arm and perpendicular arm: f

The feedforward and feedback on the luffing actuation are applied on the cylinder velocity. The displacement of the cylinder is not in the same direction as that of the z-direction of the walkway frame. Therefore, the calculated velocity at the gangway tip $\dot{z}_{WW}$ and the calculated error ε_{Z_WW} has to be multiplied by a factor. This factor is the ratio of the telescoping length L_L over the perpendicular L_C, indicated with the line L in figure 8.4:

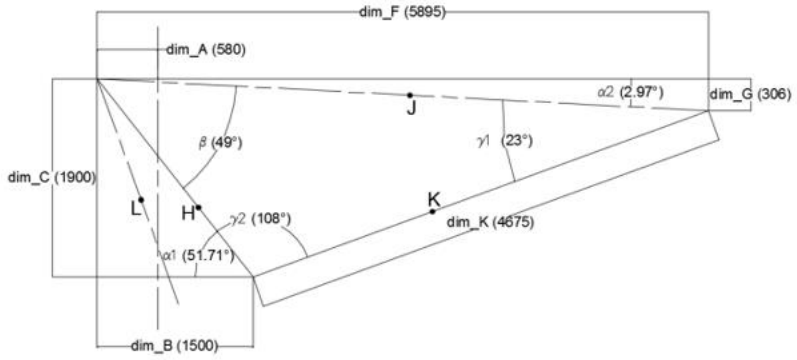

Figure 8.4 - Configuration parameters of the gangway

De perpendicular distance L_C is dependent on the luffing angle θ and can be calculated using the cosine rule:

$$f = \frac{L_C}{L_L} \tag{8.9}$$

$$L_C = J \cdot \sin \gamma_1 \tag{8.10}$$

$$\gamma_1 = J \cdot \cos^{-1} \frac{K^2 + J^2 - H^2}{2\ K\ J} \tag{8.11}$$

$$K = \sqrt{H^2 + J^2 - 2 \cdot H\ J \cdot \cos(\beta - \theta)} \tag{8.12}$$

Where

γ_1 = the angle between dimension J and K (see figure 8.4)	[deg]
β = the angle between dimensions J and H (see figure 8.4)	[deg]
θ = the actual luffing angle	[deg]
J = 5.903	[m]
H = 2.421	[m]

Step 5.1: determine the feedforward gains

After finishing step 4, the required compensation motions (velocities) for the luffing cylinder and the telescoping gangway can be calculated through multiplying the velocity with the ratio f:

$$\mathrm{V}_{\mathrm{Cylinder}} = \dot{z}_{WW\_GWT} \cdot f \qquad (8.13)$$

Where

$\mathrm{V}_{\mathrm{Cylinder}}$= cylinder velocity on which the feedforward gain has to be applied	[m/s]
$\dot{z}_{WW\_GWT}$ = the velocity of the gangway tip in the z'-direction of the walkway frame	[m/s]
f = ratio factor, as calculated in step 4	[-]

In order to determine the corresponding required flow through the cylinder to perform the required luffing actuation, the following formula is used:

$$\mathrm{Q}_{\mathrm{Cylinder}} = \mathrm{V}_{\mathrm{Cylinder}} \cdot A_{Bottom} \qquad (8.14)$$

Where

$\mathrm{Q}_{\mathrm{Cylinder}}$= required flow through the cylinder to perform the feedforward motion	$[m^3/s]$
$\dot{z}_{WW\_GWT}$ = the velocity of the gangway tip in the z'-direction of the walkway frame	[m/s]
A_{Bottom} = surface area of the bottom side of the hydraulic cylinder	$[m^2]$

Since the leakage area of the valve is assumed to be very small, losses of the flow are neglected and the calculated $\mathrm{Q}_{\mathrm{Cylinder}}$ is assumed to be equal to the required flow through the servo valve $\mathrm{Q}_{\mathrm{Servo}}$:

$$\mathrm{Q}_{\mathrm{Servo}} = \mathrm{Q}_{\mathrm{Cylinder}} \qquad (8.15)$$

In order to perform this motion the correct set point signals for these actuators has to be calculated. This is done by multiplying the obtained velocities by a feedforward gain. For the feedforward control this is simply the operation for translating the velocities back in to the corresponding set point signals. For the luffing set point, the servo valve characteristic curves of figure 8.5 can be used:

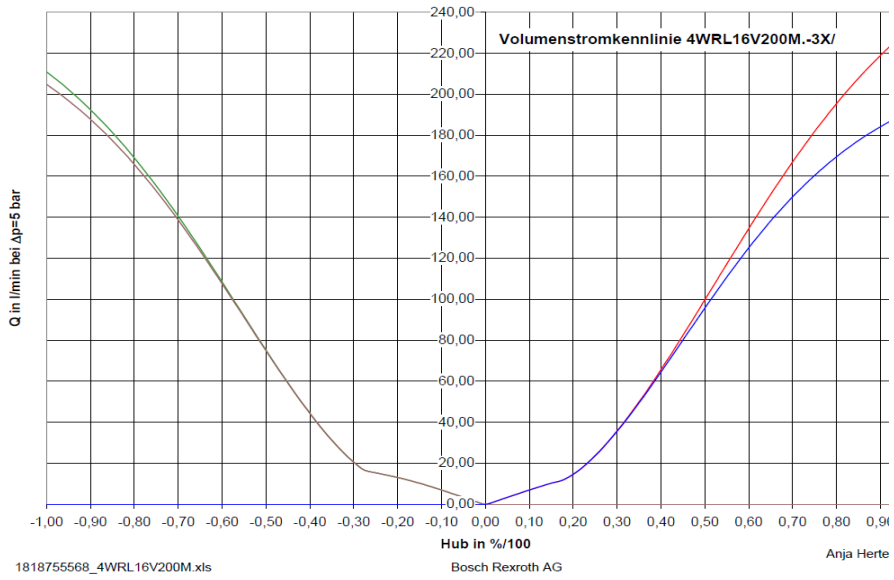

Figure 8.5 - Curve for the relationship between the flow through the servo valve and the applied set point signal [Bosch Rexroth]

As discussed in section 6.2.3, this curve is divided in 4 sections. This has also to be taken into account by converting the required flow to the corresponding signal. By taking the inverse relationship between the flow Q_{Servo} through the valve and the applied set point signal (section 6.2.3), the required set point signal given a required flow can be determined:

$$S_{Luffing} = (Q_{Servo+0.00030811)} \cdot 0.96 \quad \text{if } Q_{Servo} > 0.001084 \tag{8.16}$$

$$S_{Luffing} = Q_{Servo} \cdot 3.69 \quad \text{if } 0 < Q_{Servo} \leq 0.001084 \tag{8.17}$$

$$S_{Luffing} = Q_{Servo} \cdot 4.027 \quad \text{if } -0.00149 \leq Q_{Servo} \leq 0 \tag{8.18}$$

$$S_{Luffing} = (Q_{Servo\ -\ 0.0044314)} \cdot 1.013 \quad \text{if } Q_{Servo} < -0.00149 \tag{8.19}$$

Where:

$S_{Luffing}$= required set point signal for the control member displacement of the servo [m]
Q_{Servo}= the calculated required flow through the servo valve [m^3/s]

It's important to note that in the numerical model the set point signal for the servo valve differs from that of the control signal applied in the real servo valve. In the simulation model the orifice opening is regulated by a spring (control member displacement) and in the real world case this is done by electric signals (voltages) to the control member of the servo valve.

In figure 8.6 the construction of the feedforward block in the Simscape model is shown:

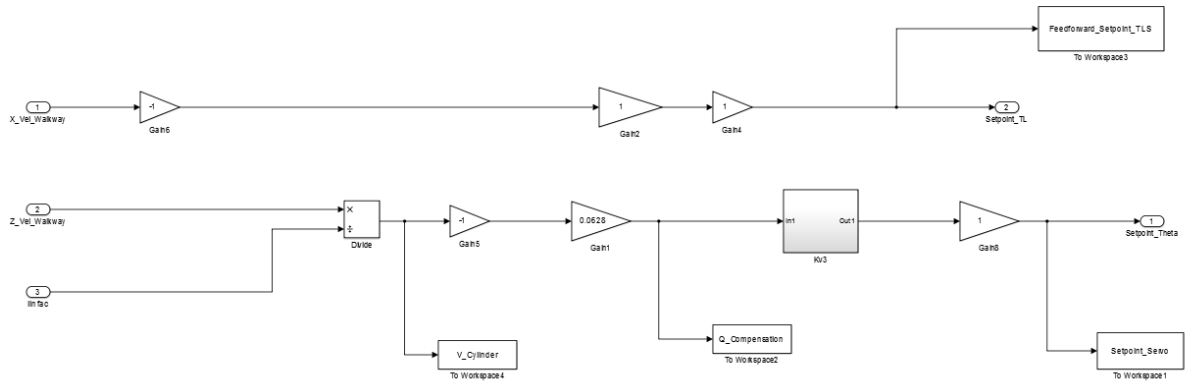

Figure 8.6 - Simscape model representation of the feedforward gain, used for the feedforward compensation

In contrast to the feedforward gain for the telescoping function, the feedforward gain for the telescoping actuation is basic. Since the telescoping function is built in such a way that it's possible to directly impose the velocity of the telescoping motion, the calculated telescoping velocity ($\dot{x}_{WW\_GWT}$) has only to be multiplied by -1 in order to compensate the telescoping motion in the right direction.

In contrast to the feedforward gains which are determined theoretically, the feedback gains are determined empirically (as mentioned in section 8.1). These gains could also be determined by an extensive analyses using control theory which was not the scope of this thesis. For the simulation model these gains are determined empirically by choosing starting values for the telescoping feedback gain $K_{P,TLS}$ and luffing feedback gain $K_{P,LF}$. This is also the way the values are determined at Kenz. From these starting points the gains will be tuned till a critical point is approached. If this critical point is exceeded, the system becomes unstable. In figure 8.7 it can be seen the critical values for the feedback gains are approached and resulted in a luffing feedback gain of 0.01 and telescoping feedback gain of 1:

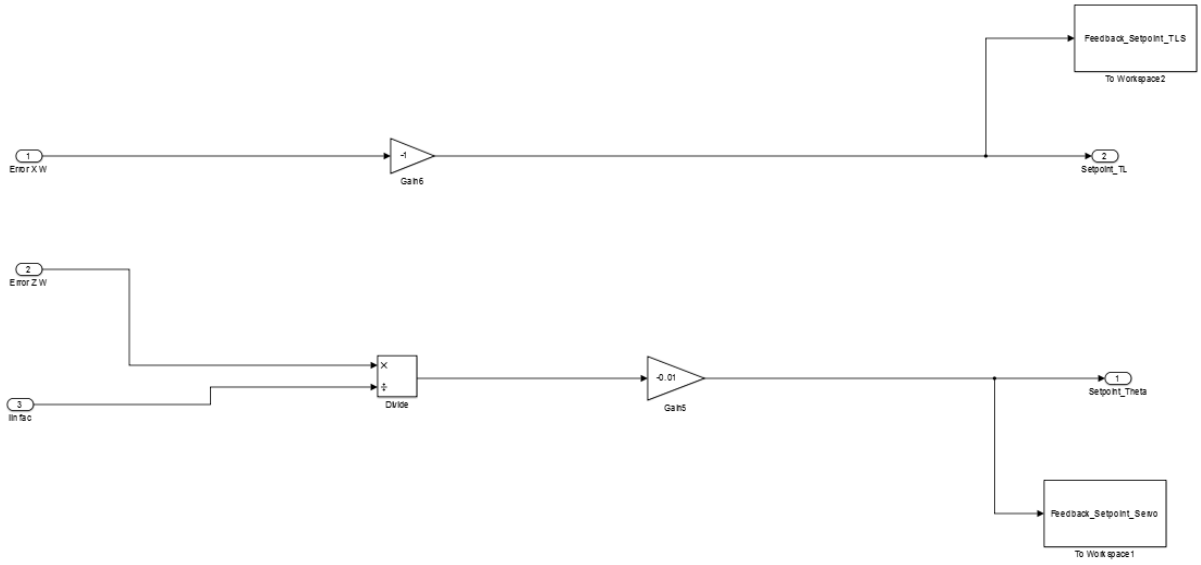

Figure 8.7 - Simscape model representation of the feedback gain, used for the feedback compensation

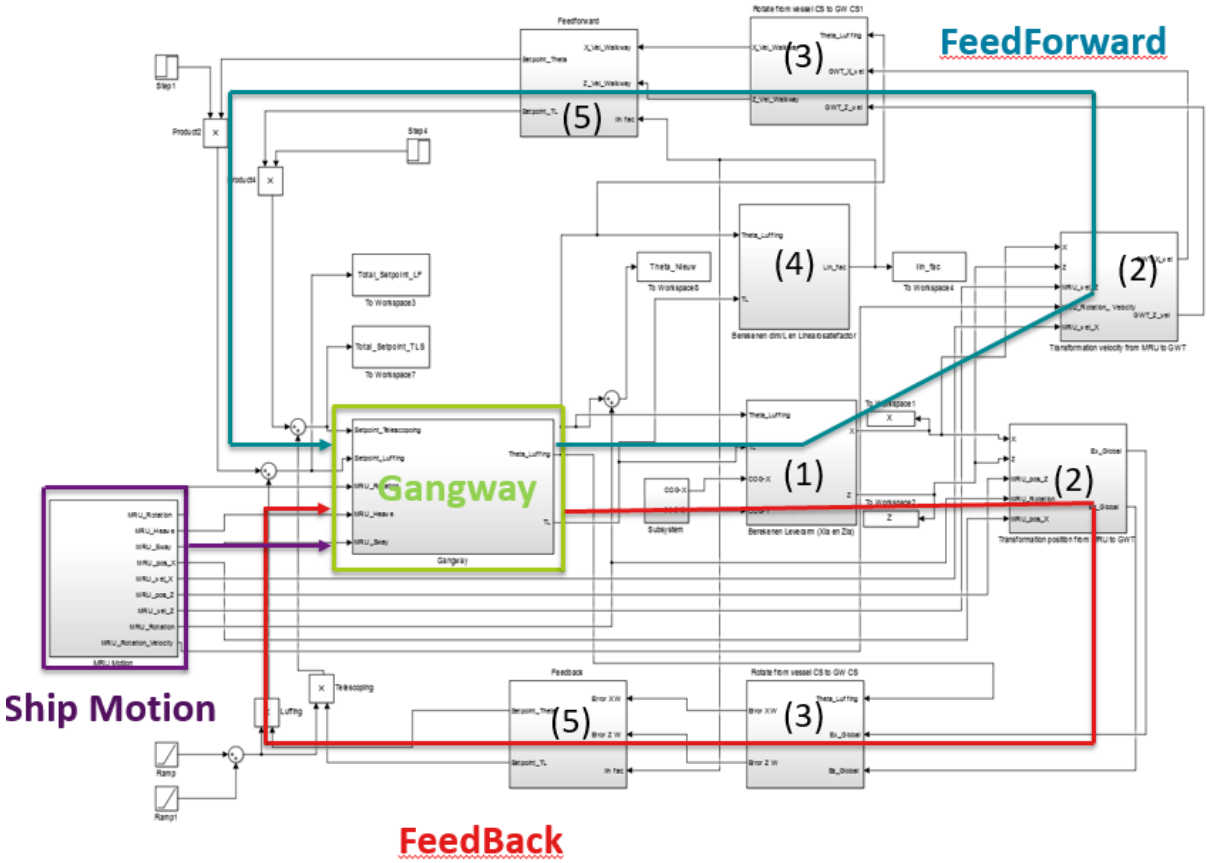

Figure 8.8 - Simscape model of the integrated control sub-system in the total gangway simulation model with the 5 steps of the feedback and feedforward loop indicated.

8 Results of the numerical 2D Simulation Model

After the control sub-system is finished, an integrated model of the mechanical, hydraulic and control sub-systems is created. After the verification of this model with simple checks presented and discussed in section 9.1, the model will be validated through analyzing and comparison of the results with experimental quayside tests conducted at the company. A lot of different tests, in order to assess the performance of the active motion compensation were conducted. These tests are called 'tracking error tests' and the main outcome is the measured error of the gangway tip with reference to a certain reference point. Besides this error tracking, a lot of other relevant parameters are logged during the tests. Interesting parameters to analyze are the cylinder pressures and the telescoping/luffing control set points, which are composed of the feedforward and feedback set point. In addition, the configuration of the parameters during the tests can be deduced from the logged luffing angle and telescoping distance at each moment. The test protocol for the conducted experimental tests at Kenz can be found in Appendix A. In section 9.3 the numerical simulation results will be shown after the same test settings from the experiments are applied on the 2D simulation model.

8.1 First Simulation Results of the integrated model

In this section, the obtained 2D numerical model will be tested through analyzing the motion of the gangway tip in three cases:

- Case 1: Response of the gangway system to applied ship motion, without any control
- Case 2: Response of the gangway system with only the feedforward loop applied
- Case 3: Response of the gangway system with the feedforward as well as the feedback loop applied on the compensation point

The gangway response is tested in these three cases to check if the model reacts on the feedforward (case 2) and feedback (case 3) as it should do in theory. In the first verification test, a roll motion is simulated by applying a sinusoidal input signal, as shown in figure 9.1 on the main luffing hinge. By imposing the motion on the main hinge, a rotation of the gangway around its pivot point can be considered which ensures that only the luffing motion is activated.

$$\alpha = 7\sin(0.2\pi t) \qquad (9.1)$$

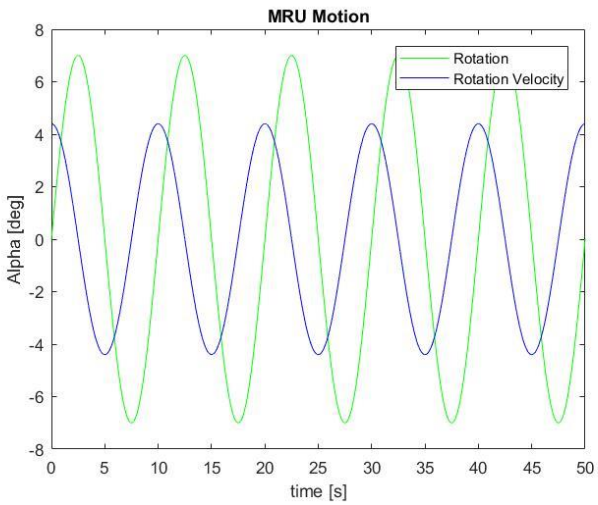

Figure 9.1 – Applied ship motion at the main hinge of the gangway structure: Amplitude = 7 [deg], Period= 10 [s], Starting telescoping distance = 1.18 [m] and starting luffing angle = 0 [deg] (gangway parallel to the vessel deck)

In the figure below the results of this first verification check are shown:

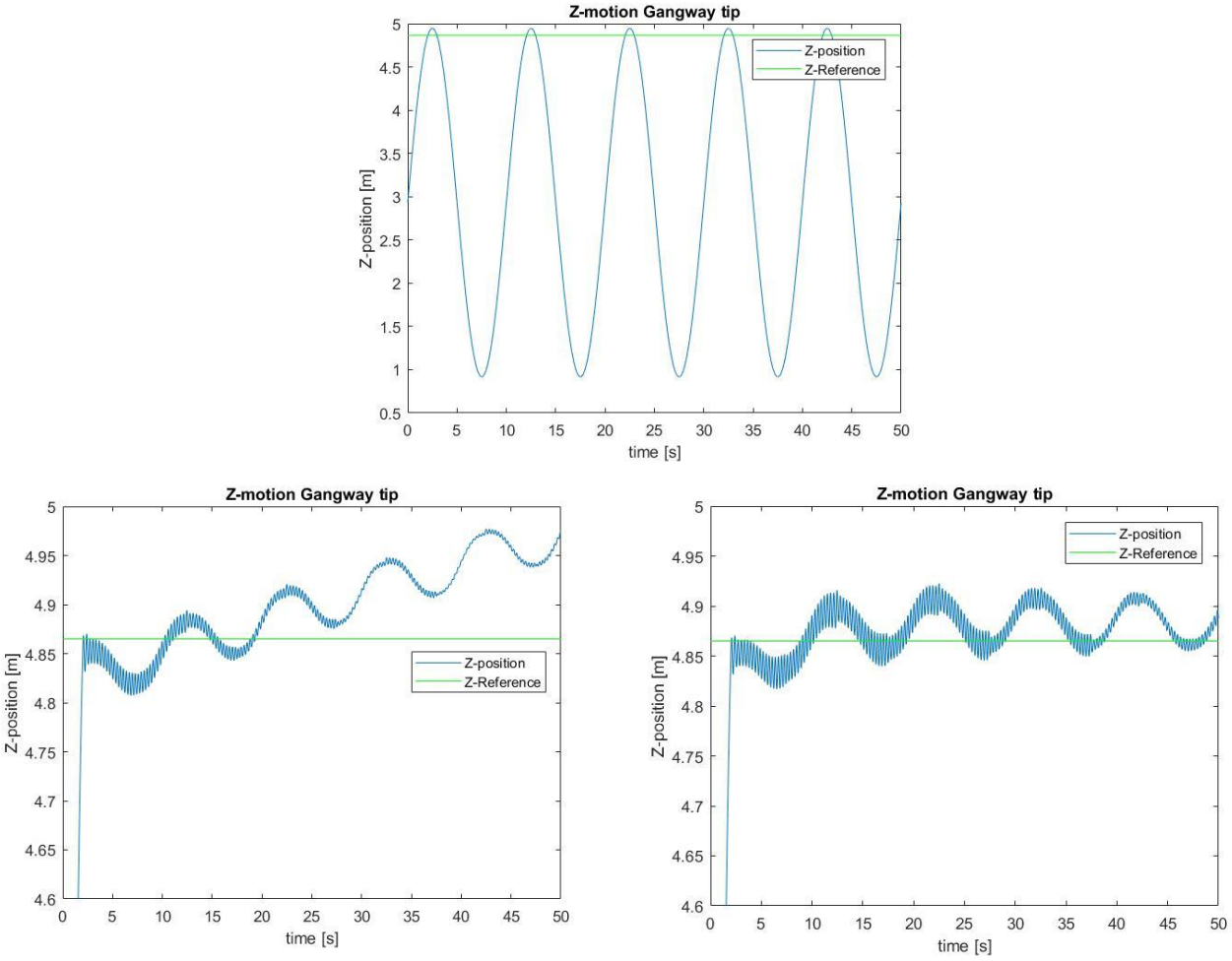

Figure 9.2 - The compensation point motion in vertical Z-direction in the situation without control (top), only feedforward (left bottom) and in the case both feedforward and feedback are applied (right bottom). Reference Z-Coordinate=4.865 [m]

In figure 9.2 the gangway response to the applied sinusoidal motion can be shown. In case 1 it can be seen that the gangway tip is just oscillating according the imposed motion. Since there is no control applied, the gangway will always follow the ship motion and will never be compensated to keep the gangway tip at the reference point. In case 2 and 3 control sub-system is activated after 2 seconds. At this moment, the actual position of the gangway tip will be set as the reference point. In figure 9.2, the Z-Coordinate of this position is indicated with the green horizontal line. The gangway tip will be compensated once the motion compensation is activated at this height. This reference point is 4.865 [m]. One can see that for case 1, the gangway tip will just move according the imposed sinusoidal roll motion. For case 2, it can already be seen that from time = 2 [s], the gangway tip is compensated towards the reference height. For case 3, a better compensation is realized. The reference point is reached earlier and the tracking error is slightly smaller than in the previous case. It can also be seen that in case 3 the gangway tip keeps oscillating around the reference height while in case 2 the gangway tip starts do drift from 30-35 [s] and starts to lose control. In figure 9.3 the results for the error in horizontal X-position are shown.

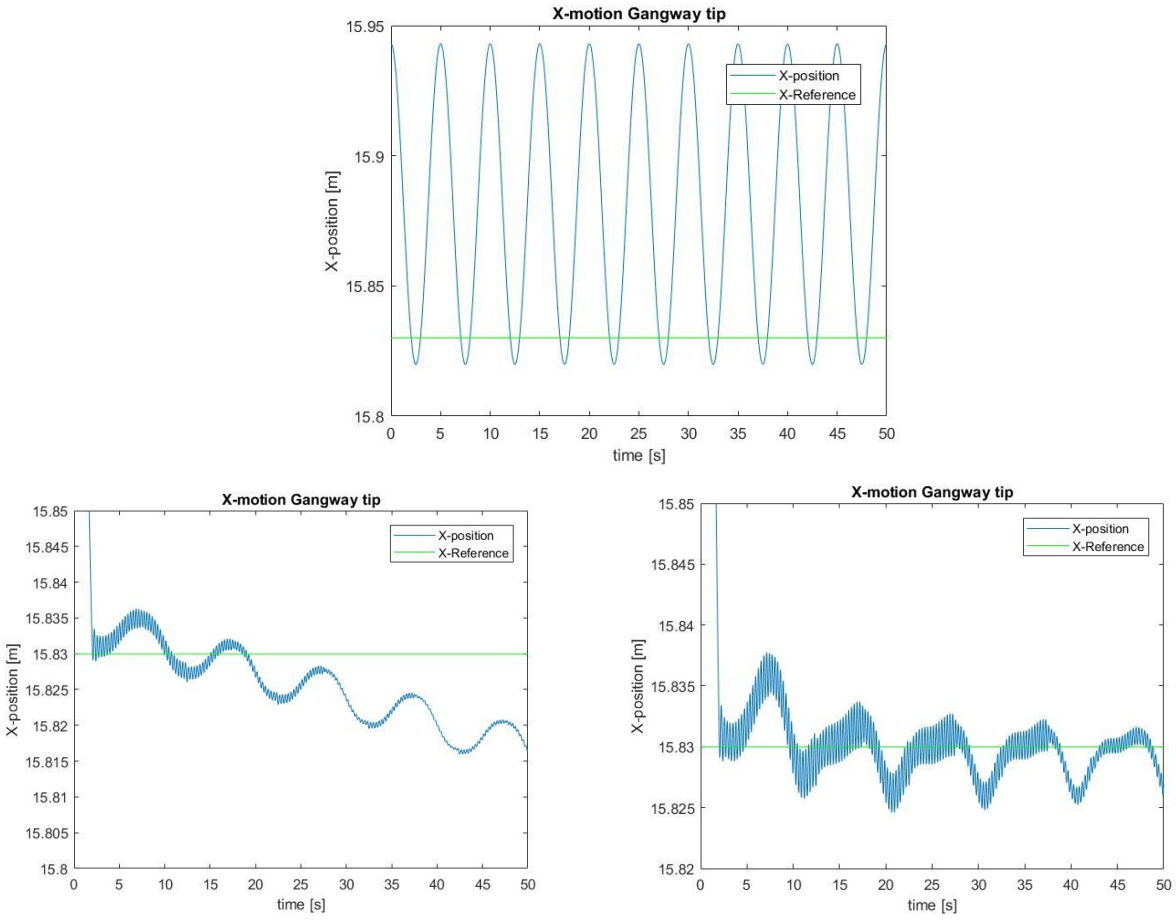

Figure 9.3 - The compensation point motion in vertical X-direction in the situation without control (top), only feedforward (left bottom) and in the case both feedforward and feedback are applied (right bottom). Reference X-Coordinate=15.83 [m]

For the error in horizontal direction, similar results can be seen as for the error in vertical direction. In both results, it can also be seen that there are two different frequencies in the charts that can be distinguished. The one with the larger period (smaller frequency) is due to the imposed motion and the high frequent motion is due to the natural frequency of the telescoping motion which is approximate 4 [Hz]. In figure 9.4, the pressure at the bottom side of the hydraulic luffing cylinder is shown for both cases is shown. The results are more or less the same except of the fact that in the case also the feedback is applied (case 3) the pressure in the cylinder has a slightly higher oscillation and frequency.

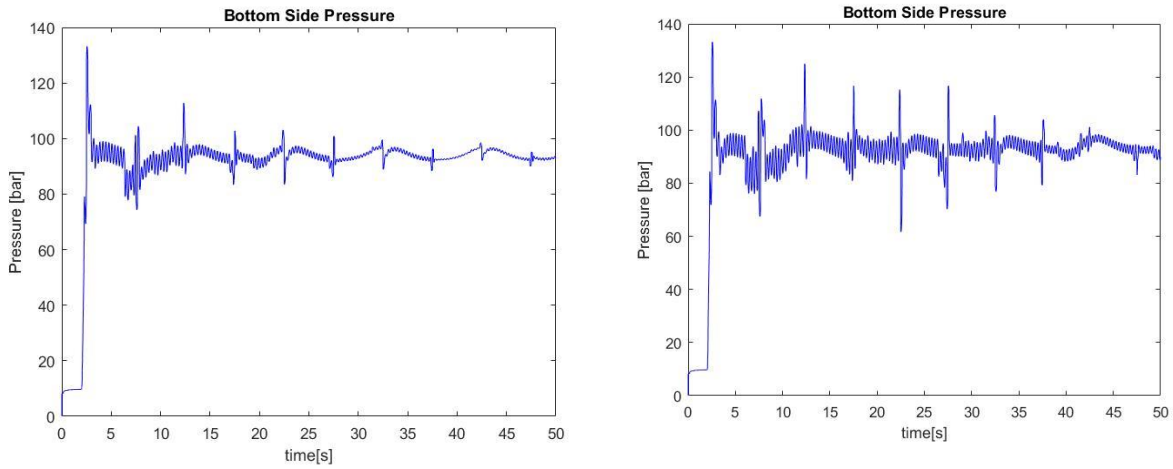

Figure 9.4 – The pressure at the bottom side of the cylinder in the case only feedforward (left) and in the case both feedforward and feedback are applied (right).

8.2 First Simulation Results/Validation of the Simulation Model

In this section the results of the created numerical model compared to the experimental quayside test results will be presented and analyzed. Quaysides tests are different from the actual situation offshore, where the vessel moves the system, and the gangway compensates the motion of vessel. In the quayside testing, the situation is reversed: the pedestal does not move and the tip of the system accelerates. In Appendix A, the setup of these tracking error tests can be found. During these tests, different sinusoidal signals are applied for the three possible motions: translation in vertical direction, which mimics the heave motion, translation in the horizontal direction, which mimics the sway motion and a rotation around the main hinge, which mimics the roll motion of the vessel. When applying only the roll motion or the sway motion, the luffing function and telescoping function respectively could be assessed separately. In theory, imposing a pure rotation (roll) around the main hinge should only cause a luffing error, which can be compensated by the luffing cylinders. This is the reason why this type of test is called the luffing test. In the same manner, the telescoping function of the gangway can be assessed by impose a pure sway motion. In the tables below, the test parameters for the luffing test and telescoping test are shown. As can be seen there are different speed settings which can be performed during the tests. In this section only the 100% speed settings are considered, since this are the most interesting results regarding the required power. Besides these three signals, combinations of these motions are also provided to assess the total performance of the system. Several variables are logged during the tests of which the compensation error, the measured control set points, and pressures in the hydraulic cylinder are analyzed thoroughly and compared with the simulation results.

Test speed [deg/s]		Amplitude [deg]	Period [s]	Test duration [s]
25[%]	1.50	6.00	25.13	320
50[%]	3.00	6.00	12.57	160
75[%]	4.50	9.00	12.57	160
100[%]	6.00	9.00	9.42	41 (1)

Table 9.1 – Luffing Test Parameters

Test speed [m/s]		Amplitude [m]	Period [s]	Test duration [s]
25[%]	0.25	2.00	50.27	640
50[%]	0.50	2.00	25.13	320
75[%]	0.75	2.00	16.76	210
100[%]	1.00	3.00	18.85	240

Table 9.2 – Telescoping Test Parameters

First, the results of the luffing test and telescoping test will be presented and analyzed. After the first analyses, the obtained numerical model will be adjusted by changing some variables or adding some physical phenomena, which were not taken into account initially. After these 'model improvements' the results will be analyzed again in order to see if the improvements make sense and verify the first conclusions.

8.2.1 Luffing test

In the figure below the imposed roll motion is shown which is used for the 100% speed setting Luffing test. As discusses in the previous section, the roll signal is ramped up and ramped down.

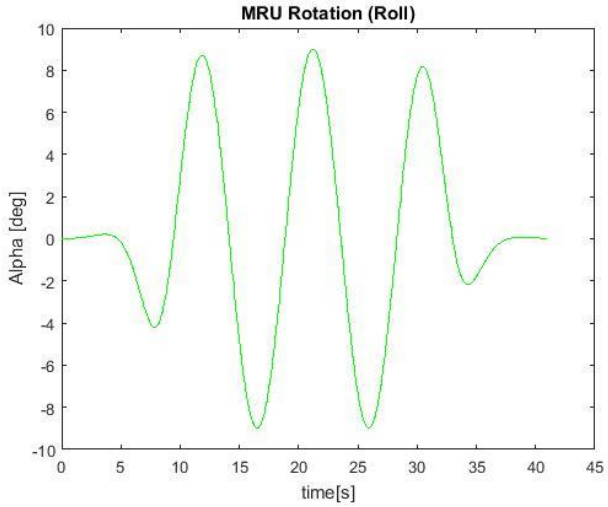

Figure 9.5 – Imposed Sinusoidal roll motion for the performance of the 100% speed setting Luffing test

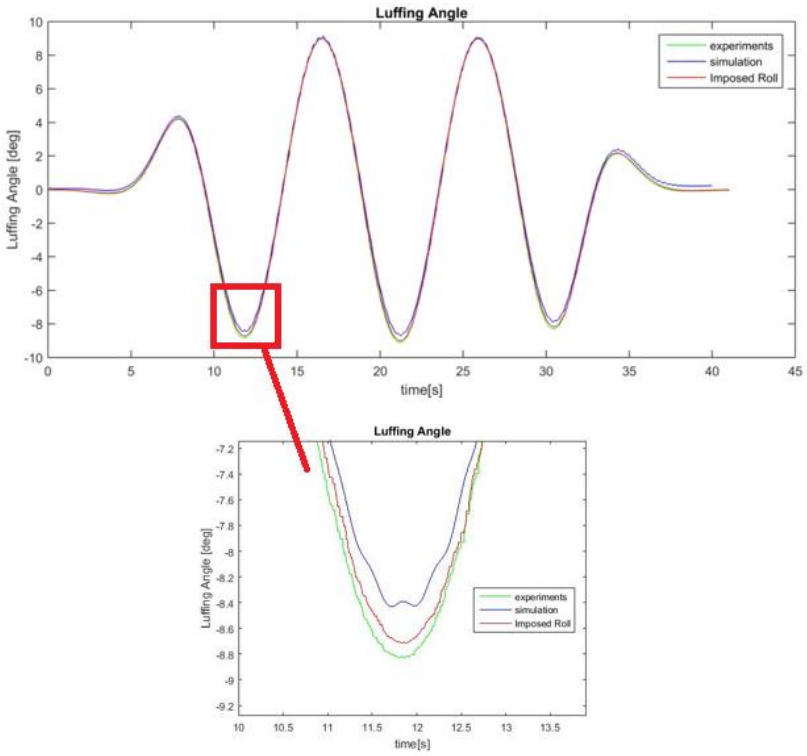

Figure 9.6 – Luffing angle of the gangway during the simulation and experimental quayside tests compared to the imposed roll motion.

In figure 9.6, the first important comparison is shown. In this chart the luffing angle during the numerical simulation is compared to the luffing angle during the quayside luffing test. Also the imposed roll motion is indicated. It can be observed that the three lines align quite well which gives the first positive conclusion that the dynamic response of the numerical model corresponds quite well with the dynamic response of the real gangway system. However, as expected, the alignment is not for 100%. The figure shows that especially when the lowest point is reached the lines starts to diverge. When zooming in on the area in which the gangway reaches its lowest point and start the upward luffing motion, interesting observations can be done. First remarkable observation is that the experiment shows that the gangway overshoots the imposed roll motion while the simulation model shows that the gangway turns back from a downwards into an upward luffing motion earlier and does not reach the depth corresponding to the imposed roll motion. It can also be observed that the blue line, which is the numerical result, contains a wave with a certain frequency in contrast to the green line (experiment). This behavior will be further investigated in the next sections.

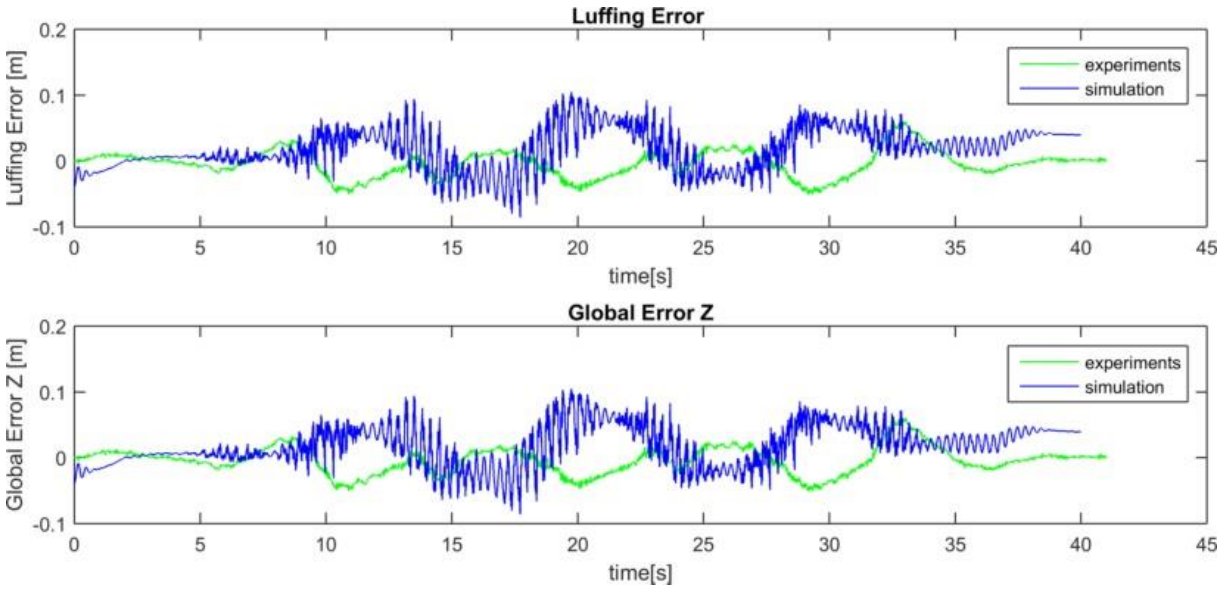

Figure 9.7 – The Luffing Error (top) and vertical global error (bottom) during the Luffing Test

In figure 9.7 the measured tracking errors are shown. Analyzing the luffing error it can be seen that the error in simulation model is larger than in the experiments. It can also be observed that it seems that the measures error of the model has the opposite sign of the tracked error during the experiments. This difference in sign is the result of the previous mentioned occurrence as shown in the bottom plot of figure 9.6. At the turning point (time = 12[s]), the experiment shows an overshoot while the simulation shows an undershoot which gives the physical explanation of the opposite results of the error.

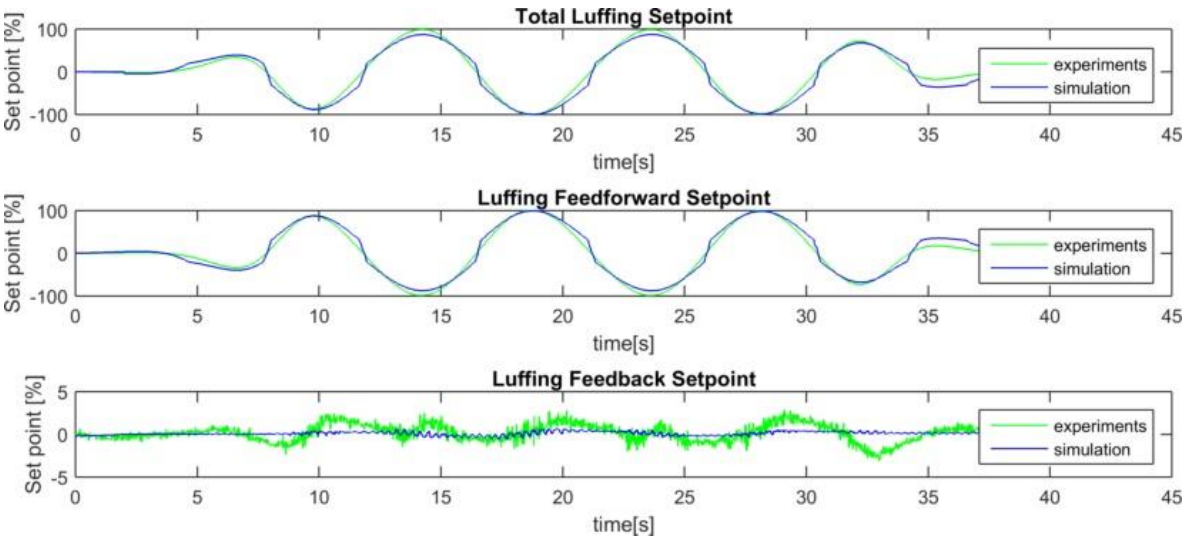

Figure 9.8 – Total luffing set point (top) which is composed of a set point due to the feedforward (middle) and the feedback loop (bottom)

In figure 9.8 the luffing set point for the compensation of the gangway tip can be seen. It can be observed that the results for the total set point aligns quite well. Again, at the turning point (from upward to downwards luffing) it can be seen that during experiments a 100% set point is reached while this is not the case in the simulation model. This can also be notices from the lower plot of the luffing feedback set point where it is clear that the feedback signal in the simulation are lower than the feedback signals in the experiments. This is an indication that the feedback does not perform as it supposed to do and probably the proportional feedback gain for the luffing motion is still too low. In the next sections this will be further investigated.

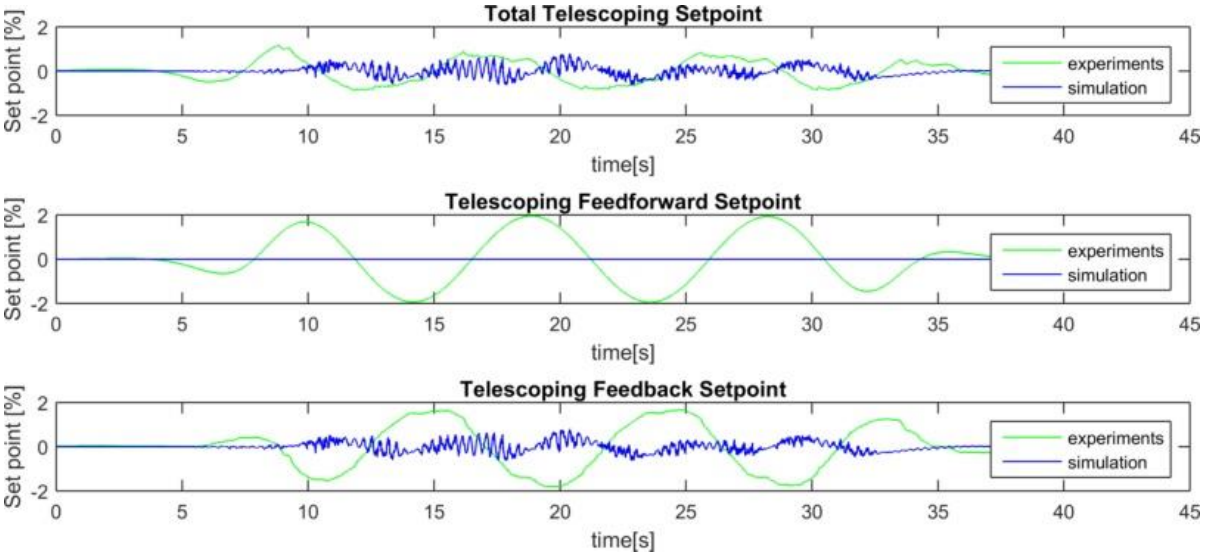

Figure 9.9 - Total telescoping set point (top) which is composed of a set point due to the feedforward (middle) and the feedback loop (bottom)

In figure 9.9 the telescoping set point for the compensation of the gangway tip is shown. This set point is of much lower interest than the luffing set point since in the luffing test, theoretically only the luffing system should be activated. However, when analyzing these telescoping set points it can be stated that the set points in the simulation model are lower than in the experiments which can be assigned to the fact that in the simulation model an ideal telescoping function is assumed.

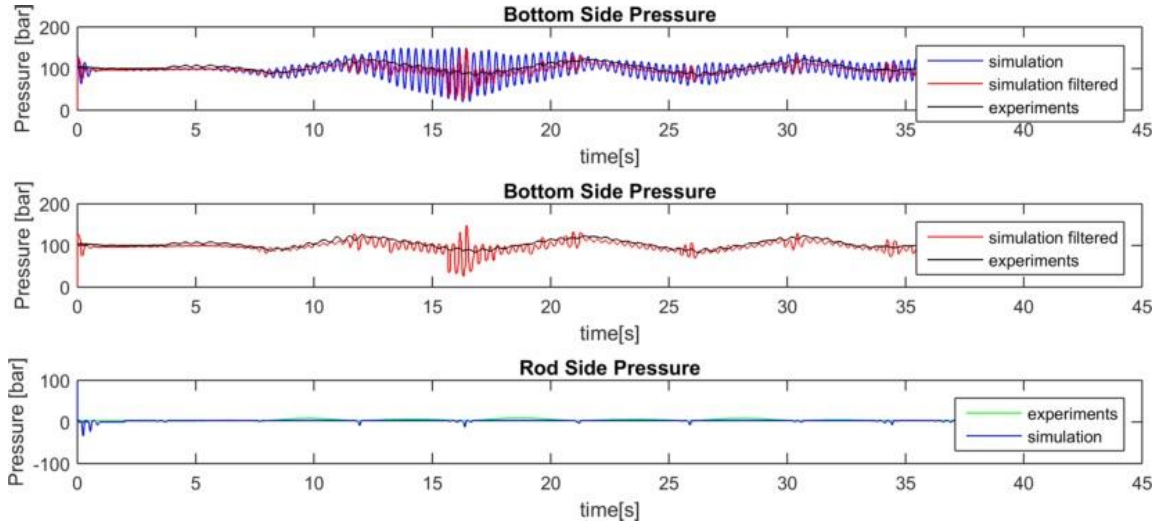

Figure 9.10 – Hydraulic Pressure at the bottom side of the cylinder (top), filtered simulation result of this pressure (middle) and the pressure at the rod side of the hydraulic cylinder (bottom)

In figure 9.10 the hydraulic pressures in the cylinder are shown. It can be observed that the (filtered) bottom side pressure of the simulation model corresponds quite well with that of the experiments. The simulation results show also a higher frequency response than the experimental results which means that the pressure is fluctuating much more during the simulation than in the experiments. It seems also that at certain points the simulation shows high peaks in the oscillation. The high oscillations and higher frequent behavior will be investigated in the next section about model improvements.

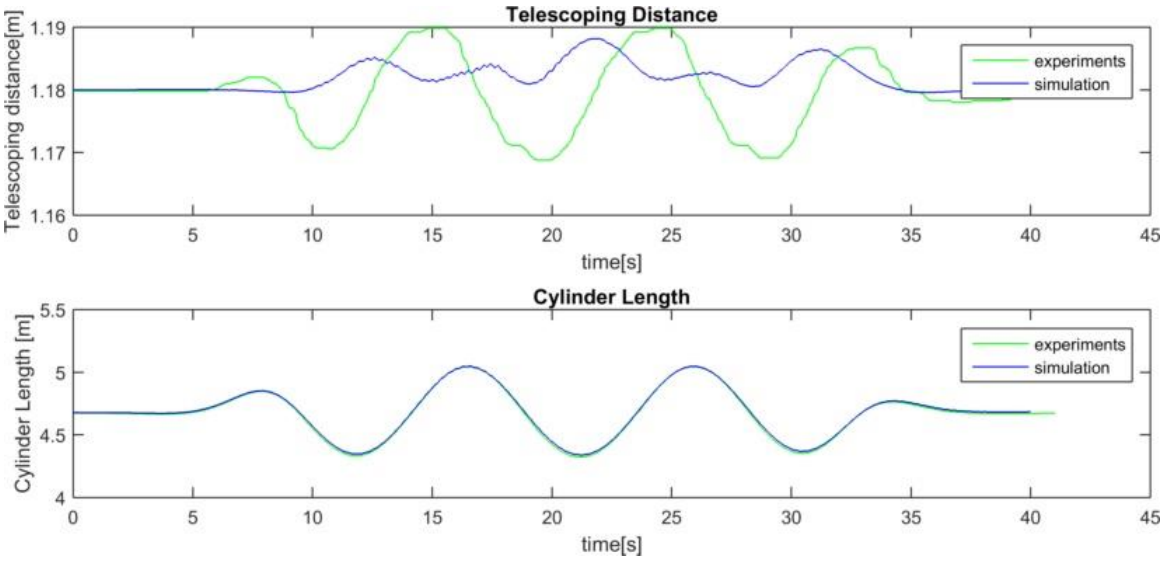

Figure 9.11 – Telescoping Distance (top) and Cylinder Length (bottom) of the gangway during simulation and experiment.

In figure 9.11 the telescoping distance and cylinder length are presented. It can be seen that at time= 5 [s] the results for the telescoping distance start to diverge which can also be assigned to the fact of that telescoping function is modeled as a theoretical ideal actuation system. Analyzing the cylinder length it can be seen that the results align much better which implied that the luffing motion (by displacement of the hydraulic cylinder) is more or less the same as in the experiments. Based on the results for the luffing angle and the cylinder length it can already be concluded that at least the numerical model shows big similarities in the dynamic response but gives visible present differences

in the hydraulic response (higher frequency in the simulation). This will be further investigated in the next sections.

8.2.2 Estimation of the required power

In general, the total required power that has to be installed in the whole system can be estimated using the following equation:

$$P_{Total} = P_{Luffing} + P_{Telescoping}$$

Where:

P_{Total} = Total required power [W]
P_{Pump} = Required power that is delivered by the pump [W]
$P_{Telescoping}$ = Required power needed for the telescopic motion [W]

The telescoping power can be calculated by the general power formula:

$$P_{Telescoping} = P_{Mechanical} = F \cdot v$$

Where:

$P_{Mechanical}$ = Total mechanical power for the telescopic motion [W]
F = The telescoping force during Active Motion Compensation [N]
v = Telescoping speed [m/s]

Since the telescoping function is barely activated during the luffing test, the telescoping is assumed to be negligible compared to the total hydraulic power. Important to notice is that the total required hydraulic power for the luffing motion is delivered by the pump and the accumulator. For the installed power only the pump power is included since the accumulator is an external power source. However, in order to perform the active motion compensation the required extra power delivered by the accumulator has to be determined precisely. Based on the estimation of the power that has to be supplemented by the accumulator, the amount and design of the accumulators can be determined. This is an important result and advantage thanks to the developed simulation model. So, the total power in order to perform the luffing motion is the summation of the power delivered by the pump P_{Pump} and the remaining required power delivered by the accumulatorP_{Accu}:

$$P_{Luffing} = P_{Pump} + P_{Accu}$$

To give an estimation of the hydraulic power the following formula can be used:

$$P_{Hydraulic} = P_{Luffing} = \Delta p \cdot \mathrm{Q}$$

Where:

$P_{Hydraulic}$ = Hydraulic power required for the luffing motion [W]
Δp = pressure drop over the power source (pump or accumulator) [bar]
Q = Flow delivered by the power source (pump or accumulator) [m^3/s]

In figure 9.12 below the estimated required hydraulic power for the active motion compensation during the simulation test is shown. It can be seen that the required power depends on the luffing

motion that has to be performed. In the upwards luffing motion the systems consumes in order to push the gangway against the gravity force. This power consuming motions can be recognized by the peaks that are visible in the plot of figure 9.28. During the luffing down motion the system does not require any power and the potential energy due to the gravity is stored in the accumulator by refilling it in this time intervals. This storage of energy is presented at the time intervals where the delivered accumulator power becomes negative. From figure 9.28 it can be seen that the maximum required hydraulic power during the luffing test is approximate 400 [kW]. The power is largely delivered by the accumulator (300 [kW]) and is supplemented by the pump (100 [KW]).

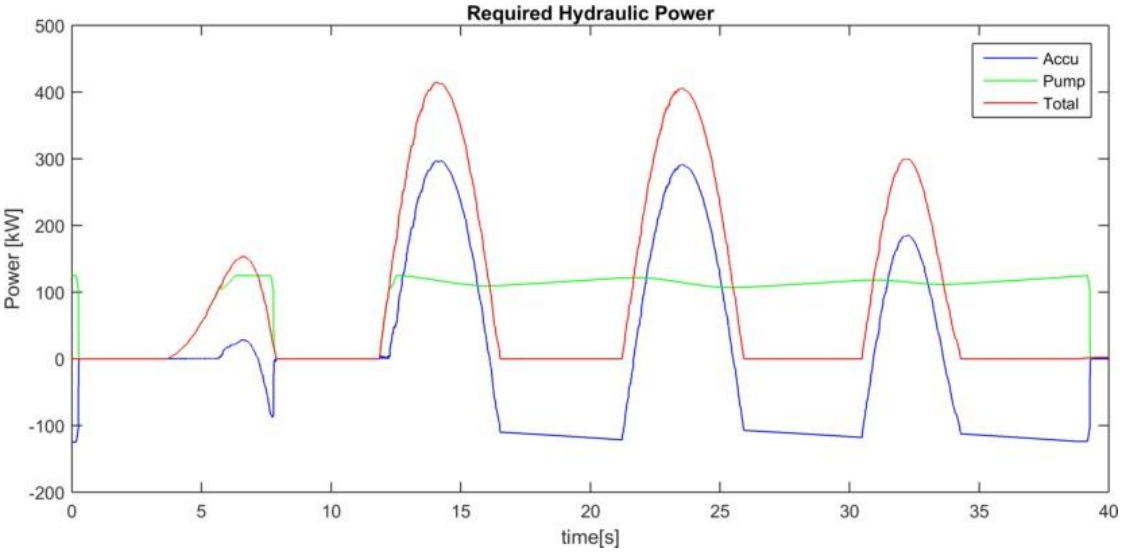

Figure 9.12 – Estimation of the required hydraulic power for the active motion compensation during the luffing test

8.3 Telescoping Test

For the telescoping test, a sinusoidal sway motion as shown in the figure below is imposed on the gangway system. The signal is ramped up and down, similar to the roll motion. For the telescoping test, the initial telescoping distance is changed to midstroke position, which means that at time = 0 [s], the gangway is telescoped 5 meters from its fully retracted configuration. The initial luffing angle is still 0 degrees, like in all conducted Personal Transfer Mode tests.

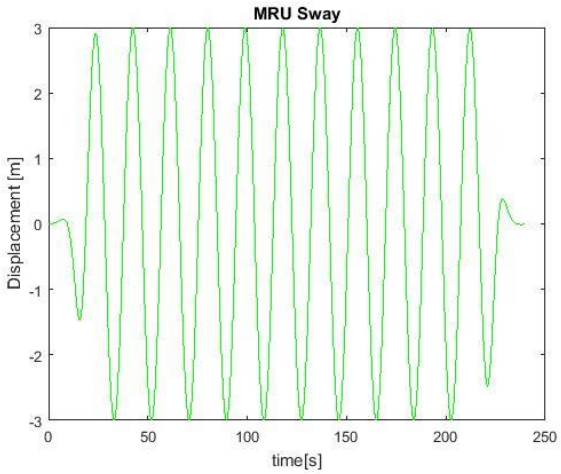

Figure 9.13 – Imposed Sinusoidal sway motion for the performance of the 100% speed setting Telescoping test

In figure 9.14 below the luffing angle during the simulation and experiments are compared to each other. Since there is no roll or heave motion imposed on the system, the luffing angle should be

theoretically zero during the whole test. However, a movement in the luffing angle can be seen in the figure below. It can be seen that during the experiments the gangway has a small negative luffing angle of approximate 0.02 [deg]. This can be assigned to the small leakages in the hydraulic luffing system which cause the hydraulic cylinder has a small inclination. The luffing angle during the simulation has a small positive value of approximate 0.04 [deg]. This can be assigned to the ideal angular velocity source which means that there is always a small amount of flow, due to the small leakages in the valves and cylinder that cause the cylinder is slightly displaced.

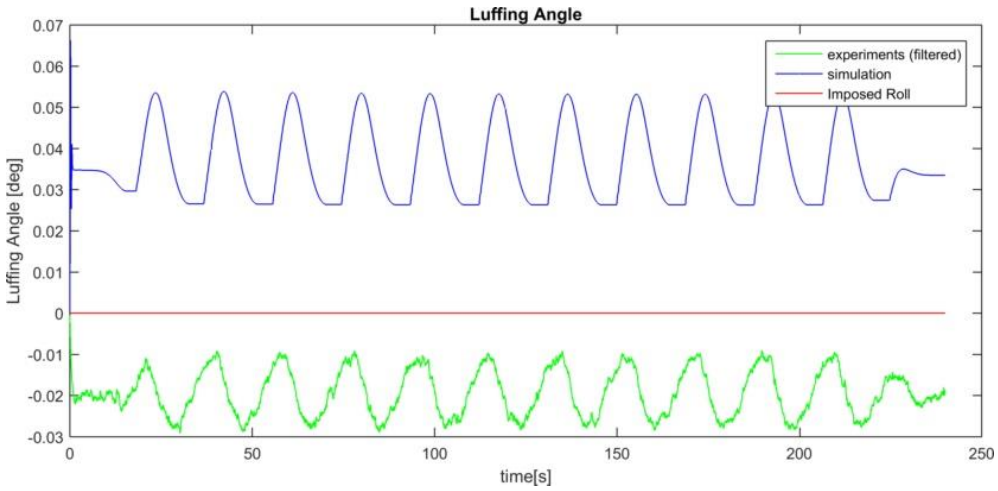

Figure 9.14 – Luffing angle of the gangway during the simulation and experimental quayside tests compared to the imposed roll motion (o [deg])

In figure 9.15 the telescoping error and luffing error during the simulation and experiments are compared to each other. When analyzing the telescoping error, it can be seen that now the simulation model gives significantly smaller errors. This is probably due to the fact that in the simulation model, the telescoping function is modeled without hydraulic sub-system in which the control signal are imposed directly. This will be further investigated in the next sections. Observing the luffing error it can be seen that this shows big similarities in shape and size.

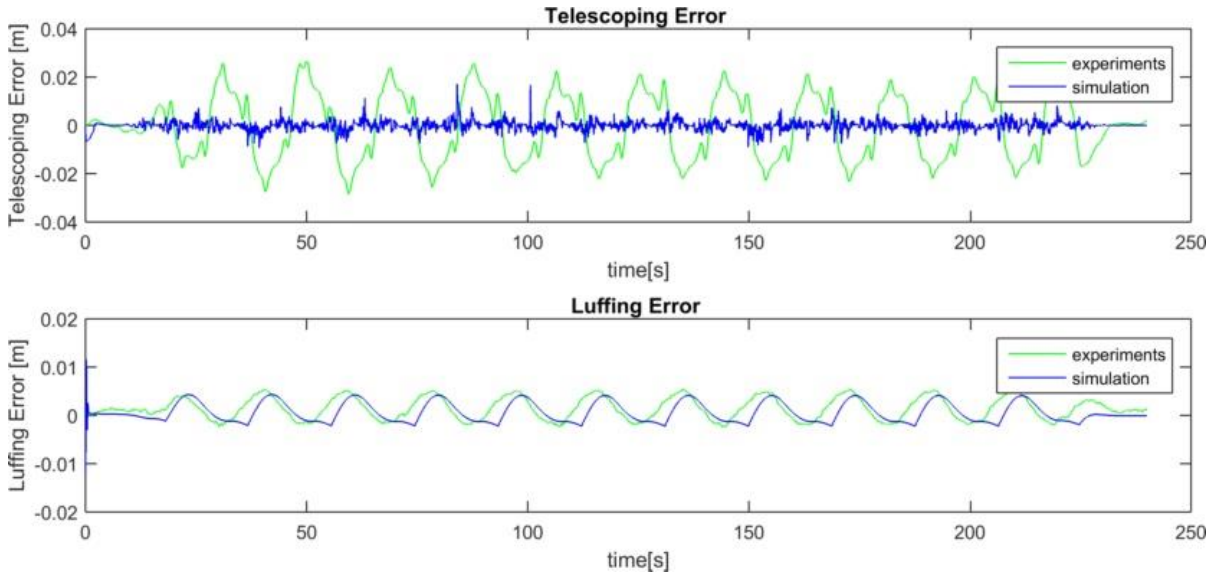

Figure 9.15 – The Telescoping Error (top) and Luffing Error (Bottom) during the telescoping test

In figure 9.16 below the telescoping set point for the compensation of the gangway tip is shown. It can be observed that the total telescoping set point and the telescoping feedforward set point has a

very strong alignment. The telescoping feedback set point during the simulation is smaller compared to the experiments which is also something that will be discussed in the next section.

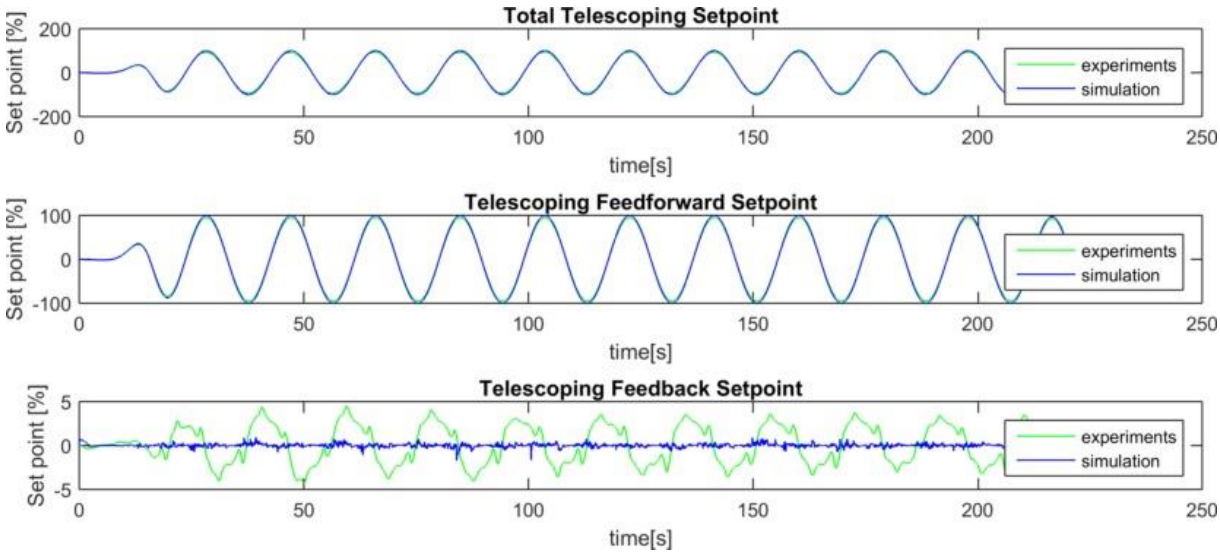

Figure 9.16 – Total Telescoping set point (top) which is composed of the telescoping feedforward set point (middle) and the telescoping feedback set point (bottom)

In figure 9.17 below the hydraulic pressure in the cylinder is shown. It can be observed that there is a similarity in shape of the charts but the pressure during the experiments is significant higher. Also, in contrast to the luffing test results, the pressure is much less frequent which implies that the high frequent response from the luffing test is due to a physical phenomenon in the hydraulic subsystem.

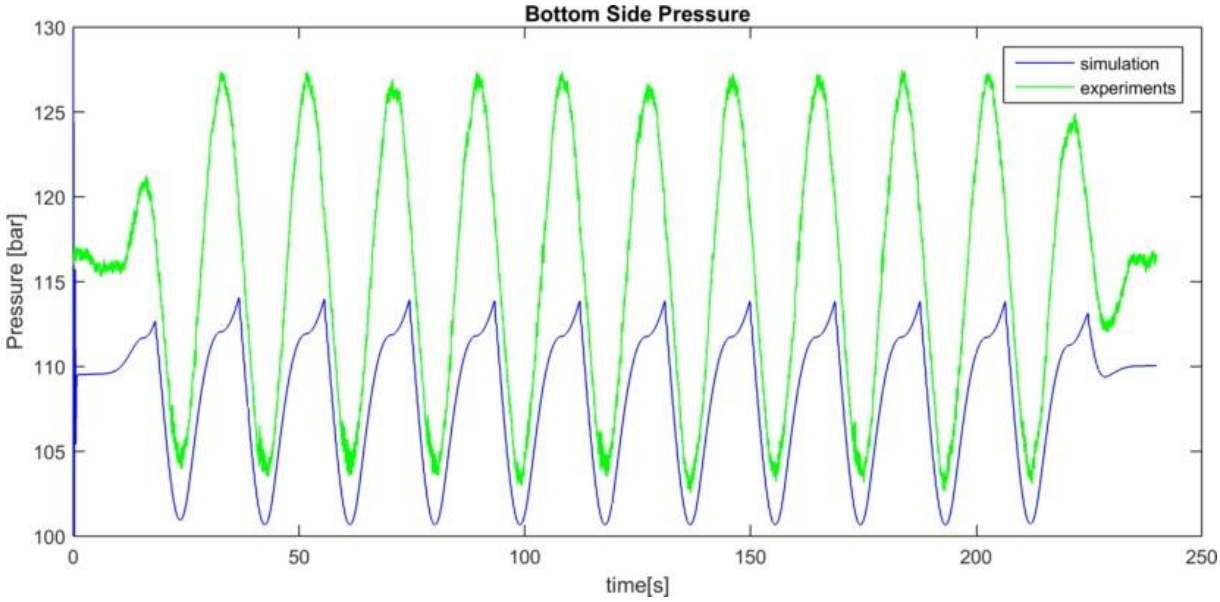

Figure 9.17 – Hydraulic Pressure at the bottom side of the cylinder during the telescoping test

In figure 9.18 the telescoping distance and cylinder length are presented. It can be observed that in both plots, the results of the experiments and that of the simulation align very well which means that also in the telescoping test, the dynamic response of the simulation model is similar to the dynamic response of the experiments. This supports the conclusion that the numerical model provides a strong basis for further development and expansion of this model.

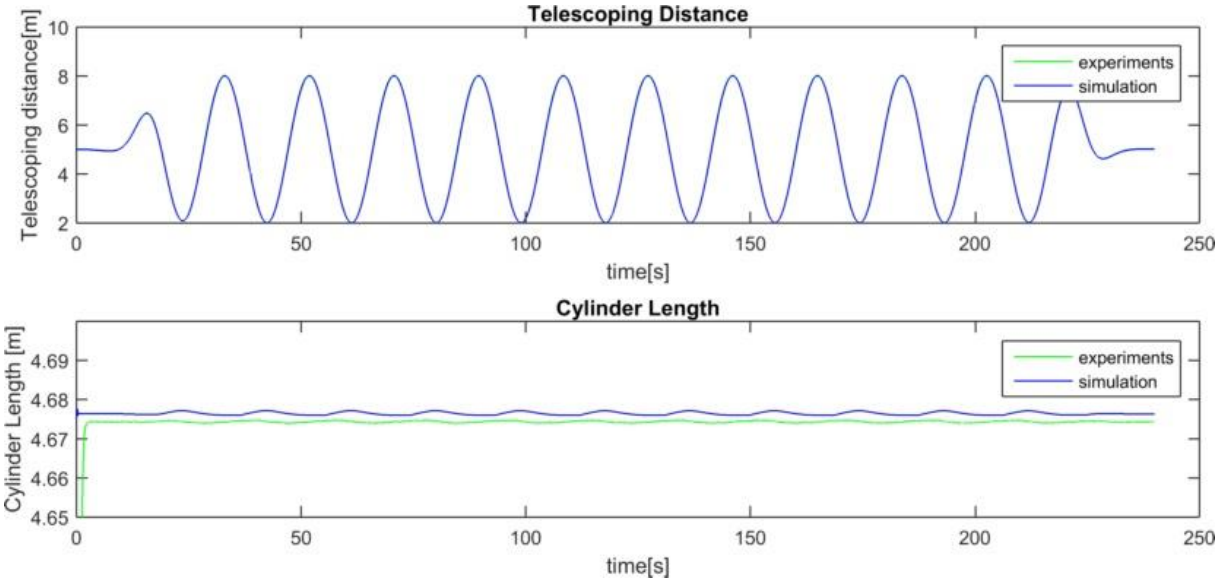

Figure 9.18 – Telescoping distance (top) and cylinder length (bottom) of the gangway during simulation and experiment

In figure 9.19, the estimated required telescoping power for the active motion compensation during the telescoping test is shown. In figure 9.20 the estimated required hydraulic power can be seen. As expected, the required hydraulic power is very small compared to the telescoping power. This should be theoretically zero since during the telescoping test only the telescoping function is activated.

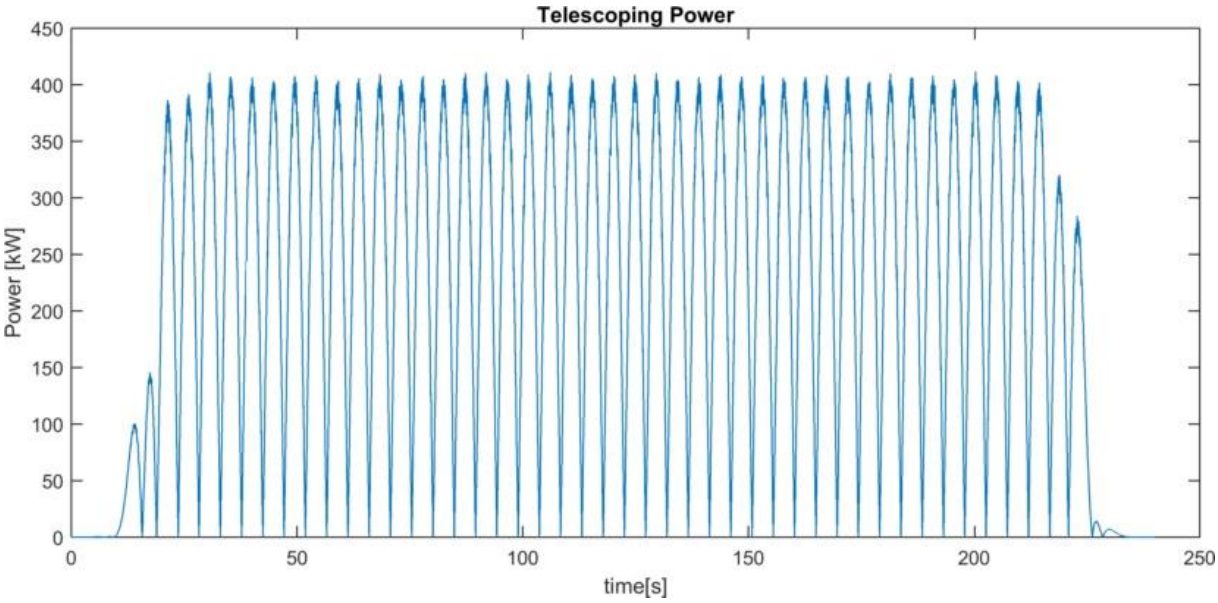

Figure 9.19 - Estimation of the required telescoping power for the active motion compensation during the telescoping test

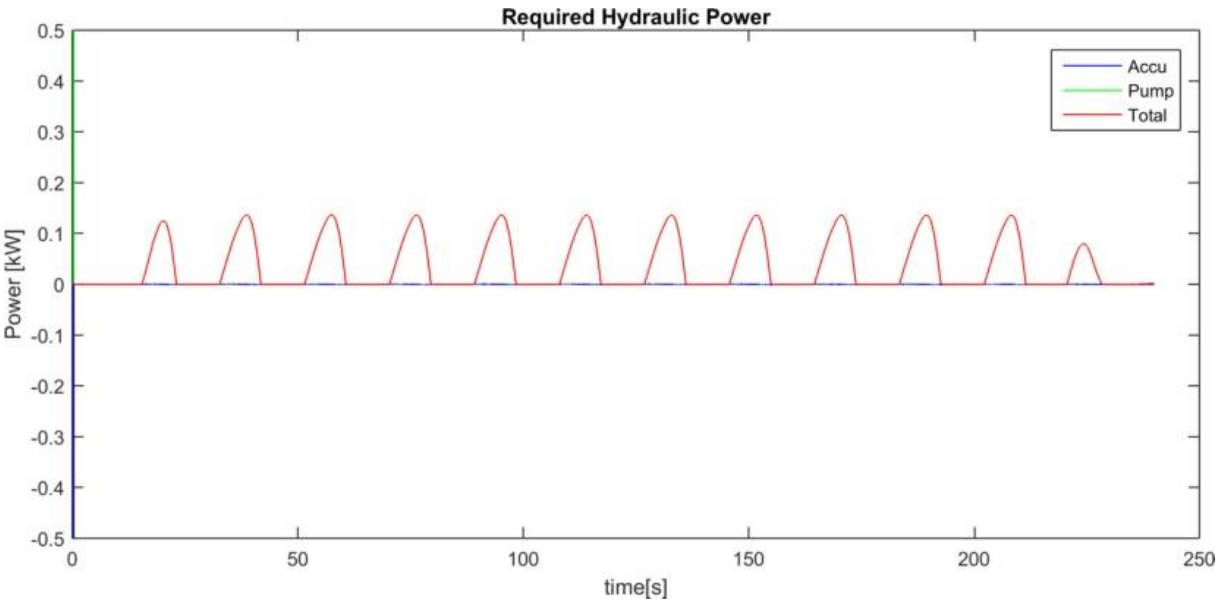

Figure 9.20 – Estimation of the required hydraulic power for the active motion compensation during the telescoping test

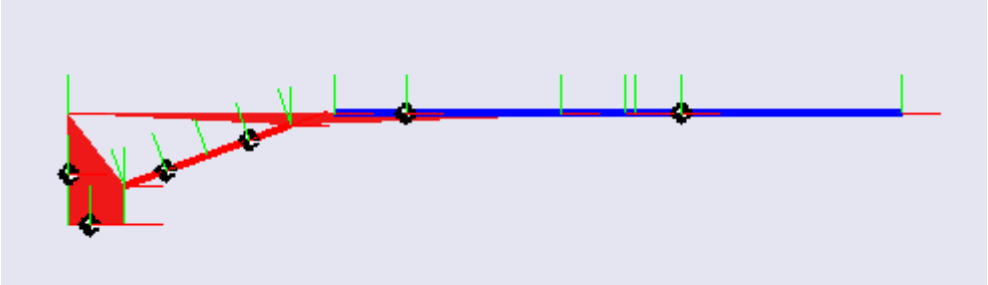

Figure 9.21 – Animation of numerical simulation during telescoping test

8.4 Model improvements

After analyzing the first simulation result, the accuracy of the model can be improved by changing some variables or adding some elements to the standard model. Before the model was developed, several assumptions were made which could be the physical explanation of the differences observed in the previous section. In order to check this is true, several adjustments are made to the model to see what impact they have on the results. The most important additions/improvements are:

- Friction between the fixed and telescoping part → Improvement of mechanical sub-system
- Delay of the telescoping function → mimics the effect of telescoping hydraulic sub-system
- Changing the bulk modulus of the hydraulic fluid (fluid property) → Hydraulic Stiffness
- Changing the viscosity of the hydraulic fluid (fluid property) → Hydraulic Damping
- Changing the density of the hydraulic fluid (fluid property) → Mass transport/Flow
- Adding an extra orifice behind the pressure compensators → Hydraulic Damping
- Changing of the luffing feedforward gain → Improvement of control sub-system
- Changing of the luffing feedback gain →Improvement of control sub-system

Friction between the fixed and telescoping part

In order to model the contact (wheel) friction between the fixed and telescoping part of the gangway, a translational hardstop block between the bodies is placed. The static and kinetic friction are calculated based on the equation:

$$F_f = \mu F_N \qquad (9.2)$$

Where:

F_f = the force of friction exerted by each surface on the other [N]
μ = the coefficient of friction, which is an empirical property of the contacting materials [-]
F_N = the normal force exerted by each surface on the other, directed perpendicular to the surface [N]

The addition to the model did not result in a significant difference in the simulation results compared to the initial results. So the friction, does not play an important role in the dynamic behavior of the gangway.

Applying a delay on the telescoping function

As stated in the previous section, the telescoping system is modelled as a theoretical ideally system in which the telescoping motion is performed by just directly imposing the telescoping velocity on the joint actuator. The whole hydraulic system behind the telescoping motion is neglected which causes the delays due to the opening of the valves and the PLC cycle time are not taken into account. This results in smaller but less realistic measured telescoping errors. In order to include this time delay a simple 'constant delay' block is added to the telescoping feedforward loop. A time delay of 0.1 [ms] is applied on the feedforward telescoping signal. This value is based on a PLC cycle time of 0.023 [s] and a time delay due to the valve opening time of 0.077 [s]. After running the exact same simulation as for the initial telescoping test, with this improvement, the next results for the measured errors are obtained:

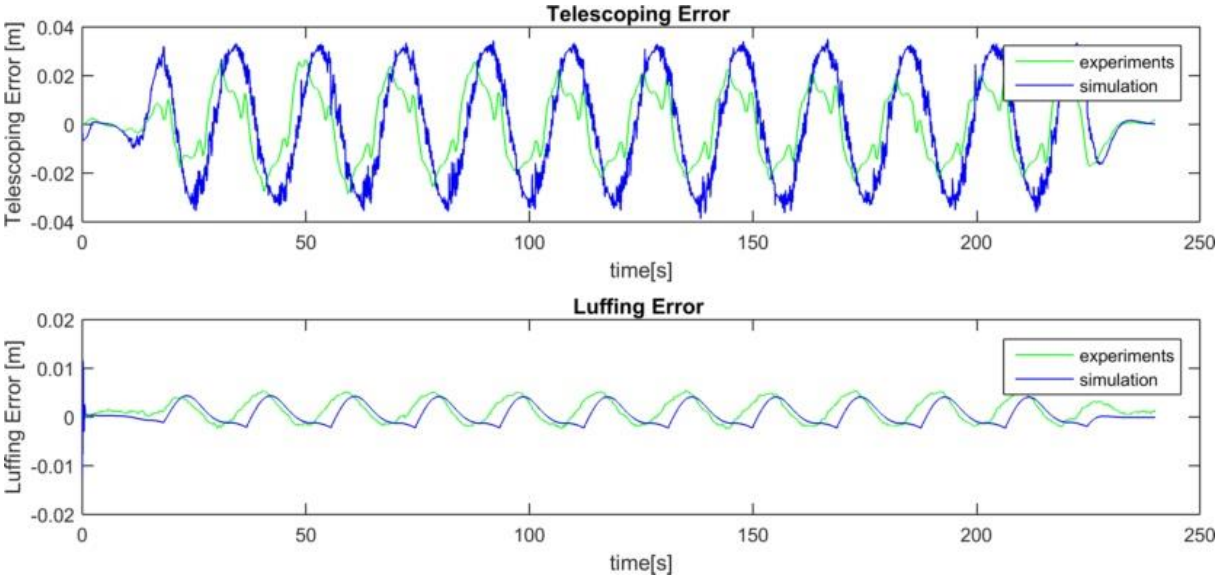

Figure 9.22 - Telescoping Error results of the improved telescoping test: addition of a time delay of 0.1 [ms] to the telescoping feedforward loop

In contrast to the initial telescoping test results, it can be seen that the telescoping error is in proximity close to the telescoping errors during the experiments. Also in the bottom plot of figure 9.23 below it can be observed that the telescoping feedback set points are much more similar than before. So the addition of the time delay is indeed an improvement to the model

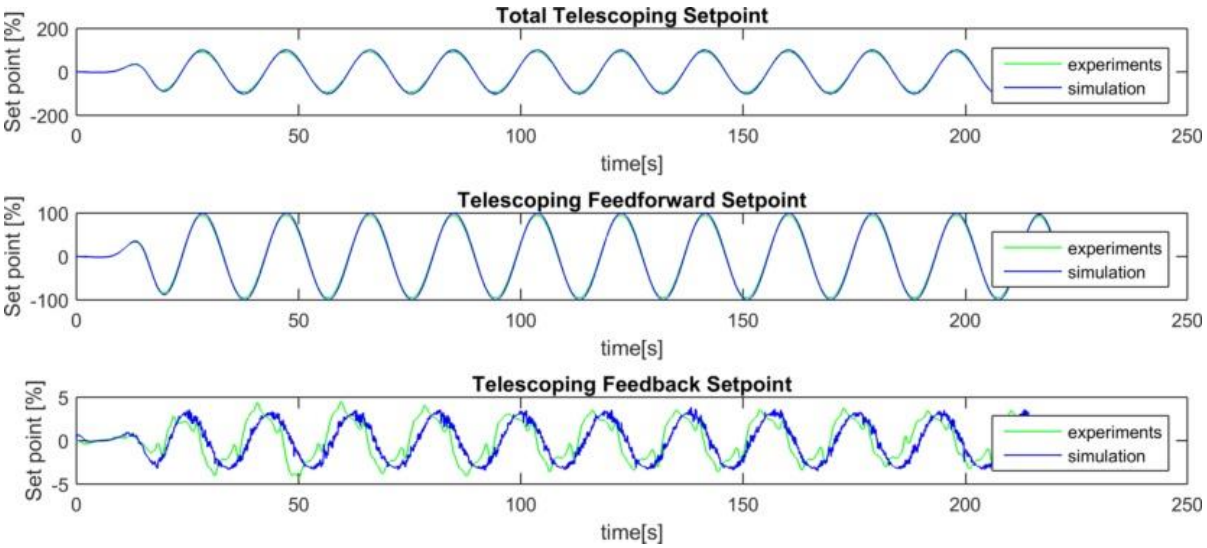

Figure 9.23 – Telescoping set point results of the improved telescoping test: addition of a time delay of 0.1 [ms] to the telescoping feedforward loop

Changing the hydraulic fluid

In the previous sections, it's observed that the simulation model has a higher oscillating and frequent response. In this section the influence of adjusting the hydraulic stiffness and hydraulic damping on the results will be investigated. There are several ways to adjust the hydraulic stiffness or hydraulic damping. First the hydraulic oil will be replaced by another type of oil to see if there any differences compared to the previous results can be observed. After this first check, more specific adjustments to the model will be done. For example the addition of extra orifices and leakages in the hydraulic components will be investigated.

In the initial numerical model 'Skydrol-5' is used as hydraulic fluid for the hydraulic luffing sub-system. Three important properties of the hydraulic fluid are the density, the viscosity and the bulk modulus of the fluid. It's important to notice that by changing the hydraulic fluid, all these properties are changing. First the results are observed after replacing the Skydrol-5 by 'Transmission fluid ATF' in order to check the influence of the hydraulic fluis. The first observed difference is shown in figure 9.24 below:

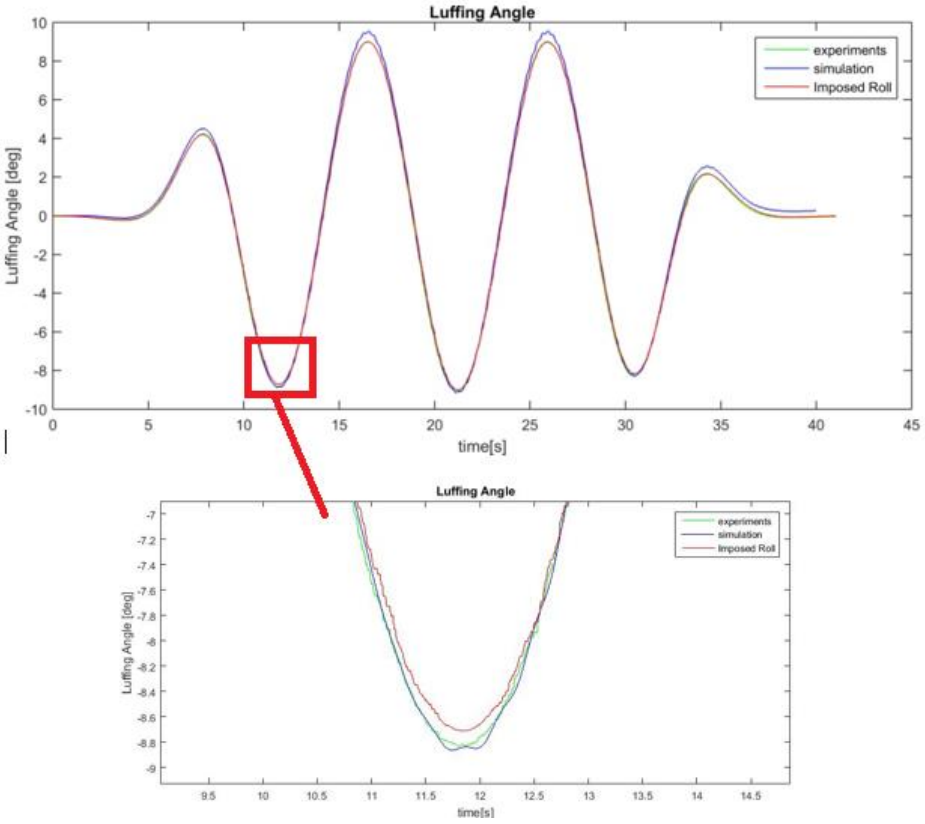

Figure 9.24 – Luffing angle during the luffing test with 'Transmission fluid ATF' instead of 'Skydrol-5' as the hydraulic fluid for the hydraulic sub-system

It can be observed that, in contrast to the initial results from the standard model, in this improved case the gangway shows also an overshoot at the lower luffing angle (at time= 12 [s]) which is a positive result. However, if the peak (for example at time = 16 [s]) is observed, it can be seen that during the simulation the gangway starts to have a bigger overshoot which means that the control system does not perform well. So, it seems like the problem is shifted from the case when the gangway reaches lower luffing angles to the peaks of the gangway motion. At the end of the simulation, there is an offset which was also visible in the initial results. This has to be further investigated in the next section.

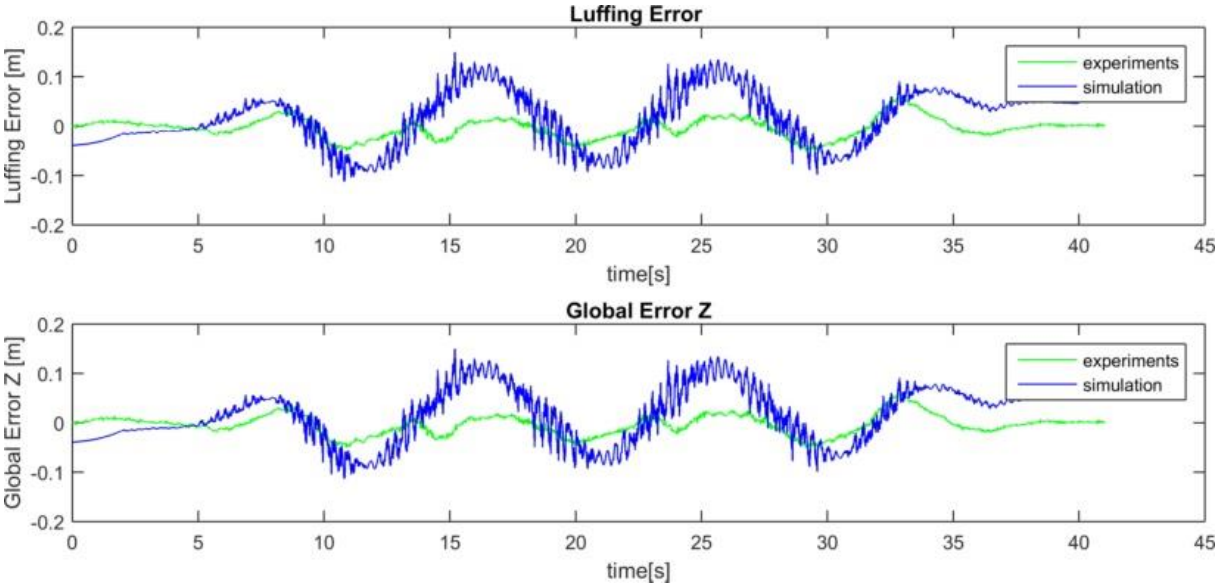

Figure 9.25 – Errors during the luffing test with 'Transmission fluid ATF' instead of 'Skydrol-5' as the hydraulic fluid for the hydraulic sub-system

In figure 9.25 it can be seen that the luffing error has more or less the same magnitude as in the previous conducted test with the standard model. The luffing error is also less oscillating than in the previous case. Observing 9.26, it can be seen that the high frequent pressure in the bottom side of the hydraulic is also present in the case of changed hydraulic fluid.

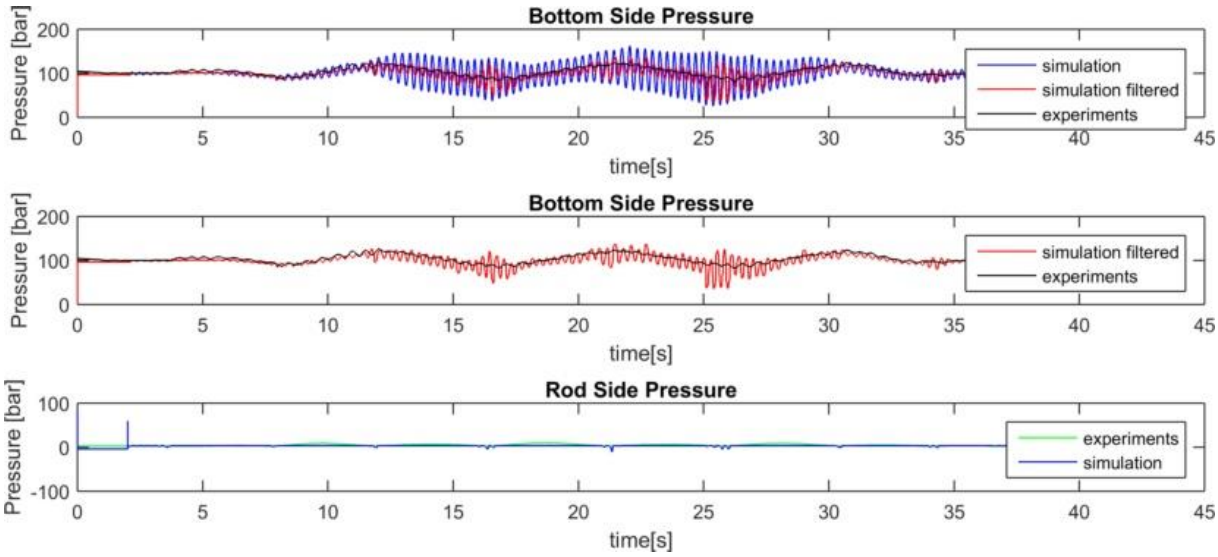

Figure 9.26 – Hydraulic pressures in the cylinder during the luffing test with 'Transmission fluid ATF' instead of 'Skydrol-5' as the hydraulic fluid for the hydraulic sub-system

Detailed investigation of changing the hydraulic fluid

From the previous section it can be changing the hydraulic fluid has an impact on the simulation results. To obtain more insight in the origin of the observed difference in the results, all the three mentioned properties of the fluid should be investigated separately to know where these differences come from. In the standard model the 'Skydrol-5' was used as hydraulic fluid. This fluid has the following properties:

$$Density = 961.4\ [\frac{kg}{m^3}]$$

$$Viscosity = 8.7\ [cSt]$$

$$Bulk\ modulus = 1.3e9\ [Pa]$$

The hydraulic fluid that is used in the quayside experiments is 'Castrol Hyspin AWS32' which has the following properties:

$$Density = 870{,}0\ [\frac{kg}{m^3}]$$

$$Viscosity = 32{,}0\ [cSt]$$

$$Bulk\ modulus = 1.0e9\ [Pa]$$

In order to see how the standard model with Skydrol-5 reacts on the adjustment of one of the three properties a 'Custom Hydraulic Fluid Block' is used which enables the adjustment of the fluid to every desired combination of the three properties. It's observed that changing the Bulk modulus and viscosity into the values above corresponding with Castrol Hyspin AWS32 this gave no significant changes/differences to the simulation results. However, after adjusting the density from 961.446 to 870 resulted in significant differences in the plots that are similar to the observed plots of the previous test with the transmission fluid ATF. In the figure below, the luffing angle of this improved model is shown.

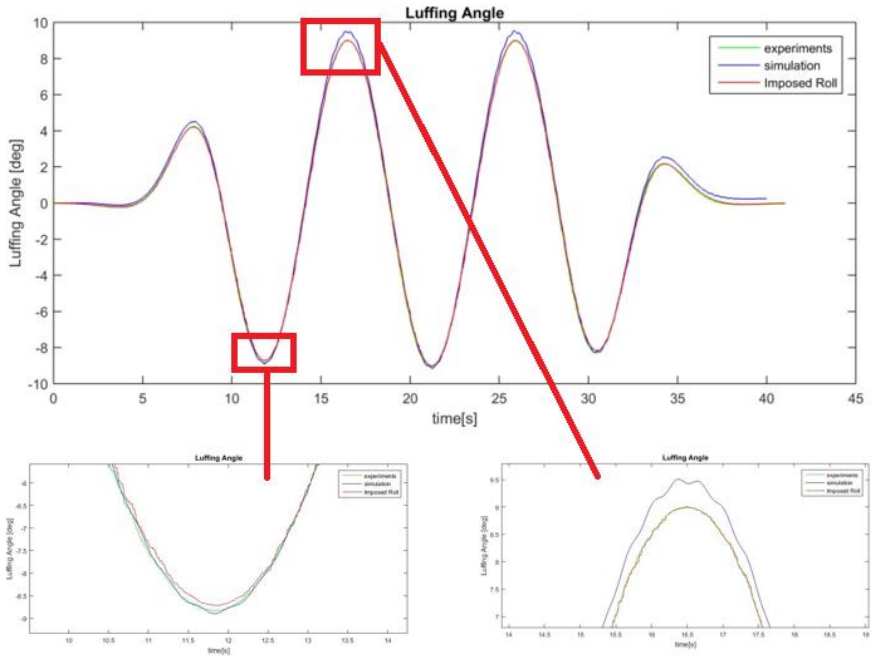

Figure 9.27 - Luffing angle during the luffing test with 'Transmission fluid ATF' instead of 'Skydrol-5' as the hydraulic fluid for the hydraulic sub-system

The results for the luffing angle are very similar to the results of the previous test with the Transmission fluid ATF which can be assigned to the fact that the density of both fluids are more or less the same (density of the transmission fluid ATF is 865.4 $[\frac{kg}{m^3}]$). Also when the other results are analyzed big similarities can be seen. This supports the assumption that the different simulation results are caused by changing the fluid density. The adjustment of the fluid density to the density of the Castrol fluid results in a better alignment around simulation time = 12 [s], when the gangway reaches its lowest luffing angle and starts to perform the luffing up motion. On the other hand, this density adjustment causes also a bigger error at the peaks, when the gangway is turning the other way around from a luffing upward into a luffing downward motion. The last effect will be further investigated by tweaking the control sub-system. This will be done by decreasing the luffing feedforward and increasing the luffing feedback gain.

During the analyses of the simulation results, also the hydraulic damping is considered by adding orifices and leakages to the hydraulic system. First an extra orifice behind the pressure compensators with a diameter of 0.1 [mm] is added. This extra orifice should give some damping effect to the model. In the results there were no significant differences visible after addition of these orifices. Also the leakages of the hydraulic components are investigated. It's observed that by increasing the leakages, in order to reach a stronger damping of the hydraulic system there was no significant decrease of the oscillations in the hydraulic pressures. Since the adjustment of the bulk modulus, which is related to the hydraulic stiffness, did not result in any significant changes it can also be stated that the high frequent response is not caused by the hydraulic stiffness that is not modeled correctly. Probably, the fact that the results are changed by the adjustments of the density has to deal with the mass transportation or flow through the system. This can be deduced from equation 6.16 which is used for the calculation of the flow through hydraulic components.

By decreasing the density, the flow through the system will increase which result in a stronger compensation at the same luffing set point. Based on the insight, which is obtained after the investigation of all the phenomena that are added to or tweaked in the model, the conclusion is made that the standard model with the Skydrol-5 fluid and with the time delay in the telescoping system included, gives the best simulation results. However, it is recommended to investigate why the system behaves better due to this difference in oil density. So, it's also recommended to figure this out first before the heave test is conducted. This will also be discussed in the next chapter.

9 Conclusions & Recommendations

The goal of this thesis is to develop a numerical model for the active motion compensation system of an offshore gangway which can be used to estimate the required power for the motion compensation. In this chapter it is indicated to what extent this goal has been achieved and how the results and conclusions can be used for further investigation and development of the numerical model.

9.1 2D (Numerical) Simulation Model

In general it can be concluded that the developed simulation model provides a good insight in the behavior of the active motion compensated gangway. Especially the dynamic response on the imposed ship motions show big similarities with the logged data from the quayside tests. The results that support this conclusion are the results of the luffing angle, cylinder length and telescoping distance, which correspond quite well with the experiments.

Besides of these big similarities, also some significant differences are observed. The most interesting differences are visible when the gangway reaches the lowest and highest luffing angles (peaks of the luffing angle chart) where the numerical model seems like to lose control and starts to generate an offset. When analyzing the errors during the simulation, it can be concluded that these errors are reasonable. The luffing error is significant larger than in the quayside test which implies that the luffing feedback and feedforward still has to be tweaked. The telescoping error shows more similarity and corresponds very well with the logged data. In order to mimic the delay caused by valve openings in the telescoping hydraulic system and the PLC cycle time, a time delay is implemented in the standard model, which is the main important improvement of the model.

Furthermore, it is also observed that the simulation results show high frequent and oscillating behavior. Especially the hydraulic pressure in the cylinder. After investigation the hydraulic stiffness (bulk modulus) and the hydraulic damping (extra orifices, viscosity of the hydraulic fluid, leakages) it is observed that this did not result in a significant decrease of the frequency response of the numerical model. However, when the density of the hydraulic fluid is decreased, it resulted in a better simulation result at the lower luffing angles but a larger offset at the positive peaks. The adjustment of the density shifted the offset. The high frequent response of the numerical model causes the simulation model to be sensitive to adjustments of the parameters.

Concluding the whole project, it can be said that the goal is reached to develop a numerical model that can be used for the estimation of the required power. Unless, the observed limitations of the current model, it provides a good insight in the behavior of the gangway system and can be used to simulate offshore tests in different virtual weather windows before testing the real gangway offshore. This is the main advantage compared to the case before this thesis is conducted. Another valuable result is the possibility, thanks to the developed model, to optimize the gangway design by adjusting the parameters.

9.2 Recommendations

In the future a more accurate simulation model can be provided by using the created 2D model and extend this to a 3D model. This can be performed relatively easy by adding a joint actuator which performs the rotation about the centerline. Secondly, the model can be improved by modeling also the telescoping and slewing hydraulic system (hydraulic motor, pump, valves etc.). As concluded, the biggest limitation of the current model is high frequent and oscillating hydraulic dynamic response. Therefore it is recommended to further investigate the hydraulic dynamic behavior or looking for the hydraulic component that causes the high frequency. In the future better AMC performances can be reached by conducting a better research in the control theory and applying this on the gangway system (for example the investigation of a PID-Control applied on the gangway system).

Before extending the current model to a 3 model, it's strongly recommended to perform the heave test after a the control sub-system is improved based on a better research of the control sub-system (feedback and feedforward). At kenz, there are already logged date for this heave test that can be used again for validation of the numerical model. In the heave test the performance of both activation systems, the luffing system and telescoping system, are tested at the same time. To compensate a vertical displacement, in order to compensate the motion, the gangway has to be rotated (luffing motion) and retracted or extracted (telescoping motion). The starting configuration of the gangway to perform the heave test is shown in the figure below. An extra hook load of 500 kg should also be taken into account since this was also the case during the performed quayside heave test.

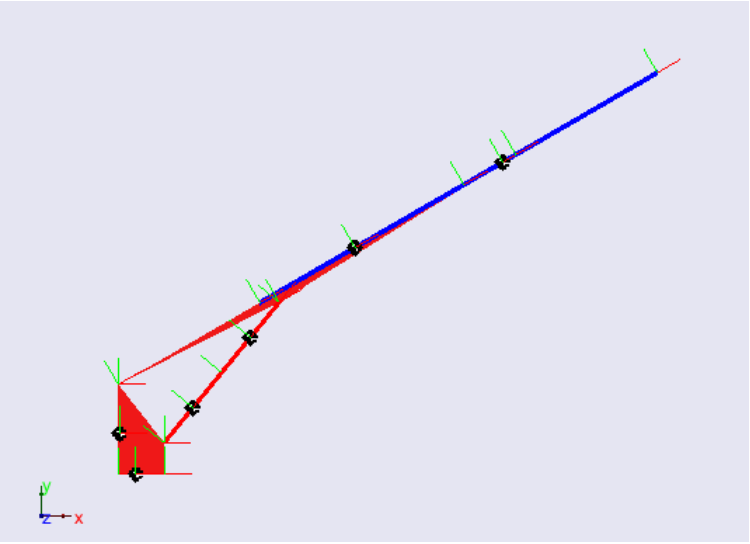

Figure 10.1 – starting configuration of the gangway for the performance of the heave test: Luffing Angle = 30 [deg], Telescoping distance = 5 [m], Telescoping Length = 20.343 [m]

LIST OF FIGURES

LIST OF TABLES

REFERENCES

[1] DNVGL-ST-0.358 (2015), *Certification of offshore gangways for personnel transfer*.

[2] G. Katsouris, L.B. Savenije (2016), *Offshore Wind Access 2017.*

[3] S. Robinson, *Simulation model verification and validation: increasing the users' confidence, in Proceedings of the 1997 Winter Simulation Conference*, edited by S. Andradoittir, K. Healy, D. Withers, and B. Nelson (Operations and Information Management Group, Aston Business School, 1997) pp. 53-59.

[4] Peter Albers (2010), *Motion Control in Offshore and Dredging.*

[5] Verope, *Technical brochure, Verope special wire ropes.*

[6] ALBERS Ingenieursbureau, *Vademecum Hydrualiek*

[7] Houman Hatami (2013), *Hydraulic Formulary,* Rexroth Bosch Group

[8] Kenz Figee (2016), *P34N001 // EH 16-26/1800 O.S. GW – Master Calculation*

[9] Kenz Figee CADFILER (2016), *2016004 P340N005 EH 16-26/1800 O.S. GW SIEM Offshore N-Sea*

[10] T. Oren, *the many facets of simulation through a collection of about 100 definitions,* SCS M&S Magazine 2, 82 (2011).

[11] R. Shannon, *System Simulation: The art and Science* (Prentice-Hall, Englewood Cliffs, New Jersey, 1975).

[12] P. Casas I, *Formal Languages for Computer Simulation: Transdisciplinary Models and Applications*, 1st ed. (IGI Global, 2013)

[13] C. Chung, ed., *Simulation Modeling Handbook: A Practical Approach*, 1st ed. (CRC Press, 1975)

[14] W. Aalst van der and M. Voorhoeve, *Simulation handbook* (Technical University Eindhoven, Dept. Of Mathematics and Computer Science, 1995).

[15] M. Law, *How to conduct a succesfull simulation study , in Proceedings of the 2003 Winter Simulation Conference*, edited by S. Chick, P. Sanchez, D. Ferrin, and D. Morrice (Averill M. Law & Associates, Inc., 2003) pp. 66-70.

[16] A. Balachandran, I. Rabuya, S. Shinde, and A. Takalkar, *Simulation & Modeling team* (2000), viewed on: 10-06-2017.

[17] A. Law and M. MrComas, *How to build valid and credible simulation models, in Proceedings of the 2001 Winter Simulation Conference*, edited by B. Peters., J. Smith, D. Medeiros, and M. Rohrer (Warwick Business School, 2001) pp. 22-29.

[18] A. Maria, Introduction to modeling and simulation, in Proceedings of the 1997 Winter Simulation Conference, edited by S. Andradottir, K. Healy, D. Withers, and B. Nelson (Warwick Business School, 1997) pp. 7-13.

[19] A. Verbraeck, *Lecture slides of simulation masterclass (spm9325),* Delft University of Technology (2014).

[20] H. Veeke, J, Ottjes, and G. Lodewijks, *The Delft System Approach* (Springer, 2008).

[21] S*. Robinson, Conceptual modelling: Who needs it?* SCS M&S Magazine 2, 1 (2010).

[22] *Hydraulics Library Manual and Tutorial,* Modelon AB, IDEON Science Park, SE-223 70 LUND, Sweden.

[23] S. Robinson, *Choosing the right model: Conceptual modelling for simulation, in Proceedings of the 2011 Winter Simulation Conference,* edited by S. Jain, R. Creaseu, J. Himmelspach, K. White, and M. Fu (Warwick Business School, 2011) pp. 1428-1440.

[24] R. Sargent, *Verification and Validation of simulation models, Simulation Research Group,* Syracusy University.

[25] C. Ekberg, *Sensitivity analysis and simulation uncertainties in predictive geochemical modelling,* Freiberg Online Geoscience 2 (1999).

[26] H. Veeke, J, Ottjes, and M. Duinkerken, *Lecture slides of discrete systems: Modelling, prototyping, simulation and control,* Delft University of Technology (2013).

[27] X. Xie, X. Li, and Y. Shen, *Static and dynamic characteristics of a long-span cable-stayed bridge with cfrp cables,* Materials 7, 4854 (2014).

[29] Mocean, Mark Paalvast (2016), *Quayside Gangway Power Test*

[30] Course Structural Dynamics (2015), *Slides of Lecture 2 about 'introduction to structural* dynamics' by A.V. Metrikine.

[31] Brien Fabien (2009), *Analytical System Dynamics – Modeling and Simulation*

[31] Mathworks, *Pressure Compensator,* https://nl.mathworks.com/help/physmod/hydro/ref/pressurecompensator.html?s_tid=srchtitle (2016), viewed on: 05-04-2017

[32] Mathworks, *Variable Orrifice,* https://nl.mathworks.com/help/physmod/hydro/ref/variableorifice.html?searchHighlight=orifice&s_tid=doc_srchtitle, viewed on: 02-04-2017

[33] Mathworks, *Gas-Charged Accumulator,* https://nl.mathworks.com/help/physmod/hydro/ref/gaschargedaccumulator.html?searchHighlight=Accumulator&s_tid=doc_srchtitle, viewed on: 07-04-2017

APPENDIX A: TEST PROTOCOL OF THE QUAYSIDE TRACKING ERROR TESTS

Report description:	**Tracking error test philosophy**
Document no.:	**9003_026**
Project no.:	P340N001
Crane type:	EH 16-26/1800 O.S. GW
Customer:	SIEM Offshore
Crane destination:	SIDDIS MARINER
P.O. no.:	P1107
Crane tag no.:	16-340
Customer doc. no.:	
Status:	**Released (d.d. 10-07-2017)**
Revision:	**A**

Revision status					
Revision	**Rev.description**	**By:**	**Date:**	**Checked:**	**Date:**
A	Updated according to client comments	JNOT	05-07-'17	FHOO	06-07-'17
0	Draft issue for client review	JNOT	27-06-'17	FHOO	27-06-'17

1 list of Abbreviations and references

1.1 Abbreviations

AP	Aft Perpendicular
BL	Base Line
CCW	Counter Clockwise
CHM	Crane Hook Mode
CL	Center Line
COG	Center Of Gravity
CS	Coordinate System
CW	Clockwise
DOF	Degrees Of Freedom
FE	Finite Element Method
GW	Gangway
LHS	Left Hand Side
MRU	Motion Reference Unit
PLC	Programmable Logic Controller
PTM	Personnel Transfer Mode
RHS	Right hand side
USB	Underside Slewing Bearing

1.2 References

	Document description	Doc. No.	Rev.	Date
[1]	Design philosophy	340_1011_020_B	B	04/04/2017

2 Test Assumptions

2.1 Gangway mode

Since the mode in which the gangway is operating (PTM or CHM) has no influence on the tracking error for luffing and slewing, all tracking error tests regarding these degrees of freedom will be performed for PTM only. However, for telescoping it is of significance whether the gangway is horizontal or in a more upright position. Therefore, tracking error tests regarding telescoping are performed in both PTM and CHM.

2.2 Gangway position

The gangway is simulated as to be positioned on the Siem N-Sea vessel (excluding the 6[m] pedestal extension), where the CL/USB (also referred to as 'equipment point') is located at:

Table 1 – Gangway position on vessel

Coordinate	Value [mm]	Measured from
X	43300	AP
Y	0	CL
Z	16345	BL

Note that the applied gangway position has no influence on the test results. The COG of the vessel, around which the vessel motions are assumed to occur, is located at:

Table 2 – Location of vessel COG

Coordinate	Value [mm]	Measured from
X	42320	AP
Y	0	CL
Z	7451	BL

Note that during several tests the COG is overridden in the PLC to ensure that only one of the gangway degrees of freedom is activated (see paragraph **Error! Reference source not found.**).

2.3 Test signals

Depending on speed and chosen amplitude a wave period is calculated for each test as follows:

$$V_{required} = \frac{2\pi}{T} A \rightarrow T = A \frac{2\pi}{V_{required}}$$

In which:

$V_{required}$	Required actuator velocity
T	Signal period
A	Amplitude of the actuator position signal

To gain sufficient insight in the motion compensation behavior, the duration of each test is chosen as such that approximately 10 cycles of each gangway motion are achieved. However, due to luffing accumulator capacity, 100[%] luffing speed cannot be achieved 10 times sequentially in one test. Two luffing cycles, during which the maximum luffing speed is achieved, can be achieved sequentially and will be tested 5 times separately. This enables the luffing pumps to refill the accumulators before each test.

In the following paragraphs, the amplitudes, signal periods and testing time, as applicable for each test, are provided. The test curve data points will be determined in MATLAB with a time interval of 10[ms] and sent to the PLC as it were a set of signals coming from the MRU (see also paragraphs **Error! Reference source not found.** and **Error! Reference source not found.**).

2.3.1 Telescoping

Table 3 – Telescoping test parameters

Test speed [m/s]		Amplitude [m]	Period [s]	Test duration [s]
25[%]	0.25	2.00	50.27	640
50[%]	0.50	2.00	25.13	320
75[%]	0.75	2.00	16.76	210
100[%]	1.00	3.00	18.85	240

([1]) For CHM the amplitudes are divided by $\sqrt{2}$ (see paragraph **Error! Reference source not found.**).

2.3.2 Slewing

Table 4 – Slewing test parameters

Test speed [deg/s]		Amplitude [deg]	Period [s]	Test duration [s]
25[%]	0.75	6.00	50.27	640
50[%]	1.50	6.00	25.13	320
75[%]	2.25	6.00	16.76	210
100[%]	3.00	6.00	12.57	160

2.3.3 Luffing

There is a non-linear relation between the gangway luffing angle and length of the luffing cylinders, this is due to the change in perpendicular arm between the cylinders and the hinge point. However, since this non-linearity can be considered small, it will, for the tracking error tests, be ignored. The maximum luffing cylinder speed is 0.24[m/s], which is equivalent to approximately 6.00[deg/s] luffing angle speed when the gangway is considered with a 0[deg] luffing angle. This results in the following test parameters as shown in Table 5.

Table 5 – Luffing test parameters

Test speed [deg/s]		Amplitude [deg]	Period [s]	Test duration [s]
25[%]	1.50	6.00	25.13	320
50[%]	3.00	6.00	12.57	160
75[%]	4.50	9.00	12.57	160
100[%]	6.00	9.00	9.42	41 (1)

(1) Duration of a single test, test will be repeated 5 times (see also paragraph 2.3).

2.4 GW configuration and vessel COG location per test

At the start of each test, except the 100[%] luffing speed test and the telescoping tests in CHM, the gangway shall be positioned in the following configuration:

Table 6 – Gangway configuration during the tracking error tests

Actuator	Value	Unit	Remark
Telescoping	5.0	[m]	Midstroke
Slewing	90	[deg]	Perpendicular to vessel CL over portside
Luffing	0	[deg]	Parallel to vessel deck

For the 100[%] luffing speed test, the telescoping stroke is reduced to 1.2[m] to minimize the boom tip accelerations in z-direction. For telescoping tests in CHM the luffing angle is changed 45[deg] upward. In the following paragraphs the applicable vessel COG location per tested actuator is given.

2.4.1 Telescoping

For the telescoping tests, no change in COG is necessary. In PTM the motion signal is applied as if it were a sway motion on the vessel since the gangway telescoping degree of freedom is in the same direction. In CHM the signals as provided in Table 3 are applied as both a heave and sway motion (in phase) to only activate the telescoping degree of freedom which is rotated 45[deg] from the horizontal. To ensure the correct telescoping speed the signal amplitudes are divided by $\sqrt{2}$. For e.g. the 25[%] test this results in a telescoping speed of $\sqrt{\left(2.00/\sqrt{2}\right)^2 + \left(2.00/\sqrt{2}\right)^2} \cdot \frac{2\pi}{50.27} = 0.25[\frac{m}{s}]$.

2.4.2 Slewing

For the slewing tests the vessel COG location is overridden in the PLC to the following values:

Table 7 – Vessel COG during slewing tests

Coordinate	Value [mm]	Measured from
X	43300	AP
Y	0	CL

Z	7451	BL

This places the COG in line with the CL of the gangway. The motion signal is applied as if it were a yaw motion on the vessel.

2.4.3 Luffing

For the luffing tests the vessel COG location is overridden in the PLC to the following values:

Table 8 – Vessel COG during luffing tests

Coordinate	Value [mm]	Measured from
X	43300	AP
Y	-580	CL
Z	19277	BL

This aligns the vessels X-axis with the boom hinge of the gangway. The motion signal is applied as if it were a roll motion on the vessel.

2.5 Communication between MATLAB and PLC

Communication between MATLAB and the PLC of the gangway will be done by means of a TCP/IP based communication. MATLAB will feed 6DOF positions and velocities in real-time as if it were a signal coming from the actual MRU. See **Error! Reference source not found.** for an overview of the test setup.

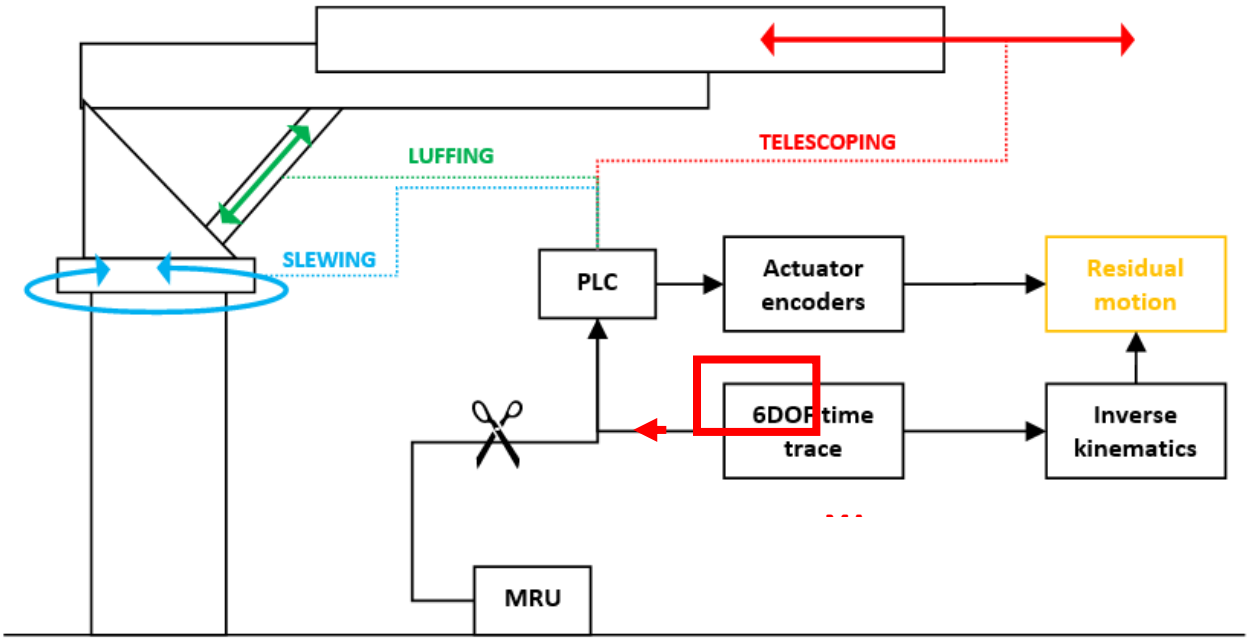

Figure 1 – Test setup on KENZ quayside during tracking error tests

The testing procedure will be as follows:

- On a separate laptop, used as a test HMI (see **Error! Reference source not found.** for a preliminary test HMI setup), one of the following tests is activated, by choosing one of the actuators:
    - Telescoping (1);
    - Slewing (2);
    - Luffing (3);

  A speed setting:
    - 25[%] (025);
    - 50[%] (050);
    - 75[%] (075);
    - 100[%] (100);

  And a gangway mode:
    - PTM (1);
    - CHM (2) - applicable only for telescoping tests.
- Based on the chosen test the PLC will send a test ID (a 5 digit test ID, e.g. '21050' for 'Telescoping – 50[%] (CHM)' or '13100' for 'Luffing – 100[%] (PTM)') combined with a 1 digit control number ('1' for initialization data) after the 'Initialize'-button is pressed.
- MATLAB will provide the following variables in a [8x1] array, corresponding with the test ID:
    - Test ID (1)
    - Gangway starting configuration (see paragraph **Error! Reference source not found.**):
        - Telescoping stroke in [m] (2)
        - Slewing angle in [deg] (3)
        - Luffing angle in [deg] (4)
    - Vessel COG location (see paragraph **Error! Reference source not found.**):
        - X-coordinate in [m] (5)
        - Y-coordinate in [m] (6)
        - Z-coordinate in [m] (7)
    - Test duration in [s] (8)
- Automatic positioning of the gangway will be used to put the gangway in the starting configuration. Once this configuration is established (encoder values for each actuator align with the requested configuration), and the AMC is enabled, the test can be started. The test is started by pressing the 'Run'-button on the test-HMI, this will send the test ID (e.g. '12075') with a control number '2' for starting the test.
- MATLAB will continuously send [13x22] arrays to the PLC with the following variables for 22 time steps (the number of time steps is based on the maximum expected communication and calculation delay between MATLAB and the PLC):
    - Relative time in [ms] (1)
    - Position values for:
        - Surge in [m] (2)
        - Sway in [m] (3)
        - Heave in [m] (4)
        - Roll in [deg] (5)
        - Pitch in [deg] (6)

        - Heading in [deg] (7)
    - Velocity values for:
        - Surge in [m/s] (8)
        - Sway in [m/s] (9)
        - Heave in [m/s] (10)
        - Roll in [deg/s] (11)
        - Pitch in [deg/s] (12)
        - Heading in [deg/s] (13)
- The PLC will interpolate between two columns of values based on its own relative time and send this relative time back to MATLAB (e.g. 241[ms]). This time value will be rounded down to the nearest 10[ms] and used as the new starting point for the [13x22] array that will be send to the PLC in the next cycle. Once the time value send by the PLC is larger than the duration of the test sending of values will be ended and the test is finished.
- If, e.g. due to larger delays than expected, the PLC needs a time step which is not in the [13x22] array, the control integer will be set to '0' to gradually stop the test by ramping down all signals to zero. Note that before testing trial runs will be done to check whether 22 time steps are sufficient or whether a larger array of values is necessary.
- Throughout the tests, PLC values are logged through an external logger, see **Error! Reference source not found.** for a list of logged values. Values will be logged every 20[ms] (might change due to final number of logged variables) with 11 significant figures (10 decimal places).

3 Safety

3.1 Maximum occurring accelerations

The gangway has been checked with regard to strength and stability of the structural steel as well as the strength of the components. Both FEM and hand calculations are based on a set of vessel acceleration occurring at the equipment point (crossing of CL/USB) as shown in the table below (see Appendix A in the Design Philosophy [1]):

Table 9 – Vessel accelerations at the equipment point

Acceleration direction	Value	Unit
Surge	-0.634	[m/s²]
Sway	0.311	[m/s²]
Heave	-0.825	[m/s²]
Roll	0.996	[deg/s²]
Pitch	3.947	[deg/s²]
Yaw	-0.614	[deg/s²]

These are converted to maximum allowable tip accelerations in the gangway coordinate system assuming a horizontal gangway (luffing angle of 0[deg]) at full telescoping stroke of 10.0[m] and slewed over one of the sides of the vessel. Note that the sign of each acceleration is chosen as such that it will result in the highest tip acceleration. The calculation results in the following allowable tip accelerations:

Table 10 – Allowable boom tip accelerations

Acceleration direction	Value	Unit
X	0.359	[m/s²]
Y	-1.105	[m/s²]
Z	-1.284	[m/s²]

The test parameters are chosen as such that during each test, the absolute values of these acceleration limits are not exceeded.

3.2 Alarm limits

All test parameters are chosen as such that during each test the gangway motions are within the applicable alarm limits:

Table 11 – Actuator alarm limits

Actuator	Min. limit	Max. limit	Unit
Telescoping	1150	8850	[m]
Slewing	-18	18	[deg]
Luffing	-18	18	[deg]

3.3 Clearance

During tests a clearance from the compensation point at the tip of the gangway towards ground level of 3.5[m] is guaranteed. Before the tracking error tests are performed a check is done on the clearance by manually moving the gangway is the most outer positions that occur during all tests. This is to ensure that no unexpected clashes can occur when performing the tests.

3.4 Ramp up/down

Using a hyperbolic tangent function the applied position and velocity signals are ramped up (and ramped down) from 0% to 100%. This is to ensure that positions, velocities and accelerations are all equal to zero at the start and the end of each test. An example of the ramp up/down signal is shown in the figure below.

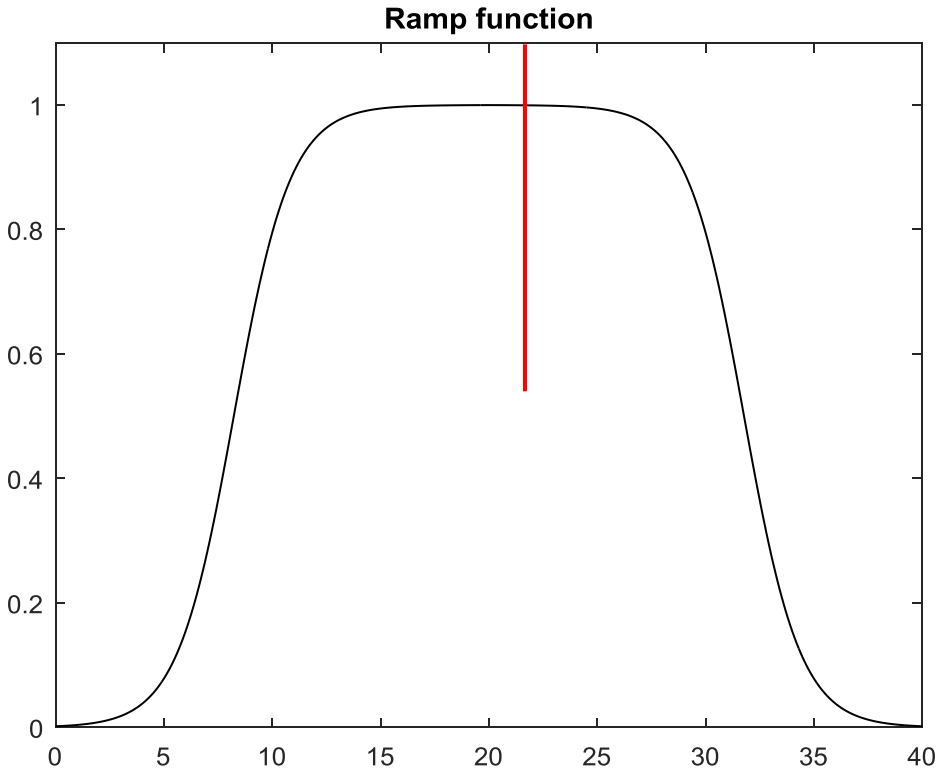

Figure 2 – Ramp up/down signal example

The left hand side of the signal (left of the red line in **Error! Reference source not found.**) is determined by the following function:

$$R_{LHS}(t) = \frac{1 + \tanh(A \cdot t - B)}{2}$$

The right hand side of the signal (right of the red line in **Error! Reference source not found.**) is determined by the following function:

$$R_{RHS}(t) = \frac{1 + \tanh\left(-A \cdot t + (A \cdot t_{max} - B)\right)}{2}$$

In which:

t	Time
t_{max}	Duration of the test
A	A scaling parameter to adjust the steepness of the ramp up/down, set to '$50/t_{max}$'. Note that for the 'Luffing – 100[%]'-test this value is set to '0.41' due to accumulator capacity (see paragraph 2.3)
B	A shifting parameter to ensure that the ramp up/down starts and ends at zero, set to 'π'

APPENDIX B: VARIABLES FOR LOGFILE

Variable		Unit	Name
Gangway mode		[1/2] (PTM/CHM)	Gangway mode
Reference point	X	[m]	Ref point X
	Y	[m]	Ref point Y
	Z	[m]	Ref point Z
Reference point locked?		[1/0]	FixAmcRef
AMC active?		[1/0]	AMC active
Telescoping stroke		[m]	Tls length
Slewing angle		[deg]	Slew angle
Luffing angle		[deg]	Luff angle
Luffing cylinder length		[m]	Luff cyl length
Surge		[m]	Surge
Sway		[m]	Sway
Heave		[m]	Heave
Roll		[deg]	Roll
Pitch		[deg]	Pitch
Heading		[deg]	Heading
Heading offset		[deg]	Heading offset
Surge speed		[m/s]	Surge speed
Sway speed		[m/s]	Sway speed
Heave speed		[m/s]	Heave speed
Roll speed		[deg/s]	Roll speed
Pitch speed		[deg/s]	Pitch speed
Heading speed		[deg/s]	Heading speed
Required telescoping compensation		[m]	TL comp req
Required slewing compensation		[deg]	SA comp req
Required luffing angle compensation		[deg]	BA comp req

Variable		Unit	Name
Required luffing cylinder compensation		[m]	LC comp req
Required compensation walkway CS	X	[m]	WW x comp
	Y	[m]	WW y comp
	Z	[m]	WW z comp
Walkway CS error	X	[m]	TLS err
	Y	[m]	SL err
	Z	[m]	LF err
Global CS error	X	[m]	ERRx
	Y	[m]	ERRy
	Z	[m]	ERRz
Telescoping joystick signal		[-100% / +100%]	TLSjoy
Slewing joystick signal		[-100% / +100%]	SLjoy
Luffing joystick signal		[-100% / +100%]	LFjoy
Telescoping feedback setpoint		[-100% / +100%]	Tele fbck sp
Telescoping feedforward setpoint		[-100% / +100%]	Tele ffwd sp
Telescoping total setpoint		[-100% / +100%]	Tele tot sp
Slewing feedback setpoint		[-100% / +100%]	Slew fbck sp
Slewing feedforward setpoint		[-100% / +100%]	Slew ffwd sp
Slewing total setpoint		[-100% / +100%]	Slew tot sp
Luffing feedback setpoint		[-100% / +100%]	Luff fbck sp
Luffing feedforward setpoint		[-100% / +100%]	Luff ffwd sp
Luffing total setpoint		[-100% / +100%]	Luff tot sp
Luffing pump pressure		[bar]	LF pump press
Luffing LHS cylinder up pressure		[bar]	LF L cyl up press

Variable	Unit	Name
Luffing LHS cylinder down pressure	[bar]	LF L cyl dwn press
Luffing RHS cylinder up pressure	[bar]	LF R cyl up press
Luffing RHS cylinder down pressure	[bar]	LF R cyl dwn press
Telescoping pump pressure	[bar]	TLS pump press
Telescoping outward pressure	[bar]	TLS out press
Telescoping inward pressure	[bar]	TLS in press
Slewing pump pressure	[bar]	SL pump press
Slewing CCW pressure	[bar]	SL CCW press
Slewing CW pressure	[bar]	SL CW press
Oil temperature	[°C]	Oil temp
Air temperature	[°C]	Air temp
Wind speed	[m/s]	Wind speed

APPENDIX C: TEST HMI EXAMPLE

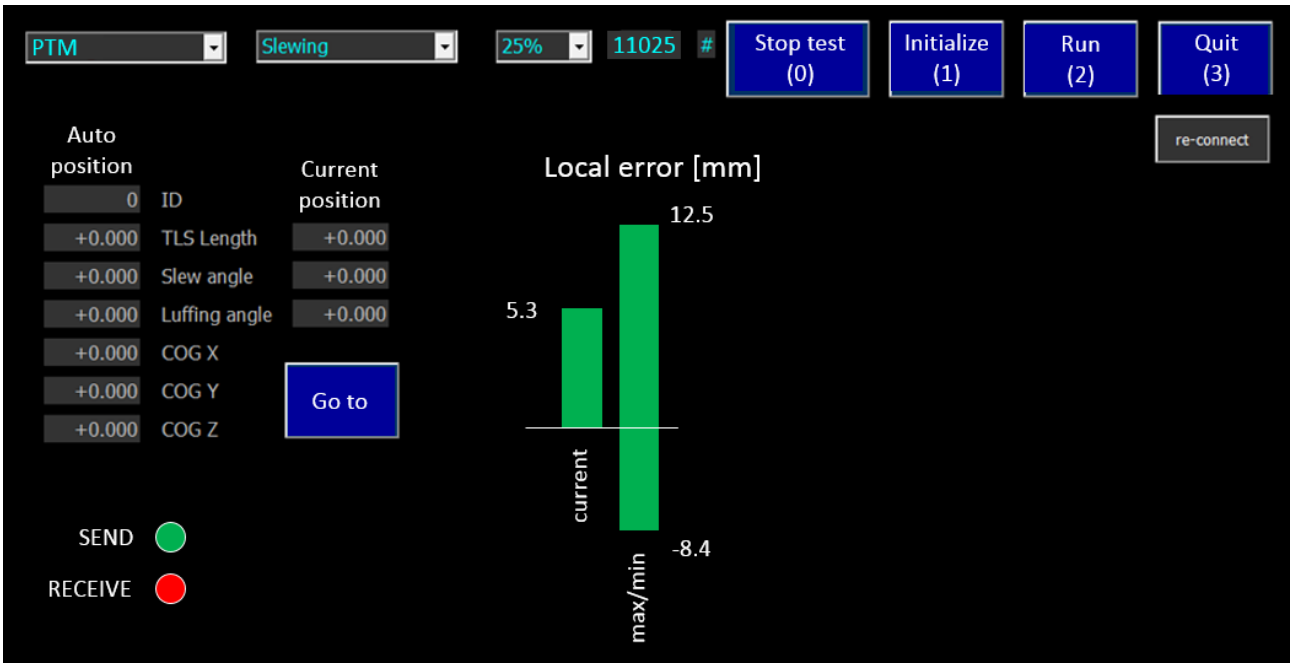

Note that this is not the final test HMI, just an indication of what it will look like.

APPENDIX D - Construction of Initial Simplified Simulink Model

First, we will construct two copies (one for each equation of motion). The first one is for the expression:

$$Sum\_Forces\_Gangway = M\ a \tag{5.7}$$

The second one is for the expression:

$$Sum\_Torque\_Pivot = J_{total}\ \ a_{Theta} \tag{5.8}$$

where 'a' is the acceleration and 'J_{total}' is the total moment of Inertia.

Therefore, we open a model and insert two Sum blocks (from the Linear Library), one above each other. We label this Sum blocks as 'Sum_Forces_gangway' and 'Sum_Torque_Pivot'. The output of each of these Sum blocks represents the sum of the forces/moments acting on the mass M_2 and around the pivot point. Multiplying by 1/M_2 and 1/J_total will give us the acceleration. Then two gain blocks are dragged into the model and each one is attached with a line to the output of the Sum blocks. These Gain blocks should contain 1/M_2 and 1/J_total. These variables will be taken from the Matlab environment. The two Gain blocks are labeled 'a_GW' and 'a_theta'. The outputs of these gain blocks are the accelerations of the mass and luffing angle. We are interested in the both the velocities and positions of the mass and the luffing angle of the gangway. Since velocity is the integral of acceleration, and position is the integral of velocity, these signals can be generated using integration blocks. Two integrator blocks are dragged into the model for the mass M_2 and the rotation around the pivot point (total mass of inertia). These blocks are connected by lines as shown in figure 5.2. The integrators are labeled 'v_GW', 'x_GW', 'v_theta' and 'Theta_luffing' since these are the signals these integrators will generate. In total 4 scopes from the Sinks library are dragged into the model and connected to the output of these integrators. They are labeled 'View_v_GW', 'View_x_GW', 'View_Theta_luffing' and 'View_v_Theta'

Now we are ready to add in the forces acting on the mass M_2 and the moments around the pivot point. First we need to adjust the inputs of each Sum block to represent the proper number. There are a total of 4 forces acting on M_2, so the Sum_Forces_Gangway block's dialog box entry is changed to: +++-

The Sum_Torque_Pivot block's dialog box entry is changed to: ---+.The first force acting on M_2 is just the input force, the Telescopic Force. A Signal Generator block from the Sources library is dragged into the model and connected to the uppermost input of the Sum_Forces_Gangway block. The Signal Generator is labeled 'F_telesc'. The same is done for the second Signal Generator which is labeled 'T_luffing' and connected to the lowest input of the Sum_Torques_Pivot block. The next force acting on M_2 is the centripetal force of the Mass M_2 if it rotates around the pivot point. This force is equal to the second term of equation 5.3:

$$F_{Centripetal} = M_2\ x_{GW}\ \ (v_{theta})^2 \tag{5.9}$$

Here we have the first coupling of the two equations of motion since in this term the two degrees of freedom are involved. This term is constructed by using the Product diagram (for the square of v_theta and multipliying this with x_GW) and a Gain block to multiply with mass M_2. These term comes in as a negative signal in the Sum_Forces_Gangway since it acts in the negative x_GW-direction.

The third force acting on the mass M_2 is the gravity force (Weight) of the mass itself:

$$F\_Weight = M2 * g * sin(Theta) \quad (5.10)$$

This term is constructed by dragging the Trigonometric Function Block into the model. The luffing angle 'Theta_luffing' is used as input for this block and the output is the Sinus of this angle. This output goes through the Gain block 'Gravity Force' which has the value M_2*g.

The final force is the translational spring force acting on mass M_2:

$$F\_spring = k\_Gangway * (x\_GW - L0 - L2/2) \quad (5.11)$$

This term is constructed by adding a constant block 'Constant', Subtract block 'Subtract' and a Gain block 'Translational Spring' and connecting to each other by lines as shown in the figure 5.2.

All the moments acting around the pivot point are constructed in a similar manner as for the forces by using the same blocks from the Simulink Library. Now there are five inputs for the 'Sum_Torque_pivot' Block and if multiplied with the 'a_theta' Gain block, the angular acceleration is obtained. During the construction of the 5 moments the coupling with the first equation of motion is made several times. That's why the figure looks quite complex but in fact it's just connecting the correct blocks and using the correct operations. The result of all previous actions results in the Simulink model as shown in figure 5.2

APPENDIX E: MATLAB SCRIPT FOR THE NUMERICAL MODEL

```
%%Pre-Processing
clc
close all
```

```
%% parameters for simplified 2D Gangway Model

current_directory = cd;

% GENERAL
M1 = 9803;                          % [kg]
M2 = 4898;                          % [kg]
M_Main_Frame = 8161;                % [kg]
M_Luffing_Cylinders = 3400;         % [kg]
g  = 9.81;                          % [m/s^2]
L0 = 1.5;                           % [m] initiele rek/ unstretched length
L1 = 15;                            % [m]
L2 = 15;                            % [m]

dim_F=5.895;
dim_C=1.9;
dim_B=1.5;
dim_G=0.306;

dim_J=5.903;
dim_H=2.421;
Beta0=49;
Gamma0=23;
```

```
% Telescopic Length and Luffing Angle at t=0 [s]
TL0=0.343;
TL1=1.18; %1.18; %5 %4;
TLstart=TL0+TL1;

GWA=0; %18.3285;


cd(current_directory);
disp('parameters are loaded')
```

```
%% In deze M-file worden de coordinaten van de belangrijkste joints van de gangway gedefinieerd

dim_GY= dim_F*sind(GWA)+ dim_G*cosd(GWA);
dim_GX= dim_F*cosd(GWA) - dim_G*sind(GWA);
dim_K= sqrt((dim_C-dim_GY)^2 + (dim_GX-dim_B)^2);
dim_D=1.032;
dim_A=0.580;
EA=1.95533e7; % Equivalente Kabelstijfheid

Alpha= acosd ((dim_C-dim_GY)/dim_K);
Beta= 90-Alpha;

X_CG_Rod= -(dim_K/4)*sind(Alpha);
Y_CG_Rod= -(dim_K/4)*cosd(Alpha);

I_x= -(dim_K/2)*sind(Alpha);
I_y= -(dim_K/2)*cosd(Alpha);

X_CG_Bottom= -(dim_K/4)*sind(Alpha);
Y_CG_Bottom= -(dim_K/4)*cosd(Alpha);
```

```
%% COG GANGWAY

COGX_FG=8.353;    % X-coordinate of the COG of the Fixed gangway(Incl winches)
COGY_FG=-0.2;     % Y-coordinate of the COG of the Fixed gangway(Incl winches)
COGZ_FG=3.239;    % Z-coordinate of the COG of the Fixed gangway(Incl winches)

COGX_FG_New= (COGX_FG + dim_A)*cosd(GWA);
COGY_FG_New= -(COGX_FG+dim_A)*sind(GWA);

COGX_TG=8.932;    % X-coordinate of the COG of the Telescoping gangway(Incl bumper)
COGY_TG=-0.009;   % Y-coordinate of the COG of the Telescoping gangway(Incl bumper)
COGZ_TG=3.209;    % Z-coordinate of the COG of the Telescoping gangway(Incl bumper)

COGX_TG_New= (COGX_TG+(dim_A-0.343))*cosd(GWA);
COGY_TG_New= -(COGX_TG+(dim_A-0.343))*sind(GWA);

COGX_MF=-0.547;   % X-coordinate of the COG of the Main Frame
COGY_MF=-0.044;   % Y-coordinate of the COG of the Main Frame
COGZ_MF=1.328;    % Z-coordinate of the COG of the Main Frame

COGX_Cyl=3.118;   % X-coordinate of the COG of the Luffing Cylinder
COGY_Cyl=0;       % Y-coordinate of the COG of the Luffing Cylinder
COGZ_Cyl=1.829;   % Z-coordinate of the COG of the Luffing Cylinder
```

```
%% Import Experimental Data

% In deze M-file worden de data in Matlab ingelezen, geselecteerd, geanalyseerd en verder verwerkt

Logged_Data2=PTMLUFF100131005;

% define time
Absolutzeit = table2array(Logged_Data2(:,3));
Absolutzeittosec = datenum(Absolutzeit)*(60*60*24) - datenum(Absolutzeit(1))*(60*60*24);
dAbsolutzeittosec = diff(Absolutzeittosec);


% Excel Kolommen vastleggen in Matlab
Roll=table2array(Logged_Data2(:,16));
Roll=str2double(Roll);
Roll=Roll;
Data_Roll=[Absolutzeittosec Roll];

Roll_vel=table2array(Logged_Data2(:,23));
Roll_vel=str2double(Roll_vel);
Roll_vel=Roll_vel;
Data_Roll_Velocity=[Absolutzeittosec Roll_vel];

Sway=table2array(Logged_Data2(:,14));
Sway=str2double(Sway);
Sway=Sway;
Data_Sway=[Absolutzeittosec Sway];

Sway_vel=table2array(Logged_Data2(:,21));
Sway_vel=str2double(Sway_vel);
Sway_vel=Sway_vel;
Data_Sway_Velocity=[Absolutzeittosec Sway_vel];
```

```
%%
Heave=table2array(Logged_Data2(:,15));
Heave=str2double(Heave);
Heave=Heave;
Data_Heave=[Absolutzeittosec Heave];

Heave_vel=table2array(Logged_Data2(:,22));
Heave_vel=str2double(Heave_vel);
Heave_vel=Heave_vel;
Data_Heave_Velocity=[Absolutzeittosec Heave_vel];
```